THE ASPERITY-DEFORMATION MODEL IMPROVEMENTS AND ITS APPLICATIONS TO VELOCITY INVERSION

A Dissertation

by

HOA QUANG BUI

Submitted to the Office of Graduate Studies of
Texas A&M University
in partial fulfillment of the requirements for the degree of

DOCTOR OF PHILOSOPHY

May 2009

Major Subject: Geophysics

THE ASPERITY-DEFORMATION MODEL IMPROVEMENTS AND ITS APPLICATIONS TO VELOCITY INVERSION

A Dissertation

by

HOA QUANG BUI

Submitted to the Office of Graduate Studies of
Texas A&M University
in partial fulfillment of the requirements for the degree of

DOCTOR OF PHILOSOPHY

Approved by:

Chair of Committee,	Richard L. Gibson Jr.
Committee Members,	Hongbin Zhan
	Akhil Datta-Gupta
	Yuefeng Sun
	Benchun Duan
Head of Department,	Andreas Kronenberg

May 2009

Major Subject: Geophysics

ABSTRACT

The Asperity-deformation Model Improvements and Its Applications to Velocity Inversion. (May 2009)

Hoa Quang Bui, B.S., University of Oklahoma; M.S., University of Oklahoma

Chair of Advisory Committee: Dr. Richard L. Gibson Jr.

Quantifying the influence of pressure on the effective elastic rock properties is important for applications in rock physics and reservoir characterization. Here I investigate the relationship between effective pressure and seismic velocities by performing inversion on the laboratory-measured data from a suite of clastic, carbonate and igneous rocks, using different analytic and discrete inversion schemes. I explore the utility of a physical model that models a natural fracture as supported by asperities of varying heights, when an effective pressure deforms the tallest asperities, bringing the shorter ones into contact while increasing the overall fracture stiffness. Thus, the model is known as the "asperity-deformation" (ADM) or "bed-of-nails" (BNM) model. Existing analytic solutions include one that assumes the host rock is infinitely more rigid than the fractures, and one that takes the host-rock compliance into account. Inversion results indicate that although both solutions can fit the data to within first-order approximation, some systematic misfits exist as a result of using the rigid-host solution, whereas compliant-host inversion returns smaller and random misfits, yet out-of-range parameter estimates. These problems indicate the effects of nonlinear elastic deformation whose degree varies from rock to rock. Consequently, I extend the model to allow for the pressure dependence of the host rock, thereby physically interpreting the nonlinear behaviors of deformation. Furthermore, I apply a discrete grid-search inversion scheme that generalizes the distribution of asperity heights, thus accurately reproduces velocity profiles, significantly improves the fit and

helps to visualize the distribution of asperities. I compare the analytic and numerical asperity-deformation models with the existing physical model of elliptical "penny-shape" cracks with a pore-aspect-ratio (PAR) spectrum in terms of physical meaning and data-fitting ability. The comparison results provide a link and demonstrate the consistency between the use of the two physical models, making a better understanding of the microstructure as well as the contact mechanism and physical behaviors of rocks under pressure. ADM-based solutions, therefore, have the potential to facilitate modeling and interpretation of applications such as time-lapse seismic investigations of fractured reservoirs.

To my family

ACKNOWLEDGMENTS

I would like to express my gratitude to whoever has directly or indirectly contributed to the completion of this dissertation.

First of all, I am deeply grateful to my advisor, Dr. Richard L. Gibson Jr., for his support, guidance, and encouragement during my stay here at Texas A&M University. Besides the incredible amount of knowledge that he has passed onto me, he has always taught and inspired me to become a good scientist and a better researcher. Without any doubt, he is one of the best academic advisors that I am fortunate enough to have known and worked with.

Secondly, I have known Dr. Anthony F. Gangi to be an excellent mathematician and physicist, a legendary geophysicist and engineer, a great philosopher and above all, a true scientist. He is always energetic about science, a real truth-seeker. I thank him for the tremendous amount of knowledge I have learned from him.

I owe my thanks to my committee members, Drs. Hongbin Zhan, Akhil Datta-Gupta, David Sparks, Benchun Duan, and Yuefeng Sun, for their thorough checking and excellent questions and advice on many topics regarding this dissertation.

Thanks also go to my friends in the research lab, John Priest, Hung-Liang Lai, Ravi Shekhar, Kyubum, Seung, Basu. I enjoyed sailing with them over the sea of hard work and have learned a lot from them throughout the years. I thank Dung Tran at the University of Oklahoma for running some code for me. My special thanks to my Vietnamese friends here in College Station who in many ways have helped me to thrive in life, spirit, and academics.

I thank Total SP and the U.S. Department of Energy for their research support.

Lastly, and most importantly, I thank my family for their patience and support during the years while I studied away from home. I dedicate this work to them.

TABLE OF CONTENTS

Page

CHAPTER Page

CHAPTER Page

CHAPTER Page

LIST OF FIGURES

FIGURE Page

FIGURE Page

FIGURE Page

FIGURE Page

CHAPTER I

INTRODUCTION

1.1 Overview

Reservoir characterization has long been an important topic in the petroleum industry. It has proved to be an important task in the process of reservoir evaluation and management, by identifying and quantifying those properties that influence the fluid mechanics, distribution and migration within the reservoir. The goal is to provide an adequate description of the physical aspects such as rock properties, porosity or permeability, etc., which are controlled by variables that change throughout the geological history of the reservoir. As computing power has become more and more robust, a reservoir can now be simulated using a computer or physical model (Sheriff, 1991). The simulation methods include quantitative, geostatistical, and stochastic modeling of field data. Capable of penetrating the reservoir depths and providing detailed images of the subsurface, seismic waves are often used to map and record the status of the reservoir at a moment in time. Hence, one challenging question in characterization is whether the seismic data and attributes can be used to detect or predict actual changes in the reservoir.

One of the most interesting applications of reservoir characterization is in carbon-dioxide sequestration. Carbon dioxide (CO_2) causes greenhouse effects that warm the earth, but possibly can be removed from the atmosphere by means of a long-term storage. One current technology is sequestration of CO_2 into geologic formations, especially known hydrocarbon reservoirs, including fractured reservoirs (Hepple and Benson, 2005). Thus, geological sequestration may help in both petroleum recovery and reducing green house effects. However, the risks lie in the fact that CO_2 could leak out of the sequestration site (due to a number of causes) and combine with water to form carbonic acid (H_2CO_3) which could react with the surrounding rocks, causing contamination of ground water as well as the atmosphere (Ha-Duong and

---

This dissertation follows the style and format of Geophysics.

Keith, 2003). It is therefore extremely important to understand the ramifications of sequestration and whether it will stand the test of time. 4D reservoir monitoring or time-lapse study is an effective way to investigate the effects of CO_2 sequestration using the seismic method.

Once the relationship between seismic attributes and reservoir variables has been established, time-lapse monitoring has tremendous potential to define the large-scale targets and therefore it is the best equipment to study a reservoir-scale model (Jack, 1997). Time-lapse or 4D seismic monitoring is the process of repeating 3D seismic surveys to determine the changes that have occurred over time, which is known as the fourth dimension (Sheriff, 1991). It allows the users to make 3D images of changes in reservoir properties as a function of time. With the use of time-lapse study, it is now possible to characterize, simulate and monitor the effects of geologic CO_2 sequestration at depth using seismic data. This technique is also currently being developed for major applications in both general and exploration seismology.

While methods of changing the pore pressure have been examined separately in the literature, current models for the effective seismic velocities of fractured rock do not consider explicitly the influence of pressure changes, which are known to be important in time-lapse applications. Therefore in this dissertation, I propose to tackle this problem by studying a theoretical model that quantitatively models the effects of pressure, allowing for simple, straightforward and accurate relations between effective pressure and elastic properties of rocks, which in turn enhances the time-lapse characterization of fractured reservoirs. The main objective of the research is to be able to answer the following question:

- *How do we effectively quantify the pressure effect for rock-physics applications such as seismic rock velocity inversion and prediction?*

The research will lead to a better physical understanding about the link between the effects of pressure on the mechanics of fractures to rock properties and seismic reflections, as well as the possibility to incorporate pressure changes into time-lapse seismic applications such as the modeling and monitoring of geologic CO_2 sequestrations.

1.2 Literature review

Time plays an important role in the description of a reservoir. In a time-lapse seismic study, it is important to understand which reservoir properties change with time

and which parameters are observable and/or predictable from the seismic. According to Jack (1997), pore (and effective) pressure, pore fluid (including saturation, viscosity, compressibility and fluid type), and temperature are among the primary reservoir variables. Other important changes include compaction, porosity, density, overburden stress, crack opening and closing, and chemical changes. The modeling and characterization of a fractured reservoir involve investigating the effects induced on the reservoir rocks by changes in the cracks, i.e. the reservoir variables. For those variables that describe or involve the mechanical behaviors of fractures such as pressures, it is necessary to have a physical model that mimics how natural fractures operate. As a result, fractured-reservoir characterization should in general go hand in hand with the study of rock physics, which include applications from fracture mechanics.

Fracture mechanics is a branch of physics and material science that deals with the mechanical performance of cracked structures (Anderson, 1995). In particular, it models and characterizes the growth and failure of cracks and the material resistance to fracturing, using analyses of stress versus strain as well as theories of elasticity and plasticity (Gdoutos, 2005). Furthermore, it uses methods of continuum mechanics, so the mechanical behaviors of the fractures are described mathematically by differential and integral equations. Reservoir rocks are certainly within the applicable domain of fracture mechanics. Once the physical model is established for a fractured reservoir, changes in the reservoir variables (e.g. pressures or stresses) will transfer into changes in the mechanical behaviors of the fractures (particularly deformations or strains) via the model differential and/or integral equations. These changes will then be linked, first to the fracture compliance (or stiffness), then to fluid and rock properties, and eventually, to seismic data. As an example, seismic modeling and characterization of CO_2 sequestration follows a similar work flow, starting with a rock-physics fracture model.

1.2.1 Fracture modeling

Fractures in rocks and in other types of materials have been studied intensively in the past. However, since natural fracturing is an integrated function of many variables, usually one or a few simple behaviors are separated and modeled at a time, while others are kept constant. Several physical models have been proposed and examined,

in which rock fractures are considered to be thin, planar layers (Walsh, 1965; Gangi, 1978; Hudson, 1980; Fehler, 1982), linear-slip surfaces (Schoenberg, 1980), or aligned vertical cracks with anisotropic poro-elasticity (Crampin, 1981; Gibson and Toksöz, 1990). The first group simulates natural fractures as planar distributions of "imperfect interfacial contacts" (Liu et al., 1996). In contrast, the second group considers fractures as areas of slip surfaces, which can be incorporated into finite difference modelling of seismic wave propagation and fluid flow simulation. The last approach involves "anisotropic poroelasticity" (APE) which models the orientations of cracks directly under specific pressure configurations. The most common physical model currently used in time-lapse seismic is the Walsh (1965) model, generalized for an effective medium by Hudson (1980), which treats fractures as ellipsoids with aspect ratios whose concentrations make up the total porosity of the rock.

Though all of these models are accurate descriptions of natural fractures, some of them are too detailed and complicated for a reservoir-scale quantification model, which means a computationally expensive cost for reservoir simulation, while others contain non-unique solutions or a trade-off between simplicity and accuracy. Hence it is particularly important for reservoir modeling and characterization to have a simple but accurate model that is applicable to the field scale. Of the many available models, it appears that the Gangi (1978) asperity-deformation "bed-of-nails" model (ADM, or BNM) is one that very well suits this purpose. This model is simple and effective because it allows for direct, straightforward mathematical relations between effective pressure and seismic rock velocities (of both compressional and shear waves), so data measurements in the reservoir can be readily and easily inverted for parameter estimates. Moreover, the existing (analytic) ADM solutions (Gangi, 1981; Carlson and Gangi, 1985) themselves are relatively simple mathematical formulae, with just a few meaningful parameters, so the inversion performance can be quite stable and reliable. Hence, ADM needs to be thoroughly investigated in terms of accuracy in data fitting and velocity prediction. This motivates my research.

1.2.2 The link between fracture characterization and seismic data

What can be observed on seismic data as a result of reservoir properties changes are changes in seismic travel time and amplitude attributes. Amplitude variations with offset (AVO) analysis is the study of seismic amplitudes taken into account the re-

flectivity that depends on the angles of incidence at the boundary of contrast. AVO analysis is a powerful tool for predicting the presence of hydrocarbons in petroleum exploration because it enables the detection and mapping of pore fluids in the subsurface. This technique was first employed by Ostrander (1984) as a means to identify a high-porosity gas sands embedded in shale, which causes an amplitude increase with offset on the seismic section. Koefoed (1955) proposed a set of rules to relate the change in reflection coefficient to the change in Poisson's ratio, which is an indicator of lithology, across the boundary between two media. Further AVO developments include attempts at approximating the exact reflectivity, given by the Zoeppritz equations, as a function of angle of incidence (Bortfeld, 1961; Richards and Frasier, 1976; Aki and Richards, 1980; Shuey, 1985; Smith and Gidlow, 1987), categorizing different sands groups based on AVO characteristics (Rutherford and Williams, 1989; Castagna et al., 1998), and AVO analysis, crossploting and interpretation (Castagna and Backus, 1993; Castagna et al., 1998). Nowadays, AVO attributes extracted from seismic data are being used as direct hydrocarbon indicators (DHIs) in petroleum exploration.

The importance and effectiveness of AVO analysis are the main reasons why seismic data is usually used as the measurement of change in reservoir properties. Thus, time-lapse seismic modeling and analysis have the potential to predict, map and illuminate the dynamic changes in reservoir properties and enhance reservoir management, especially for fractured reservoirs. Once having a fracture model, i.e. a physical representation of natural fractures, the obvious question for the user then would be: how does one go from this mechanical model to seismic data? Obviously the answer has to do with the rock or the medium characterized by this fracture model. Alternatively, what is the link between rock physics and seismic data? The answer lies in the elastic moduli, of the fracture and of the fractured rock. The elastic modulus is an indication of stiffness (or its inverse, compliance). And seismic velocities are proportionally related to the stiffness of the material they travel within. Stiffer materials tend to conduct seismic waves faster. In a Schlumberger lecture-award paper, Pyrak-Nolte (1996) demonstrates the link among fracture "specific stiffness", fluid flow, and seismic properties. Basically, the seismograms will change if seismic velocities across the fracture change, and that happens when the fracture stiffness changes; consequently, anything that brings about a change in the elastic moduli of the fracture will induce a change in the seismic, of which pressure and fluid are among

the main cause factors. Thus, the key link between a fracture model and the seismic is how the fracture elastic moduli are being modeled, over which pressure has a strong influence.

1.2.3 Seismic modeling of CO_2 sequestration in fractured reservoirs

The basic idea in this type of study is to use the time-lapse changes in reservoir properties as a tool to forward model the change in seismic amplitudes as a result of the CO_2 sequestration model. The simulation of CO_2 sequestration begins with the process of injecting CO_2 into the reservoir. Presumably maximum changes in the reservoir occur during injection, and after that chemical reactions take effect while the fluid flows into the low-permeability matrix (e.g. Kumar et al., 2008). In reality, the system takes a long time to reach equilibrium due to pressure relaxation. A reservoir rock-physics quantification model is necessary to predict and monitor the changes that happen during and after injection of CO_2. This model will relate the change in the reservoir properties to that in the seismic data. Time-lapse seismic study is used to investigate the feasibility and performance of the model.

For example, Yuh (2004) used the time-lapse seismic methods to model, simulate and monitor CO_2 sequestration. One important conclusion from his study is that since the acoustic properties of CO_2 are different from those of hydrocarbons and water, it is possible to image even the saturation of CO_2 using time-lapse seismic. Furthermore, a comparison of amplitude changes after injection can differentiate between supercritical fluid CO_2 and liquid CO_2. He also demonstrated the practice of time-lapse seismic monitoring by integrating actual production and petro-physical data, with rock-physics modeling, seismic wave propagation simulation and AVO analysis, to interpret the effects of pore pressure on the seismic amplitudes of two actual field data. In his rock-physics modeling works however, instead of a fracture model, he used empirical equations from Eberhart-Phillips et al. (1989), Dvorkin and Nur (1996), and Gardner and Harris (1968), for unconsolidated sandstone reservoirs, to account for the effects of pressure and porosity, and the Gassmann (1951) equation for fluid effects.

Recently, Shekhar and Gibson (2005) used the Hudson (1980) fracture model and applied theoretical solutions set forth by Pointer et al. (2000) to simulate AVO response for randomly isotropically fractured reservoirs embedded in a porous medium

and predict changes in velocity and attenuation for a reservoir-scale model. Differentially tuned, frequency-dependent thin-bed AVO response are incorporated using equations from Lin and Phair (1993). Their results suggest possible seismic discrimination between fluid types: brine, CO_2 , and supercritical CO_2-saturated reservoirs. In a related study, Shekhar et al. (2006) integrated engineering, geochemistry, geology and geophysics into a time-lapse study of CO_2 injection into hydrocarbon reservoirs and model the change in reservoir rock and fluid properties. Their results not only show a reduction in bulk modulus and velocity (and thus change in seismic amplitudes with time), but also find that the rate of change is slow after 10 years and thus difficult to be detected on a noisy data. They conclude that geochemical processes of CO_2 may have negligible effects on seismic data.

These studies, along with many others, justify the use of time-lapse seismic in modeling and monitoring geologic sequestration of CO_2.

1.2.4 The influence of pressure

Although such studies have modeled well the effect of CO_2 sequestration on seismic data, the change in effective pressure for fractured reservoirs has not been a factor of consideration. Actually, for decades now the effects of pressure on seismic velocities have been included in empirical equations for rock-physics modeling of sandstone reservoirs, such as by Eberhart-Phillips et al. (1989), Dvorkin and Nur (1996), Endres and Knight (1997), Han and Batzle (2006), and usually in combination with some other factors such as porosity or clay content. Theoretically, the effects of pressure and stresses on the mechanical and physical properties of rocks, such as elastic moduli and seismic velocities, have also been modeled extensively (e.g. Gangi, 1978; Mavko and Nur, 1978; Walsh and Grosenbaugh, 1979; Oda, 1986). Many studies have modeled the effects of pressure in relation to the shape and geometry of the pores in the rock. One common practice is the representation of cracks as a "spectrum" of ellipsoidal pore-aspect ratios (e.g. Cheng and Toksöz, 1979; Xu and White, 1995; Tran et al., 2008). Originally, Walsh (1965) treated all cracks and pores as ellipses (i.e. "penny-shaped" cracks) and modeled the applied stress in terms of the small aspect ratio of the elliptical cracks it closes. Toksöz et al. (1976) extended the work to cover for oblate spheroidal cracks of all aspect ratios from very thin, linear cracks to very spheroidal ones. Cheng and Toksöz (1979) used a linearized method to invert for the (discrete)

spectrum of pore-aspect ratios in rocks, using velocity-versus-pressure data. However, notwithstanding the successful modeling of pressure influences, the implementation and incorporation of pressure models in time-lapse seismic applications have been limited due to computational intensity and a trade-off issue between simplicity and accuracy.

In reality, pressure plays an extremely important role in anisotropy and fractured reservoirs at depth. The influence of pressure on rock properties is an essential part in the study of rock mechanics. Confining pressure has been known to strongly influence rock properties (e.g. Gangi, 1981; Carlson and Gangi, 1985). Pore pressure effects are important in many cases (e.g. Crampin and Zatsepin, 1997; Liu et al., 2004; Vlastos et al., 2006). As CO_2 is injected into the formations, the increase in pore pressure could lead to the opening of some cracks which affects the elastic properties of the whole rock. Attempts have been made to model the pore-pressure effects on fractured reservoirs. Recently, Vlastos et al. (2006) modeled the compliance of fractured rocks due to pore-pressure change and found noticeable changes on the waveform, amplitude and attenuation of the final seismogram. However, due to the specific set-up of their model, they concluded that the effect of pore pressure is negligible on the P-wave signal and only significant on the S- and coda-waves signals. In reality, pressure changes may cause enough change in the fracture compliance (or stiffness) that leads to measurable changes in seismic velocities and/or attenuation, and such effects should be included in the reservoir model. For the special case of sandstone reservoirs, the aforementioned empirical equations also confirm that reservoir rock properties are highly sensitive to pressure.

1.3 Research objectives

With the motivation of incorporating the influence of pressure into time-lapse seismic studies of fractured reservoirs, the primary goal of the research is to integrate and extend some of the innovative works aforementioned to develop a reservoir-scale model that is capable of describing the general behaviors of previous solutions, while quantifying the effects of pressure on the fracture modulus, and hence rock properties, particularly seismic velocities, which are the link to seismic attributes. Starting with the Gangi (1978) "bed-of-nails" model and its original solutions (Gangi, 1981; Carlson and Gangi, 1985), I will investigate its applicability in terms of a field-scale

rock-physics reservoir quantification model. Then I will try to improve the accuracy of its solution in terms of inversion and data fitting by slight modifications to the original model. The main novelty in this research is the validation, extension and improvement of a forward model that
(1) relates the effective pressure to the seismic velocities of the reservoir,
(2) is computationally simple enough for field-scale implementation, and
(3) accurately applicable to all reservoir rock types.
Below I present an outline of the key steps in developing this model.

1.4 Dissertation outline

Beside the introduction, this dissertation will consist of four main chapters and a final chapter for concluding remarks and suggestions for future work.

1.4.1 Chapter II - Theoretical study of the asperity-deformation model and its existing analytic solutions

1.4.1.1 Summary

Motivated by the Gangi (1981) and Carlson and Gangi (1985) formulae as simple and straightforward means to model and predict the effects of pressure on seismic velocities (and thus, time-lapse seismic), I investigate the accuracy and applicability of these equations in terms of data fitting and velocity inversion. In lieu of using them as black-box inversions, it is important to understand the physical model on which these solutions are based, the asperity-deformation model (ADM) (Gangi, 1978). More than a mere review of these papers, I first complement and contribute to the understanding and applicability of this model (which have been discussed briefly so far in the literature), by showing thorough and complete theoretical and practical examinations of ADM and its existing solutions. Theoretically, I show a detailed description of the model, how it operates, its assumptions and physical meanings in modeling fractures and effects of pressure, regarding rock deformation. Starting with a representation of natural fractures, the Gangi (1978) "bed-of-nails" model (BNM), I show that ADM models pressure as proportional to the infinitesimal deformation volume of contact asperities, while the distribution of contact asperities governs the

fracture behavior proportionally through induced change in elastic moduli. As a result, by making different assumptions about the significance of the host rock moduli, I show mathematical derivations of the existing analytic power-law ADM solutions: the Gangi (1981) "rigid-host" and Carlson and Gangi (1985) "compliant-host" equations. I will also discuss and interpret the physical meaning and definition of each parameter in these solutions as well as the equations relating among them.

1.4.1.2 List of contributions in chapter II

- Provide complete understanding and description of ADM and solutions
- Complement to current literature on theory and practice of ADM by discussing undiscussed topics, assumptions and implications.

1.4.1.3 Outline

- ADM, BNM and all physical meanings
- Topics regarding the rigid-host solution
- Topics regarding the compliant-host solution

1.4.2 Chapter III - Effects of pressure on seismic velocities of fractured rocks - Applications of existing power-law asperity-deformation model solutions in nonlinear inversion of laboratory data

1.4.2.1 Summary

Viewing a rock differently as consisting of fractures and either a rigid or a compliant host, Gangi (1981) and Carlson and Gangi (1985) respectively delineated ADM-based velocity-versus-pressure relationships for fractured rocks and illustratively showed sample applications of those solutions to a few low-porosity, hard, crystalline rocks taken from a specific site. Recently, Genova (2008) used the Gangi (1981) rigid-host solution to perform stochastic modeling and linearized inversion, using a method set forth by Parrish and Gangi (1981), on the velocity and permeability data from a Wilcox shale (Kwon et al., 2001) and several other rocks previously examined by

Gangi (1978), Carlson and Gangi (1985), and Gangi and Carlson (1996). His study mainly focuses on modeling the effects of random noise and of the zero-pressure measurement on the uncertainty and sensitivity of parameter estimates from the rigid-host equation. Here, I follow a different path and contribute to the practice of ADM by carrying a complete study of systematic nonlinear inversion results, applying both rigid- and compliant-host solutions to the compressional and shear wave velocities (V_p and V_s) of a broad total of twenty low- and high-porosity rocks of different types (sandstones, carbonates, and granites) from the published laboratory data sets of Coyner (1984), King (1966), and Nur and Simmons (1969).

The good quality of the Coyner (1984) measurements allows for a precise study of the sensitivity of model parameters, the non-uniqueness of results and working mechanisms of each solution. By studying the sensitivity of each solution parameter using synthetic and actual laboratory data, I have been able to determine which parameters can be more accurately and uniquely identified. Altogether, these results indicate a non-uniqueness in solution parameter estimates, expressed in terms of uncertainties and trade-off relationships among model parameters. Additionally I find that random noise effects can be restrained by putting constraints on the possible outcome values of estimates. To ensure the stability of inversion, I employ different methods including the Levenberg-Marquardt, Nelder-Mead, Differential Evolution, Simulated Annealing, and Random Search algorithms, which are built in as options of Mathematica functions such as NonlinearRegress and NMinimize. My inversion results in chapter III illustrate that while the rigid-host solution fits reasonably well with the data from several rocks, systematic misfits exists in other rocks comparatively larger than the measurement error. In contrast, the compliant-host solution returns negligible and random errors in all rocks, for both V_p and V_s data. However, the compliant-host inverted parameter values fall uninterpretably out of their possible range as constrained by ADM. These results lead to the conclusion that although ADM-based solutions can be applied to all rocks, modifications are in order to improve the rigid-host fit and interpret the seemingly unphysical estimates of compliant-host parameters. ADM-based solutions therefore have the potential to facilitate time-lapse seismic applications for fractured reservoirs.

1.4.2.2 List of contributions in chapter III

- Present applications to published data (i.e. inversion results to broad data sets), proving that although the ADM method is applicable for all rocks, modifications are necessary.
- Demonstrate solution behaviors and interpretation of results regarding ADM.

1.4.2.3 Outline

- Existing analytic ADM solutions
- Inversion results
- Topic discussions

1.4.3 Chapter IV - Numerical inversion of the distribution of asperity heights - Model improvements from the rigid-host perspective

1.4.3.1 Summary

An elastic property of a rock is a funciton of the properties of both the inclusion pores/cracks and that of the host rock. The contribution of the host rock property to the overall rock property is either significant or negligible depending on how it compares to that of the fractures. Nevertheless, ADM allows the users to assume that the host rock is always much more rigid and thus its compliance is negligible compared to the cracks, equating the rock elastic moduli to those of the fractures and attributing all natural rock physics to the linear elastic deformation of the asperities as they come into contact in the "bed-of-nails". From this perspective, the distribution of asperity heights dictates rock behaviors while it does not have to obey a simple power law such as assumed by Gangi (1978) or by the existing ADM solutions. Hence, I employ a numerical method to generalize and invert for the distribution of asperity heights in the experimental rocks. I discretize the deformation axis at a number of sample points using a logarithmic sampling scheme, and invert for the value of the cumulative distribution function (CDF) of the asperity-height distribution at each of the sample points by grid-searching over its possible range of values, while linearly interpolating in between these points. Pressure and velocity are evaluated numerically

corresponding to the interpolated distribution function and matched with the data for the best fit in a least-square sense. Similar to a discrete finite element method (DFEM), the interpolating function affects the result of the numerical asperity-height inversion (AHI) at any particular point, but does not change the general behavior of the inverted distribution. As a result, our numerical grid-search inversion does a better job of fitting the data compared to the rigid-host analytic solution, but at the expense of using more parameters to describe the distribution function, as well as much more computation time. The results confirm our initial postulation that from the rigid-host point of view, the asperity-height distribution varies arbitrary from rock to rock, and does not have an universal form (such as a simple power-law).

One important motivation for this discretization is to simplify comparisons to results from a well-known linearized inversion scheme made popular by Cheng and Toksöz (1979). The concept of a pore-aspect ratio (PAR) has been widely used in the industry, especially for describing the pore geometry and microstructure of the rocks as well as specifying an effective medium for time-lapse seismic modeling. This method inverts for a PAR spectrum from the V_p and V_s pressure profiles of the rock, assuming the properties of the grain solid are known. The spectrum contains discrete concentrations of the porosity for different bins of aspect-ratios. An increase in pressure closes the porosity made up by all elliptical cracks having ratios in between the bin boundaries. Pressure is related to PAR using the Walsh (1965) formula for closure stress while velocities are related to PAR using the Kuster and Toksoz (1974) model. Here I postulate that the distribution of asperities which determines the rock behaviors will bear some resemblance to the PAR spectrum. The analogy is both in the indirect relation of pressure and velocity through a third variable (either asperity height or PAR), and in the physical meaning of that variable. Longer asperities are first-in-line to be brought into contact and deformed just like the thinner ellipsoidal cracks with smaller pore-aspect ratio getting closed before the more spherical ones do. Due to the non-uniqueness of the sampling scheme and of the bin-interpolation function, it is difficult to come up with two different sampling schemes which will hopefully display comparable features on both inverted distributions; therefore, I relate both distributions to effective pressure. Finally, I compare the two methods in terms of accuracy and computing resource. The comparison results suggest that two models describe the same physical phenomenon which is the general increase in contact area due to pressure.

1.4.3.2 List of contributions in chapter IV

- View every rock as having a rigid-host, generalize and invert for the asperity distribution (grid-search AHI).
- Comparison with a known, standard method for velocity inversion, pore-aspect ratio (PAR); relate to rocks' physical behaviors.

1.4.3.3 Outline

- Rigid-host and power-law assumptions
- Methods and results: numerical implementation of ADM and PAR
- Comparison of the two methods in terms of results and physical meaning

1.4.4 Chapter V - Nonlinear deformation and the pressure dependence of the host rock - Model extension from the compliant-host perspective

1.4.4.1 Summary

In this chapter I look at the experimental rocks from the compliant-host perspective and provide a theoretical extension of ADM to incorporate the dependence of the host on pressure variations. First, I postulate that the unphysical parameter estimates from compliant-host inversion reflect the fact that the compliant-host solution has not taken into account the pressure dependence of the host rock moduli, which is caused by the nonlinearity of deformation. I attempt to incorporate the host-rock pressure dependence into ADM by modifying the original ADM and let the properties of the asperity material change with the fracture closure according to another power law, separate from the Gangi (1978) power-law number of asperities in contact. Naturally, when the host rock depends on pressure, its compliance is negligible at low pressures (which is why the rigid-host solution works well for all rocks in the low pressure range), but increases with increasing pressure and becomes significant at high pressures (i.e. comparable to that of the fractures). In the "bed-of-nails", since the fracture faces are considered rigid, I attempt to build the modulus decreasing-with-pressure of the host

rock into the asperities. In other words, I have the host-rock pressure dependence built into the "bed-of-nails" by letting the "nails" (or asperities) weaken with increasing applied pressure.

This extension of ADM leads to the same equation for velocity as a function of pressure as the compliant-host solution, but with a new, different parameter which simultaneously accounts for both the linear elastic deformation of contact asperities and the pressure dependence of the host rock moduli, in contrast with the original compliant-host solution which accounts for only the linear elastic deformation alone. The model extension unties the positive constraint on the new parameter, making negative-valued estimates possible and meaningful, thereby successfully explains the outcome of inversion. I interpret the negative-valued estimates from compliant-host inversion such that for these softer rocks, the host material deforms faster than the original linear-elastic contact asperities. Practically, the applied pressure range of 0-100 MPa is indeed too large for deformation to be approximated as infinitesimal strain (i.e. linear elastic) in these rocks. As a result, the extended compliant-host rock model works universally well for all rocks under this pressure range. This is supported by the evidence that while the rigid-host solution returns larger and larger RMS error when fitting to data of progressively increasing pressure inputs, the residuals from the compliant-host inversion remains random and below the measurement error. Because the noise effect is minimal as the quality of the data is very good, this evidence supports my original postulation that the rigid-host assumptions become more and more invalid as the applied pressure increases, while the compliant-host assumptions remain valid.

Another fact that points towards this model extension is the application to fluid substitution. Gangi and Carlson (1996) provides the methods and formulae for the fluid inclusion using an approximation of the ADM contact area. These formulae use the compliant-host solution per se. Here my hypothesis is that although their formulae can give a close prediction of the fluid effects, their calculation of contact area is based solely on the elastic contact asperities without including the deformation of the host-rock material; therefore, either their predictions are not feasible for negative-valued compliant-host estimates, or such predictions are systematically off compared to measured data, in the case of positive estimates. My initial experiments with such fluid substitution supports this hypothesis.

1.4.4.2 List of contributions in chapter V

- View every rock as having a compliant host and power-law mechanisms of elastic contact asperities and host deformation.
- Extend ADM to cover for nonlinear deformation and pressure dependence of the host, interpret the seemingly unphysical compliant-host parameter estimates and improve data fitting compared to rigid-host, while statistically applicable to all rocks.
- Include fluid substitution (Gangi and Carlson, 1996) and interpretation using this extended model

1.4.4.3 Outline

- Nonlinear deformation and the pressure dependence of the host rock
- Model extension: derivation of equations and corresponding physical meanings
- Supporting evidence
- Fluid substitution (Gangi and Carlson, 1996) and interpretation using the extended model

1.4.5 Chapter VI - Conclusions and future work

This dissertation investigates two different ways to improve misfits and interpret laboratory data : (a) non-linear inversion using the analytic compliant-host solution with a power-law asperity-height distribution, and (b) a generalized inversion using the rigid-host model with an arbitrary asperity-height distribution. The compliant-host solution attempts to analytically solve the case when the modulus of the fracture is comparable to that of the host rock (i.e. the rock frame and the cracks have similar stiffness). The generalized inversion is a discrete, numerical method that allows for the discretization and perturbation of the distribution of asperity heights in order to find one that allows a good match of modeled and measured velocity. Compare to an existing method of pore-aspect ratio spectrum inversion, the ADM method is more suitable for ease of implementation as well as accuracy. Finally, I extend ADM to interpret nonlinear deformation and provide evidence to support the theory.

The link between the velocity inversion methods of pore-aspect ratio spectrum and asperity-height distribution can be better established via the relation to the contact area, which should be proportional to both porosity and the number of asperities in contact. Thus, any future work can expand on this idea to account for the pressure-induced increase in contact area and application to fluid substitution.

CHAPTER II

THEORETICAL STUDY OF THE ASPERITY-DEFORMATION MODEL AND ITS EXISTING ANALYTIC SOLUTIONS

2.1 Introduction

Quantifying the influence of pressure changes on elastic rock properties is important for optimal use of time-lapse seismic surveys in fractured-reservoir characterization, such as applications to carbon-dioxide (CO_2) sequestration. Specifically, a valid quantification model should relate changes in the reservoir effective pressure (and/or pore pressure) to changes in the seismic parameters, and it should be easily applicable to reservoir-scale simulation models for straightforward use in large seismic studies. Additionally, simulations of field-scale fluid flow and seismic-reflection data require a model that is computationally simple enough for fast and easy implementation in conjunction with reservoir simulation. Although models for seismic velocity variation with pressure are common for granular media such as sandstone formations, (e.g. Gardner and Harris, 1968; Eberhart-Phillips et al., 1989; Dvorkin and Nur, 1996; Endres and Knight, 1997; Han and Batzle, 2006), most recently developed models for the effective seismic properties of fractured media (ESPFM, popularly used in time-lapse seismic modeling and characterization of fractured reservoirs) do not include the influence of pressure (e.g. Pointer et al., 2000; Liu et al., 2000; Chapman, 2003). While many studies use the ellipsoidal crack model to relate between pressure and velocities through pore-aspect ratios (e.g. Cheng and Toksöz, 1979; Xu and White, 1995), the method requires the use of the Kuster and Toksöz (1974) model for elastic moduli, with a differential effective medium (DEM) (e.g. Norris, 1985; Mukerji et al., 1995) in addition to a "self-consistent" iterative implementation (e.g. Berryman, 1980), which is computationally expensive and difficult to implement on a field scale (e.g. Keys and Xu, 2002). Other solutions do attempt to include pressure effects by modeling the closure of fractures depending on their orientation with respect to stress fields (Zatsepin and Crampin, 1997; Crampin and Zatsepin, 1997; Angerer, 2002). However, all of these approaches tend to require the specification of many parameters that would be difficult, or even impossible, to constrain on the scale of a

complete reservoir formation.

Therefore, I investigate the utility of a simpler quantification model that allows a relatively straightforward calculation of the influence of pressure on seismic velocities of fractured rocks, developed by Gangi (1978; 1981). Because the primary effects of pressures and stresses involve the opening and closing of cracks, it is important to have a physical model that simulates these realistic effects, and/or describes the mechanical behaviors of natural fractures under the influence of external forces/stresses. Here the mechanics of fracture allows the user to select and/or develop the simplest but most accurate representation. Gangi (1978) described an useful model for this purpose. Noting that fractures in rocks have complex, irregular surfaces that are in contact at many asperities, this model reproduces such behavior by representing the fracture as two ideal planar surfaces, one of which has a set of cylindrical rods of variable height. Gangi (1978) pictured this as the "bed-of-nails" model. At any particular value of applied pressure, some of these "asperities" are in contact (with the fracture faces) and supporting the fracture; but as pressure increases, more asperities (rods) come into contact and deform, increasing the stiffness of the fracture. Thus the model is also known as the "asperity-deformation model", or ADM (Gangi, 1978; Carlson and Gangi, 1985). The deformation is assumed to be linearly elastic, i.e. following Hooke's law, so the rods are spring-like. Furthermore, the original (pre-pressure) length of the asperities is assumed to follow a certain distribution. Depending on this distribution, the number of asperities that come into contact, deform and change their lengths accumulates as pressure is applied to the system. Elastic rock properties are related to effective pressure through the change in length of the asperities in contact as pressure changes. This in turn allows an estimate of how seismic velocity changes with increasing (and/or decreasing) pressure. A set of analytic solutions has previously been derived for the "bed-of-nails" model: one for a "rigid-host" rock and one for the "compliant-host" case (Gangi, 1981; Carlson and Gangi, 1985). Because both solutions assume that the distribution of asperity lengths (or heights) is a simple power-law, I will use the term "power-law solutions" to refer to these existing solutions.

2.2 The asperity-deformation model

Gangi (1978) first described and used the "bed-of-nails" model (BNM) to model the

effect of confining pressure on the permeability of rocks. Later on, it has been called the "asperity-deformation model" (ADM) (Gangi and Carlson, 1996) after the main physical phenomenon that the model describes. In this dissertation, I will use these two names interchangeably to refer to this physical model.

2.2.1 Modeling pressure in terms of deformation - The concept of elastic asperities in contact and deformation

Figure 2.1 shows the "bed-of-nails" representation of a natural fracture. A natural fracture is characterized by two ideal planar surfaces which are separated by a number of asperities of maximum height L at zero pressure. Other asperities of height $h < L$, or "shortness" $s = L - h > 0$, are distributed on one of the fracture surfaces. Consequently, L is also the maximum aperture of the fracture, and h and s range from 0 to L. When a pressure P is applied, the two fracture faces move towards each other a distance x and deforming (linear elastically) the asperities already in contact while bringing the longer ones into contact during the process. The net effect is that the fracture faces are now supported by asperities currently of height $h = L - x$ (i.e. of shortness $s = x$) but originally taller than or equal $L - x$ (i.e. having shortness less than or equal to x), and the number of asperities in contact (and deformed) $N(h)$ (or equivalently, $N(s) = N(L - h)$) has increased. This increases the overall stiffness of the rock and, therefore, seismic velocity. Here, the term "asperities in contact" refers specifically to those deformed asperities that are in contact with the fracture faces and supporting the fracture under the influence of a particular applied pressure.

2.2.1.1 Mathematical representation

The mechanical behavior of this model is described by an integral equation that relates the total pressure P acting on the fracture to the closure (or displacement) x by way of the distribution of asperity heights (or shortnesses) (Gangi, 1978):

$$P(x) = \frac{EbL}{A} \int_0^x (x - s) n(s) ds = \frac{k}{A} \int_0^x (x - s) dN(s). \tag{2.1}$$

where s is the shortness of the asperities in contact at pressure $P(x)$, which varies from 0 to x. All asperities are assumed to be made from the same material with Young's modulus E and have the same spring constant $k = EbL$, where b is an

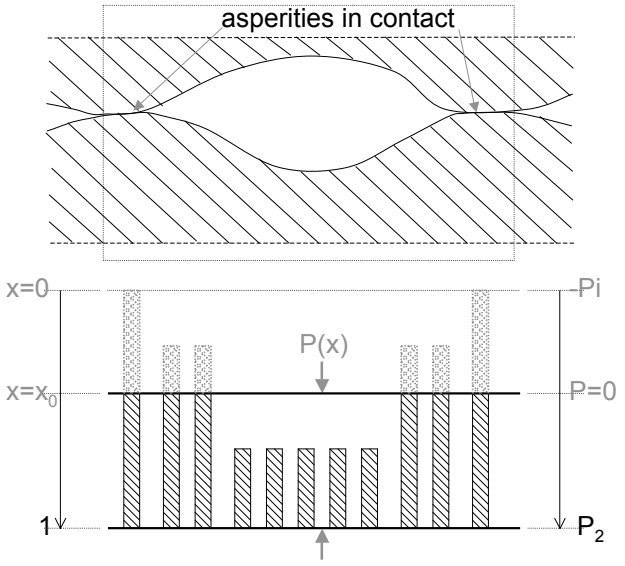

Fig. 2.1. The "bed-of-nails" representation of a natural crack

unitless constant, L is the maximum crack aperture at zero pressure (i.e. equal to the length of the tallest asperities), and A is the surface area of the crack, such as defined by Gangi (1978). Here $EbL/A = k/A$ is a proportionality constant describing the maximum possible force per volume (at which the system still maintains linear elasticity). In other words, this constant can be thought of as a volume-averaged measure, and is characteristic of the material that makes up the asperities. Note that since this material is assumed to be linear elastic or spring-like (i.e. following Hooke's law), there is only one universal spring constant k for all asperities, and it stays constant with pressure.

When there is no force acting on it (i.e. at $P = 0$), the fracture is characterized by a distribution of asperities whose heights (or shortnesses) vary between 0 and L. The function $n(s)$ describes the "number density" of asperities having shortness s and $N(s)$ describes the number of asperities having shortness less than or equal to s. In other words, $n(s)$ is the number of asperities having shortness between s and $s + ds$, while $N(s)$ is the number of asperities with shortness between 0 and s, which is also the number of asperities that will be in contact when the closure x is equal to s, i.e. under a pressure $P(x)$ (Gangi, 1978). Notice that both $N(s)$ and $n(s)$

are equivalently a representative picture of the internal microstructure of the rock because the distribution of asperities dictates the rock behaviors according to this model.

As a result of an applied pressure $P(x)$, all asperities with shortness s smaller or equal to x are now in contact, therefore s varies from 0 to x in equation (2.1). Note that although Gangi (1978) assumes for convenient purposes that all asperities have the same Young's modulus ($E_i = E$) and the cross-sectional area of each asperity a_i is proportional to its length l_i (i.e. $a_i/l_i = k/E = bL$) so as to have an universal spring constant k, it is possible to instead make the asperities have the same cross-sectional area ($a_i = a$) while having their Young's moduli E_i differ proportionally to their lengths. As a consequence, the number of asperities in contact $N(s)$ may also be considered to represent the area of contact in the direction perpendicular to the measurement direction (if each asperity is to have the same normalized cross-sectional area). In addition, $x - s$ is the deformed length of the asperity originally having shortness s and currently in contact due to pressure $P(x)$. Thus, the physical meaning of equation (2.1) is that pressure is proportional to the deformed volume (length times area) of asperities in contact (i.e. the change in volume). All natural physics occurring under the influence of pressure are attributed to the change in lengths of the asperities as they come into contact.

2.2.1.2 Normalization

Note that although x and s describe length quantities, they can be normalized by the maximum crack aperture L, such that $0 \leqslant x, s \leqslant 1$. Similarly, $n(s)$ and $N(s)$ can also be normalized by the "total number of asperities" N_T, such that $0 \leqslant N(s) \leqslant 1$. Both constants of normalization L and N_T can be combined with the proportionality constant EbL/A to create one single constant P_2 describing the maximum possible pressure (with respect to linear elasticity), such that

$$P_2 = \frac{EbL^2N_T}{A} = \frac{kLN_T}{A}. \tag{2.2}$$

The physical meaning of P_2 is that it characterizes the asperity material (through the spring constant) as well as the total number of asperities (N_T). The notation P_2 is conveniently invented to make distinct with the other pressure constants (e.g. P_0 and

P_1) defined by Gangi (1978). Equation (2.1) is then equivalent to:

$$P(x) = P_2 \int_0^x (x-s)n(s)ds = P_2 \int_0^x (x-s)dN(s) = P_2 \left[\int_0^x N(s)ds - xN(0) \right], \quad (2.3)$$

where x and s represent fractional lengths (with respect to the maximum aperture L), and $N(s)$ represents the fractional number of asperities in contact. The behavior of the system does not change after the normalization. So now instead of having x vary from 0 to L in equation (2.1), the variable x in equation (2.3) actually varies from 0 to 1 and becomes an elastic strain measure. $P(x)$ now becomes the pressure-versus-strain response curve, while the number of asperities is now a fractional number. Note that it is mathematically safe to assume $N(0) = 0$ because otherwise we can make the change in the coordinates system $N^*(x) = (N(x) - N(0))/(1 - N(0))$. This makes $N(s)$ equal the cumulative distribution function (CDF) of fractional shortness s ($0 \leqslant s \leqslant 1$), and thus $n(s)$ is the probability density function (PDF) of the same distribution: $dN(s) = n(s)ds$. Beside the advantageous facts that the concepts of PDF and CDF are widely used in statistics and probability theory and that stress-versus-strain analyses are an important and well-known part of rock and fracture mechanics, the goal of normalization is to produce the same constant P_2 as can be deduced from the original Gangi (1981) derivation, which will benefit the inversion results as will be demonstrated later.

2.2.1.3 Physical meanings

As a consequence of normalization, the integral in equation (2.3) represents the bulk strain (or volume strain) caused by an applied pressure P which is a function of the (elastic) strain x in the measurement direction. The physical meaning of equation (2.3) is that pressure is modeled as the combined effect (product) of the asperity material property and the deformed volume (i.e. the volume strain corresponding to the strain x caused by the deformation of the asperities in contact under the influence of pressure). The former is represented by P_2, the pressure required to make the material (that makes up the asperities) yield (i.e. deform plastically). The latter is represented by a sum (over the asperities in contact whose shortness s varies from 0 to x) of the product of the deformed length $x-s$ with the induced change in contact area $dN(s)$. Note that since the model assumes linear elastic deformation, P_2 is treated as a constant throughout the process of asperity deformation, while the deformed asperity

volume (i.e. volume strain) depends solely on the distribution of asperity shortnesses. As a result, the distribution of asperity shortnesses dictates the behaviors of the model as it controls the volume strain (which is always proportional to the applied pressure), while the material property is assumed constant as pressure changes. From equation (2.3), because $0 \leqslant x, s \leqslant 1$ and $N(s) \leqslant 1$, we have $P/P_2 = \int_0^x (x-s)dN(s) \leqslant 1$, indicating that ADM applies (i.e. the fracture behaves linear-elastically) to pressure values P not greater than P_2. An intuitive and logical corollary would be that for $P > P_2$, all asperities in the rock have been deformed, all fractures have been closed and the host takes up all the energy applied to the system. Thus P_2 should also be known as the (crack) closure pressure.

Another excellent point about this model that resembles nature is the mechanism in which the fracture operates under applied pressure. An applied pressure simultaneously increases the fracture stiffness and closes the aperture by deforming (elastically) the asperities in contact. These effects can be seen from equation (2.3) as it consequently models the fracture elastic modulus M, i.e. the ratio between infinitesimal stress over strain which is equal to the derivative of pressure P with respect to closure x, to be:

$$\frac{dP}{dx} = M(x) = P_2[N(x) - N(0)]. \tag{2.4}$$

Equation (2.4) relates the stiffness response of the "bed-of-nails" (i.e. the fracture) to an applied pressure P as proportional to the total increase in number of asperities in contact $N(x) - N(0)$. Since $N(s)$ is the number of asperities in contact, it is a monotonic non-decreasing function. Thus, the fracture stiffness will either increase or stay the same with pressure through the increasing strain x, depending on the function $N(s)$. This confirms the above remark that in the "bed-of-nails" model, the distribution of asperity shortnesses dictates the behaviors of the fracture.

2.2.2 Pre-pressure deformation

Taking $N(0) = 0$, the mathematical representation of ADM is

$$P(x) = P_2 \int_0^x N(s)ds \Rightarrow \begin{cases} M(x) = P_2 N(x) \\ x \geqslant 0 \end{cases} \tag{2.5}$$

At zero deformation $x = 0$, $P(0) = 0$ and $M(0) = 0$, meaning when there is no force or pressure acting on it, the fracture is actually two separate pieces with no contact or connection between them. Thus, it is important to understand the implication that the asperities may have already been in contact and deformed before pressure is applied in the recorded experiments. Corresponding to this model behavior may be physical phenomena such as cementation, grain interlocking, or even plastic damages of the micro-contacts among cracks if the rock has been previously cycled through pressure. This pre-pressure deformation $x_i \geqslant 0$ can be represented by an "initial" pre-pressure P_i as such:

$$P(x) = P_2 \left[\underbrace{\int_0^{x_i} N(s)ds}_{P_i \geqslant 0} + \int_{x_i}^{x} N(s)ds \right] \Rightarrow \begin{cases} M(x) = P_2 N(x) \\ x \geqslant x_i \geqslant 0 \end{cases} \tag{2.6}$$

The start of experimentally applied pressure is marked by the pre-pressure deformation x_i and therefore:

$$\begin{cases} P_{app}(x) = \int_{x_i}^{x} N(s)ds \\ P(x) = P_i + P_{app}(x) > 0 \\ M(x) \geqslant P_2 N(x_i) \geqslant 0. \end{cases} \tag{2.7}$$

Note that $M(x) = 0 \Leftrightarrow x = x_i = 0$ happens only if $P_i = 0$ or the pre-pressure is negligible. Thus, pre-pressure deformation is a very important property of ADM.

2.3 From fracture modeling to rock-physics modeling

Since the fracture faces are assumed to be infinitely rigid, this fracture model applies to a rock whose dry frame is much stiffer than its cracks/porous portion. For a rock whose fracture modulus is of the same order as that of the host (frame) rock, the iso-stress Reuss lower-bound average can be used to compute the rock's effective elastic modulus M_r as an average of the rock frame/matrix portion and the porous/cracks portion:

$$\frac{1}{M_r} = \frac{\phi}{M_{crack}} + \frac{1-\phi}{M_{matrix}} \tag{2.8}$$

where ϕ is the porosity of the rock, and M_{matrix} and M_{crack} are the total rigidities of the solid frame matrix and the cracks, respectively. This is similar to the approach by

Gangi (1981) to average between the cracks and the unfractured portion of the rock. For "low-porosity hard, crystalline rocks" such as those studied by Gangi (1981) and Carlson and Gangi (1985), the frame portion (i.e. the frame matrix effective modulus) $\frac{M_{matrix}}{1-\phi}$ is usually much stiffer than the cracks portion (i.e. the fracture effective modulus) $\frac{M_{crack}}{\phi}$, so its effect is indeed considerably negligible. Gangi (1981) takes advantage of this fact and makes several other assumptions to derive his rigid-host solution from the "bed-of-nails" model.

2.4 The rigid-host solution

The original derivation of this solution is described in details by Gangi (1981). Here I will summarize, discuss and interpret the key results and the underlying assumptions. The main and final equation that describes the relationship between velocity and effective pressure in a fracture with an infinitely rigid host rock is, for $P \leqslant 100$ MPa (Gangi, 1981),

$$V(P) = V_0 \left(1 + \frac{P}{P_i}\right)^{\frac{(1-m)}{2}}, \tag{2.9}$$

where $V(P)$ is the velocity at effective pressure P, and V_0 is the velocity at zero effective pressure ($P = 0$). The parameter P_i reflects the deformation of asperities at zero effective presssure (i.e. pre-stress deformation), as seen in equation (2.6). It accounts for the asperities already in contact (and deformed) when no experimental pressure is applied. The rock behaves as if it was under a pressure of P_i when in fact there is no applied pressure. Hence, P_i may represent the amount of cementation in the rock. The exponent m ($0< m \leqslant 1$) depends on and characterizes the power-law distribution of asperity shortnesses. Its value changes from rock to rock and with intensity of fracturing. In particular, the power-law asperity-shortness distribution is represented by either the probability density function (PDF) $n(s)$ or the cumulative distribution function (CDF) $N(s)$:

$$\begin{cases} n(s) = (m^{-1} - 1)s^{(m^{-1}-2)} \\ N(s) = \int_{z=0}^{s} n(z)dz = s^{(m^{-1}-1)} \end{cases} \tag{2.10}$$

where s is the normalized (fractional) asperity shortness, as in the description of the "bed-of-nails" model. Here, $n(s)$ and $N(s)$ have also been normalized by the

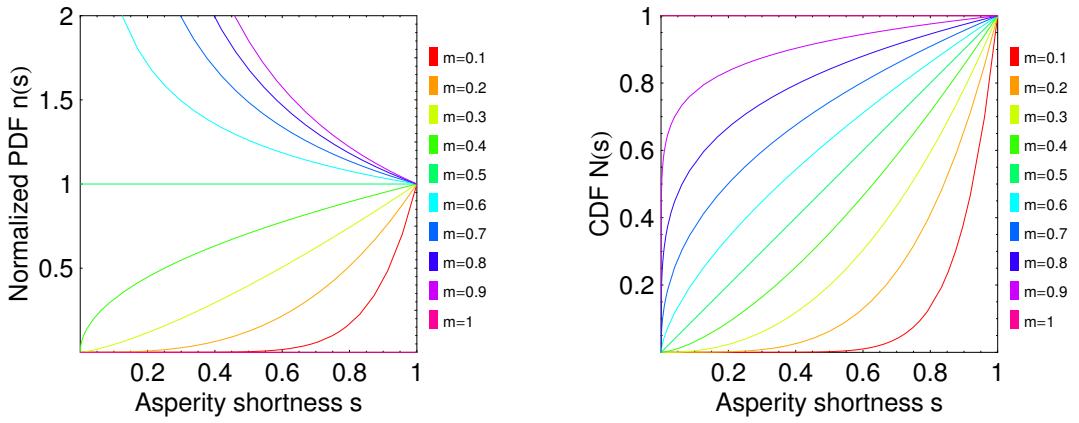

Fig. 2.2. The PDFs and CDFs of power-law distributions

total number of asperities N_T (see section 2.2.1.2). The parameter m characterizes the shape of the power law. The constraint $0< m \leqslant 1$ comes from the fact that $N(s)$ must be monotone non-decreasing. Figure 2.2 shows the power-law distribution functions $n(s)$ and $N(s)$ for different values of m. Recall that $n(s)$ and $N(s)$ are actually a representative picture of the microstructure of the rock being modeled, so the value of m varies from rock to rock.

Here, it is important to note the first assumption, explicit in the derivation of this solution. For the low-porosity, hard rocks in his study, Gangi (1981) assumes that the rock frame is much stiffer than the rock fractures, such that its effect on the whole rock is negligible. Indeed, if the effective host-rock elastic modulus is infinitely larger than that of the fractures $\frac{M_{matrix}}{1-\phi} \gg \frac{M_{crack}}{\phi}$, then the effective elastic modulus of the whole rock is in effect equal to that of the cracks portion of the rock, $Mr \approx Mcrack/\phi$. Thus, this solution can be descriptively referred to as the "rigid-host" solution. Note the presence of both porosity ϕ and the grain matrix modulus M_{matrix} in the assumption.

Another important assumption is that the distribution of asperity heights obeys a simple power law. Similar to the exponential function, the simple power law is a good statistical approximation to natural contact deformation (e.g. Dieterich and Kilgore, 1996; Schlueter et al., 1997). The inversion results using the existing power-law analytic ADM solutions in this research further supports this conclusion. Moreover,

the power-law is mathematically useful because it conveniently allows for a direct relation between pressure and velocity (as opposed to an indirect relation via a third parameter such as the deformation x), as demonstrated below.

Effective pressure P, elastic modulus M, and velocity V are related to (and controlled by) the power-law distribution of asperity shortnesses. We can re-derive equation (2.9) by substituting the above power-law $N(s)$ into the "bed-of-nails" (equation 2.7) as follow:

$$\begin{cases} P + P_i = mP_2 x^{m^{-1}} \Leftrightarrow x = [(P + P_i)/(mP_2)]^m \\ M_{crack} = dP/dx = P_2 x^{m^{-1}-1} \\ V = \sqrt{M_{crack}/(\rho\phi/3)} \\ P_i = mP_2 x_i^{m^{-1}} = P_1 x_i^{m^{-1}} \\ V_0 = V(P=0) = V(x=x_i) = \sqrt{(mP_2/P_i)^m P_i/(m\rho\phi/3)} \end{cases} \tag{2.11}$$

where x is the pressure-induced strain (i.e. the fractional displacement or closure), x_i is the initial pre-pressure deformation and $h = 1 - x$ is the (fractional) crack aperture. Here ρ is the density of the rock and $\phi/3$ is the linear porosity in the measured direction, which are both assumed to be constant for a rock of unit length. Note that as a result of the power-law assumption, V_0 is actually a function of m, P_i and P_2, and by comparing equations (2.11) to equation (22) from Carlson and Gangi (1985), $P_1 = mP_2$ is, just like P_2, a constant that accounts for the physical properties of the asperities (e.g. crack strength), which varies from rock to rock. Thus, P_1 is the closure pressure for the rock being modeled in the rigid-host power-law case, and $P_1 \approx M_{frame}$, the modulus of the rock frame (Gangi, 1978). The fracture closes completely when $x = 1$, or $P + P_i = P_1$. Again, the pre-pressure P_i is the shifted pressure corresponding to an initially deformed length x_i at $P = 0$ (note that P_i has a power-law relation to x_i).

To summarize, three assumptions underlie the Gangi (1981) rigid-host solution. Gangi (1981) assumes that the frame portion of the rock is always much more rigid than the cracks portion, and that the distribution of asperity shortnesses, which inherently dictates the behaviors of the "bed-of-nails" model, is a power law. His rigid-host solution also presumes a non-negative pre-pressure deformation of asperities which is an intrinsic property of ADM. As noted by Gangi (1981), the rigid-host

solution works well when the rock is considerably rigid over the applied pressure range, generally within 100 MPa. As an attempt to improve on the applicability of this solution (to a higher pressure range), Carlson and Gangi (1985) maintain the power-law assumption while allowing the rock frame to be accounted for, as an additional parameter, in their compliant-host solution to the "bed-of-nails" model.

As pressures in the first few kilometers in the crust of the earth (i.e., where the hydrocarbons are) are well within 100 MPa (Barton, 2006), this model solution satisfies normal reservoir conditions. In addition, because it directly relates velocity to effective pressure, straightforward use of the solution is feasible as measured data is usually available in the form of pressure versus velocity. Moreover, because of its simplicity as a mathematical equation and as a model with just a few parameters, this solution is absolutely convenient for inversion purposes and for use in reservoir simulation. Thus, I will later investigate its accuracy in terms of fitting laboratory data from a broad variety of rocks.

2.5 The compliant-host solution

The idea about a "bed-of-nails" solution to rocks whose frame compliance is non-negligible compared to that of the fractures has originally been mentioned (but not discussed) by Gangi (1981). The details and derivation of this solution is given in Carlson and Gangi (1985), and the key results are summarized and discussed below. The basic idea is that for a rock whose fracture modulus is not too much smaller than that of the host rock, the host is not significantly stiffer than the cracks and so its compliance is not negligible (e.g. see equation (2.8) for verification).

Generally, the solid matrix rigidity M_{matrix} should be much larger than the crack modulus M_{crack} for most rocks, but when normalized by the volume concentrations (see equation (2.8) and section 2.3) the effective rigidity of the frame portion may become more or less comparable to that of the cracks portion of the rock. Therefore, according to Carlson and Gangi (1985), for pressure values that are low enough ($\leqslant$ 500 MPa for the low-porosity igneous and metamorphic rocks in their study), small pressure changes do not significantly affect the modulus of the grain matrix, but will affect the modulus of the cracks. Thus the rate of change that an applied pressure P (in the order of less than 500 MPa) brings to the grain matrix is negligible, $\frac{\partial M_{matrix}}{\partial P} \approx 0$, so M_{matrix} can be treated as a constant as pressure changes. Here, Carlson and

Gangi (1985) essentially made the argument that the Gangi (1981) solution applies well only specifically to the cracks portion of the rock $\frac{M_{crack}}{\phi}$ but has not accounted for the frame portion (i.e. the host rock) $\frac{M_{matrix}}{1-\phi}$. So they attempted to account for it with an additional parameter $V_g = \sqrt{M_{matrix}/\rho}$, a constant with pressure, noting that velocity generally increases with pressure until it asymptotes a value equivalent to the velocity of seismic waves traveling in the rock frame material only. This velocity is theoretically equal to the velocity of the grain matrix. Conclusively, the compliant-host model assumes that applied experimental pressure only has an effect on the cracks portion of the rock (M_{crack} and ϕ), and not on the grain matrix of the host rock. It takes into account the compliance of the host rock, but not the dependence of it on pressure changes.

Specifically, Carlson and Gangi (1985) used the "bed-of-nails" model with a power-law distribution of asperity heights to relate pressure to velocity in a compliant-host rock, where the range of values for pressure is extended to $P \leqslant 500$ MPa:

$$\frac{1}{[V(P)]^2} = \left(\frac{1}{V_c^2} - \frac{1}{V_g^2}\right)\left(1 + \frac{P}{P_i}\right)^{(m-1)} + \frac{1}{V_g^2} \tag{2.12}$$

where m and P_i and $V_0 = 1/\sqrt{(1/V_c^2 - 1/V_g^2)}$ are precisely those parameters from the Gangi (1981) rigid-host solution, while V_g is the velocity "in the mineral grains", or the "solid rock" host material, and V_c is the velocity of the cracks portion of the rock. The term $G^2 = 1/V_g^2$ represents the rigid host which does not comply to pressure, while the term $C^2 = 1/\left[V_0^2\left(1 + \frac{P}{P_i}\right)^{(1-m)}\right]$ is the pressure-induced velocity which represents the pressure-compliant portion. Notice that at very high pressure the rock velocity $V(P)$ approaches the velocity of the grains V_g as it describes a rock having no cracks or porosity.

This solution attempts to account for the rock frame which is not always much stiffer than the cracks portion as assumed in the Gangi (1981) rigid-host solution. Nevertheless, it still uses the original "bed-of-nails" and all relations and equations from the rigid-host solution, while both porosity reduction and the pressure dependence of the host-rock (grains) modulus are considered negligible. Note that this solution can be thought of as an average between the rigid term G and the compliant term C, assuming the density, porosity and the rigid term stay constant, while the compliant term changes under the influence of pressure exactly like in the rigid-host

case:

$$\begin{cases} 1/[V(P)]^2 = 1/[V_{cg}(P)]^2 + 1/V_g^2 \\ V_{cg}(P) = V_0 \left(1 + \frac{P}{P_i}\right)^{(1-m)/2} \\ V_0^2 = 1/\left(1/V_c^2 - 1/V_g^2\right) = (mP_2/P_i)^m P_i/(m\rho\phi/3) \end{cases} \tag{2.13}$$

It can thus be stated that the Carlson and Gangi (1985) solution is an extended version of the Gangi (1981) solution. The same physical "bed-of-nails" model is used with a power-law aspeirty-height distribution assumption. From the mathematical point of view, the same parameters (with the same physical meanings) are used (m, V_0, and P_i), whereas one more (V_g) is added to account for a new physic (i.e. the host-rock compliance) which should make the solution applicable to a larger variety of rocks. Therefore, it is expected to enhance accuracy in fitting laboratory data. However, this solution still neglects the pressure dependence of the host-rock compliance, and hence the pressure dependence of the host-rock velocity. This was mentioned by Carlson and Gangi (1985), and can be verified by equation (2.12) as V_g is treated as a constant with respect to pressure changes. Carlson and Gangi (1985) also discussed that this effect can be included in the asperity-height distribution. However, they used the same power-law for the asperity-height distribution in their derivation of the compliant-host solution (as in the rigid-host solution). For the hard, crystalline rocks in their study, the inversion results are not greatly affected since host-rock velocity variation with pressure in such rocks had indeed been proven to be very small for low pressures (Carlson and Gangi, 1985). Yet when the inversion is applied to a broader data set including softer rocks such as clastics and carbonates, this effect (i.e. pressure-compliant grain matrix) may become large enough that can cause the parameter estimates to be largely uninterpretable (i.e. values out of range). In fact, as the inversion results will show later, the values of the parameter m are negative for many rocks in the Coyner (1984) data set, as well as the high-porosity sandstones in King (1966), which violates the constraint $0 < m \leqslant 1$ set to guarantee the non-decreasing behavior of the asperity distribution function $N(s)$.

2.6 Summary

Therefore, there could be a room for improvement in the compliant-host solution that is the host-rock material, albeit being accounted for (by the grains velocity parameter

V_g), is assumed to be independent of pressure changes. Taking this into consideration, I will later postulate that the host does comply to pressure in most rocks, and that this effect can be large enough to cause false interpretation of parameter estimates when this solution is used to fit with data from many experimental rocks. As a result, I will attempt to extend the model in order to account for this effect (i.e. host-rock pressure compliance), by allowing the asperity spring constant to decrease with pressure or with the induced deformation. Note that both power-law solutions assumes a negligible reduction of porosity and density with pressure.

CHAPTER III

EFFECTS OF PRESSURE ON SEISMIC VELOCITIES OF FRACTURED ROCKS - APPLICATIONS OF EXISTING POWER-LAW ASPERITY-DEFORMATION MODEL SOLUTIONS IN NONLINEAR INVERSION OF LABORATORY DATA

3.1 Introduction

It is well understood that crustal rocks are greatly fractured due to various causes such as stress and strain from geological events, e.g. compression and extension, folding and compaction, uplifts and earthquakes, etc... Fracturing occurs on all scales and intensity, from micro cracks to normal rock joints to large-scale faults. Natural rock fractures have been studied extensively in the past, for they have been known to influence the overall physical, mechanical, and transport properties of the rock, such as normal and shear stiffnesses (i.e. elastic moduli) (e.g. Goodman, 1976; Brown and Scholz, 1986; Liu et al., 1996) or permeability and fluid flow (e.g. Gangi, 1978; Brown and Bruhn, 1998; Walsh et al., 1997). For this reason, many authors have attempted to characterize and model natural fractures (e.g. Brown, 1995; Xia et al., 2003; Jiang et al., 2006). Basically, natural rock fractures are composed of surfaces that are neither planar or smooth, but are rough, mismatched and in contact at discrete locations (Brown, 1987). Brown and Scholz (1985) described this irregular geometry of the fracture surfaces, generally known as "surface roughness", as "a collection of peaks, summits and valleys," and showed that in general two rough elastic surfaces in contact are equivalent to a surface with a "composite topography" being the sum of heights of both surfaces along the fracture plane.

In addition, it is well established that micro and macro fractures are statistically similar in behaviors and rock-property influences, thus a single fracture/crack can represent the whole rock as long as the statistical distribution of fractures is known (or else, assumed). This has before led to the idea of an effective-media theory (e.g. Liu et al., 1996; Walsh et al., 1997) to describe the overall effective properties of fractured rocks, which has been commonly used in time-lapse studies. Inarguably, the statistical distribution of surface heights (also referred to as surface roughness,

rough walls, composite tomography, aperture, asperities or asperity heights, etc...) determines fracture and rock properties. Greenwood and Williamson (1966) first developed the contact theory for two rough elastic surfaces and showed that the normal distribution is a good approximation in many cases. Since then, numerous efforts have been made to characterize realizations of the distribution of asperity heights. While it can be characterized by the mathematical concept of fractals for rock joints (e.g. Brown, 1995; Jiang et al., 2006), a common practice is to assume one of the three probability density functions for the asperity-height distribution: exponential, Gaussian, or power-law (e.g. Greenwood and Tripp, 1967; Gangi, 1978; Swan, 1981). Walsh et al. (1997) noted that "roughness profiles of all surfaces can be expressed with sufficient accuracy as power-law spectral density function," while experiments with rock thin sections and images from the scanning electron microscope (SEM) have also indicated a power law for the contact area and the distribution of asperity heights (e.g. Hadley, 1976; Schlueter et al., 1997; Zamora-Castro et al., 2008). Gangi (1978) first used a "bed-of-nails" together with a power-law density function to model the roughness in rock fractures.

The "bed-of-nails" model (Gangi, 1978) is a simple and accurate representation of the mechanism in which rock fractures behave under effective pressure influence. It views natural fractures as rough surfaces that are in contact at many asperities, and represents that by a "bed of nails" with variable heights, sandwiched by two rigid fracture faces (Gangi, 1978). At any particular value of effective pressure, some of these "asperities" are deformed and in contact (with the fracture faces), supporting the fracture; but as pressure increases, more asperities (rods) come into contact and deform, increasing the stiffness of the fracture. Thus the model is also known as the "asperity-deformation model", or ADM (Gangi, 1978; Carlson and Gangi, 1985). The deformation is assumed to be linearly elastic, i.e. following Hooke's law, so the rods are spring-like. Furthermore, the original (i.e. pre-pressure) "asperity shortness" (the difference between the maximum length and the length of each rod at zero pressure) is assumed to follow a certain distribution. Depending on this distribution, the number of asperities that come into contact, deform and change their lengths accumulates as pressure is applied to the system. Elastic rock properties are related to the effective pressure through the change in length of the asperities in contact as pressure changes. This in turn allows an estimate of how seismic velocity changes with increasing (and/or decreasing) effective pressure. Existing analytic results from

the "bed-of-nails" model include the Gangi (1981) rigid-host rock and the Carlson and Gangi (1985) compliant-host case. Both solutions assume mathematically that the distribution of asperity heights (or shortnesses) is a power-law.

The above pioneer studies have also demonstrated that the power-law set of solutions can reproduce velocity data quite well, though they have in general been tested with data from a few low-porosity, hard, crystalline sample rocks (Gangi, 1981; Carlson and Gangi, 1985). Following these studies, Genova (2008) performs stochastic modeling and rigid-host inversion using a linearized method (Parrish and Gangi, 1981) on velocity and permeability data of a Wilcox shale (Kwon et al., 2001) and several other rocks previously examined by Gangi (1978), Carlson and Gangi (1985), and Gangi and Carlson (1996). His study mainly focuses on modeling the effect of random noise and of the zero-pressure measurement on the uncertainty and sensitivity of parameter estimates from the rigid-host equation. He also experiments with the extrapolation of synthetic data to check the accuracy of velocity prediction, assuming that there is no modeling error (i.e. all errors come from random noise artificially introduced into data).

In my research, I contribute to the practice of ADM by carrying a complete study of systematic nonlinear inversion results applying both rigid- and compliant-host power-law solutions to the compressional and shear wave velocities (V_p and V_s) of a broad total of twenty low- and high-porosity rocks of different types (sandstones, carbonates, and granites). The results indicate that while the rigid-host solution fits reasonably well with the data from several rocks, systematic misfits exists in other rocks comparatively larger than the measurement error. In contrast, the compliant-host solution returns negligible and random errors in all rocks, for both V_p and V_s, but with uninterpretably out-of-range parameter estimates. Thus, although ADM-based solutions can be applied to all rocks, modifications are in order to improve the rigid-host fit and interpret the seemingly unphysical estimates of compliant-host parameters. The conclusions drawn from this study act as a guide to help find the direction in the next phases of the research.

3.2 Data

Applying ADM solutions to sandstone data has not been done in the literature. For granular media like sandstones, at first it may not make sense to apply ADM, because

they are generally softer, much more porous, and the microstructure is very different from that of the low-porosity, hard, crystalline rocks (which have previously been proved applicable). However, the behavior of the rock is still controlled by a set of grain-to-grain contacts that play the same role as the asperities, suggesting the model will be useful. Nevertheless, it would be difficult to classify sandstones as having a rigid frame and being a linear-elastic material, because they are generally softer than crystalline rocks, while their high porosity affects total deformation (i.e. more undeformed asperities). In reality among sandstones, the stiffness and porosity vary greatly, and so does the pore geometry, as well as grain size, shape, sorting, and cementation. These factors influence the classification of sandstones using the "bed-of-nails" model parameters, making the results more widespread and uncertain. Nevertheless, the flexibility in the model specification of the asperities (see chapter II) may be able to account for some (if not all) of the differences among different types of sandstones, allowing ADM to still be valid and applicable. This remark can be verified by fitting ADM solutions to observed data for sandstones.

In this chapter, I use both existing power-law solutions to perform non-linear inversion for large sets of compressional- and shear-wave velocity data from a total of twenty igneous, carbonate and clastic rocks. These data sets are published laboratory measurements of sonic velocities versus pressure from separate, independent studies (Coyner, 1984; King, 1966; Nur and Simmons, 1969). The King (1966) data set contains all high-porosity sandstones, while the Nur and Simmons (1969) data set has low-porosity granites and low- and medium-porosity carbonates. The measurements from these two data sets are slightly scattered and of slightly lower quality (e.g. King (1966) reported a precision of about $\pm 0.3\%$ for velocities) than compared to the Coyner (1984) data set ($\pm 0.2\%$). The Coyner (1984) data set is particularly valuable because it contains dense, high-quality measurements on a broad variety of rock types of various porosity (including four sandstones, two carbonates and three igneous rocks), and because it has not been widely used in previous investigations of this type. From this data set, I use only the measurements made for dry rocks, with the purpose of isolating the effect of pressure (from the combined effect with the fluids). The measurements are made at constant zero pore pressure and increasing confining pressure up to 100 MPa. Most of the experimental rocks are well-known, and their porosity ranges from very low (0.5-1% in granites) to low, medium and quite high (0.5-10% in carbonates and 12-22% in sandstones). Another important

point is that this particular data set is of very high quality. Coyner (1984) reported in his PhD dissertation that extreme care was taken to make sure the measurements are performed properly and precisely, and that measurement error is approximately within ±0.2% which translate to about ±0.01km/s or ±10 m/s (using an average velocity of 5 km/s) to ±0.015 km/s or ±15 m/s (using a maximum velocity of 7.5 km/s) for velocities. Data of this quality is extremely valuable, because all random errors are very small and the goodness of the fit will justify the accuracy of the fitting model.

Effective pressure is modeled such as by Gangi and Carlson (1996) and many other workers as a function of confining and pore pressures: $P_e(P_c, P_p) = P_c - nP_p$, where $n = n(P_c, P_p)$ is a factor whose functional form can depend on the precision of the measurement. This is a good reason for taking $n \approx 1$, at least for the high-quality Coyner (1984) dataset. It has also been commonly accepted that $n \approx 1$ for unconsolidated, high-porosity sandstones (such as those in the King (1966) data set). Here, velocity measurements of dry rocks are made at zero pore pressure, therefore the applied confining pressure is also the effective pressure. Anisotropy is assumed to be negligible, since the stress applied to the samples is uniform in all directions and will not result in crack alignment.

3.3 Methods

Gangi (1978; 1981) and Carlson and Gangi (1985) theoretically showed that the "bed-of-nails" model (BNM) is applicable to both fractured and unfractured rocks because the asperities account for the physical change in the solid component of the rock only, while the pores and/or cracks make up the void portion (i.e. porosity) which is assumed unchanged. Note that the BNM assumptions include constant porosity, rigid host rock, linear elastic deformation, power-law contact regime, and pre-pressure deformation (i.e. cementation). To certain extents, these are reasonably valid and good approximations to natural rock behaviors under pressure, thus the power-law solutions are arguably applicable to all rocks, although the goodness of fit should differ for a certain rock or rock type, depending on how close the rock is to these assumptions. For instance, the stiff carbonates may be more suitable as having a rigid host than compared to sandstones, while the low-porosity, hard, crystalline rocks may exhibit more linear-elastic behavior than compared to sandstones, or the

consolidated sandstones are better cemented than the unconsolidated ones, etc...

In other words, although the model assumptions should not statistically limit the application of ADM, they may affect the ability of its solutions to fit and interpret observed data. Thus, a broad examination of fitting ADM solutions to laboratory-measured data will allow us to verify this important remark and make statistical conclusions about the applicability of ADM. For example, Gangi (1978) showed that the Hertz-Mindlin "packing of spheres" model for sandstones induces a value of $m \approx 0.67$ for the power-law asperity-height distribution in the rigid-host solution. His study also suggested that the physical meaning of the parameter P_i (i.e. the "initial" pre-pressure) is to account for the degree of cementation in the experimental rock. Thus, it would make sense to apply the power-law rigid- and compliant-host solutions to consolidated and unconsolidated sandstones to see whether the parameter estimates agree with such theoretical conclusions which have previously been tested with a restricted number of crystalline rocks.

Because the power-law ADM solutions (equations (2.9) and (2.12)) are relatively simple formulae, conventional non-linear inversion methods provide straightforward estimates of parameter values. Here, I first obtain the data by discretizing the graphs and tables from the above data sets. I then use the built-in functions NonlinearRegress and NMinimize from the software package Mathematica to find the solution curves that best fit the velocity versus pressure data in the least-square sense. I ensure the stability of the inversion results by trying different techniques for finding the global minimum, including Levenberg-Marquardt, Simulated Annealing, Differential Evolution, Nelder-Mead, and Random Search, which are built in as options to the above functions, until the results from these different algorithms converge to the same value. The reason for this is because depending on the search algorithm, the initial guess might cause the engine to search on values that would return a complex value somewhere in the process, or having too big / too small a step size, etc..., that would return a false value (e.g. a local minimum) before it actually converges to the global minimum. My test results have shown that no single initial guess works universally on all methods and for all data. That also justifies the use of the different methods to verify and see if they agree on the final inversion result. The initial guesses that work for each inversion method are found through trial and error. A slight note here that I have also tried least-squared inversion in the natural logarithm domain. The results differ slightly when compared to conventional non-linear inversion.

For both applications of forward modeling and inversion, the objective function is defined as the root-mean-square (RMS) of the differences between the modeled velocity and the velocity measurement at each applied pressure. For example, the rigid-host objective function is a function of the three independent parameters m, P_2 and P_i as follow:

$$f(m, P_2, P_i) = \left\{ \frac{1}{n} \sum_{j=1}^{n} \left[V_{mod}(P_j, m, P_2, P_i) - V_{dat}(P_j) \right]^2 \right\}^{1/2} . \tag{3.1}$$

For nonlinear inversion problems such as this one, although the inversion algorithm will perform a search over a range of values for all parameters and return a best-fit set of parameter estimates that minimizes the value of the objective function, a non-uniqueness is always associated with the results due to the presence of noise (coherent and incoherent) in the data. Therefore, the inversion result is always a region from which although we cannot locate exactly which point corresponds to the "correct" parameter or set of parameters, we know that statistically there is a large chance the "correct" point is somewhere within that region. In statistics, this is termed the confidence region. Thus, my inversion results are statistically shown in the form of a 95% (ellipsoidal) confidence region around the best-fit parameter set, meaning there is a 95% chance of having the correct set of parameters fall within the specified region. The confidence region indicates the uncertainties of the inverted parameters; a larger confidence region means larger uncertainties for parameter estimates and vice versa, while a smaller confidence region implies less noise effects, assuming no modeling error.

In all studied cases, the objective function is a well-behaved function with a well-defined global minimum so the problem is only with constraining the search range of the parameters. Here let us consider the rigid-host solution for an example, and address the issue of having a negative (out of range) estimate value for P_i and what it physically means in terms of constrained inversion. For rigid-host inversion, it is not necessary to constrain values of m and P_2 (i.e. results with and without constraints are the same) because the rigid-host objective function changes significantly for values out of range. However, that is not the case with P_i. A close and detailed investigation with synthetic and laboratory data reveals that while the forward rigid-host model is insensitive to values of P_i near the minimum, the inverted estimate for P_i is sensitive to the data measurements at low pressure. Thus, although the physical meaning of

P_i constrains it to be non-negative (see chapter II), the noise-induced uncertainty associated with the data might cause the estimate to be negative. In real life, this is especially feasible at the low-pressure measurements, because the signal-to-noise ratio for these measurements are usually low. However, taking into account that there is always a non-uniqueness associated with the inverted solution, and that objective function is well-behaved in most cases, it is usually possible to constrain the value of P_i to be non-negative (or effectively and equivalently, V_0 no less than some value V_c, which will automatically apply the constraint $P_i \geqslant 0$ according to equation (2.11) - i.e., if $P_i < 0$ then V_0 is a complex value). Doing that however will cause the inversion to return either the global minimum or an estimate exactly equal to the constrained value (i.e. $P_i \to 0$, or $V_0 \to V_c$) due to the monotonic behavior of the objective function away from the minimum. In the former case it makes no difference whether to use a constraint, while in the latter case, the outcome estimate of P_i is certain and predictable and the RMS of the fit residuals will increase although not by much because of the model insensitivity to values of P_i. Therefore, although it is possible to eliminate the noise effect on P_i by putting constraints on its estimate value, it is unnecessary to do so for the inversions.

As an illustration, I show in figure 3.1 example fits of the Berea sandstone from the Coyner (1984) data set with and without a constraint on the search values of P_i. On the left panel, P_i is left to vary freely over the real axis, while on the right panel, P_i is constrained to be non-negative. The rigid-host inversion returns an estimate of $P_i \approx -2$ (i.e., $V_0 \approx 2.8+0.8i$ is a complex value) for the first case, and $P_i \approx 0$ ($V_0 \approx 0$) for the second case. Recall that we invert for the parameter P_i and the code returns a real value; however, the corresponding value of V_0 can be complex by equation (2.11). The RMS error increases from 0.021 to 0.084 which slightly worsens the fit, but the fit residuals remain following a similar systematic pattern. Moreover, rigid-host inversion returns a larger confidence region for m, from $(0.823, 0.838)$ to $(0.758, 0.830)$, and for P_2, from $(3817, 4149)$ to $(3871, 5615)$, respectively for model without (shown on the left panel) and with (shown on the right panel) the non-negative P_i constraint. Estimates for m and P_2 also change as a result. Indeed a negative value for P_i or equivalently, a complex value for V_0 is physically unmeaningful. Hence, it is only possible to identify a "correct" value if we have more measurements near zero pressure. In fact, it is noticeable that many rocks lacking the measurement near zero pressure have a negative P_i inversion estimate (e.g. the King (1966) sandstones and a few

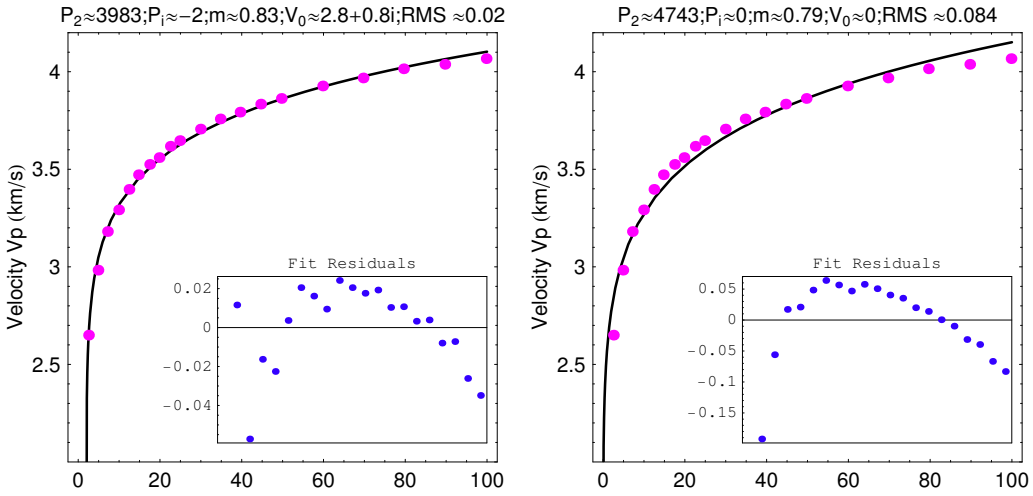

Fig. 3.1. Examples of rigid-host inversion for Berea sandstone (Coyner, 1984) with (left) and without (right) the constraint $P_i \geqslant 0$ on the search values of P_i.

Coyner (1984) rocks). A previous study by Genova (2008) concludes that the reason for the uncertainty of P_i is because of the lack of measurements near zero effective pressure. My inversion results not only agree with such conclusion, but also show that the lack of measurements near zero pressure can lead to an unphysical estimate of $P_i < 0$.

3.4 Results and discussion

Figures 3.2 to 3.22 show my inversion results for all experimental rocks from the aforementioned data sets. The measurement data points are ploted as dots, while the best fit analytic solution is plotted as a solid curve (the rigid-host in black and the compliant-host in green). The panel onsets show associated fit residuals (blue dots) which also gives a sense of the RMS error of the fit.

3.4.1 Inversion results using the power-law rigid-host solution

Figures 3.2 to 3.11 show the rigid-host best fits with confidence regions (plotted as ellipses and errorbars) and RMS errors for the V_p and V_s of all twenty rocks.

Figures 3.10 and 3.11 summarize the rigid-host parameter estimates and their confidence regions (as ellipsoids and error bars) in these rocks. These figures plot

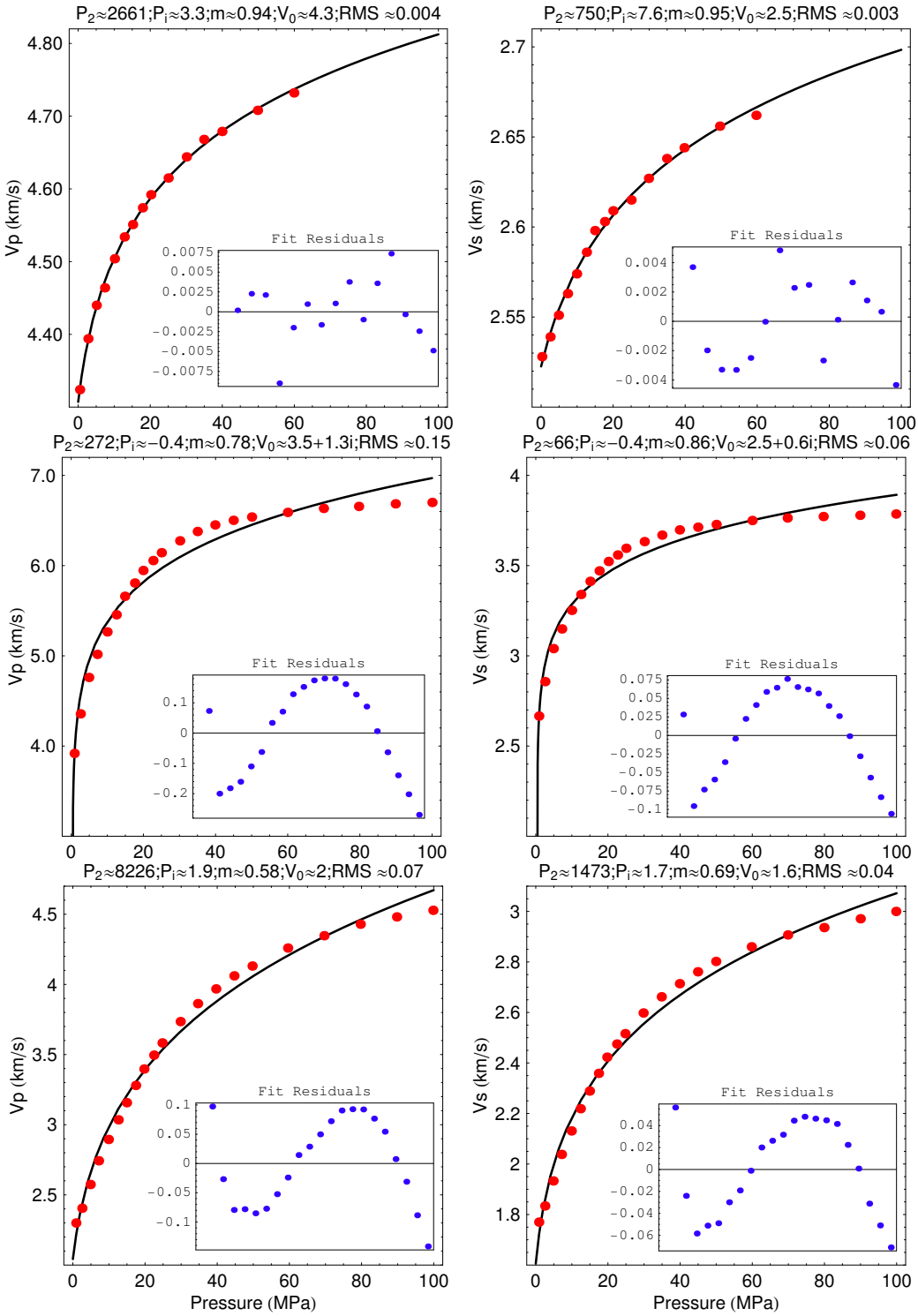

Fig. 3.2. Rigid-host fitting curve and residuals for Bedford limestone (top), Webatuck dolomite (middle) and Weber sandstone (bottom) from the Coyner (1984) data set.

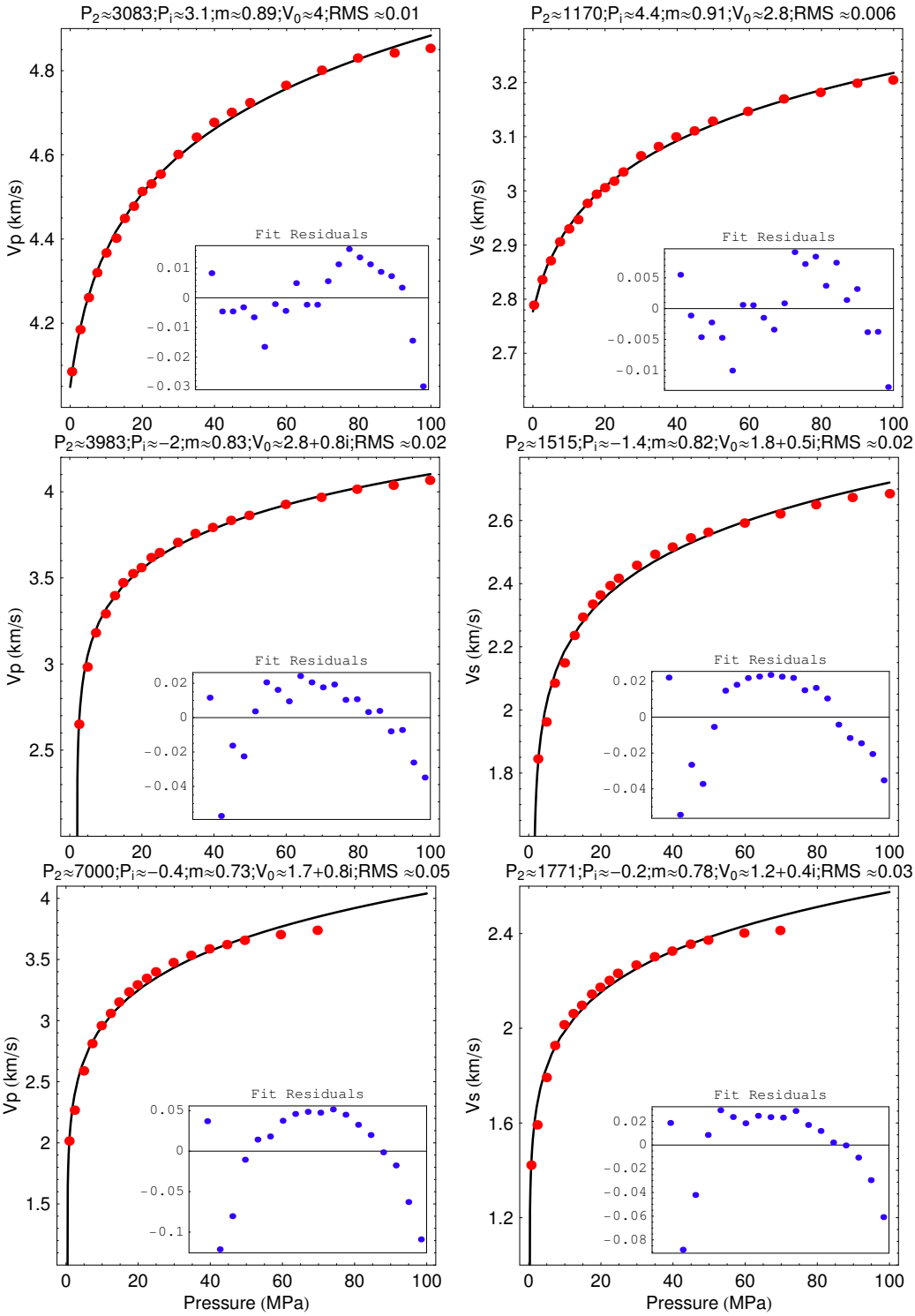

Fig. 3.3. Rigid-host fitting curve and residuals for Navajo (top), Berea (middle) and Kayenta (bottom) sandstones from the Coyner (1984) data set.

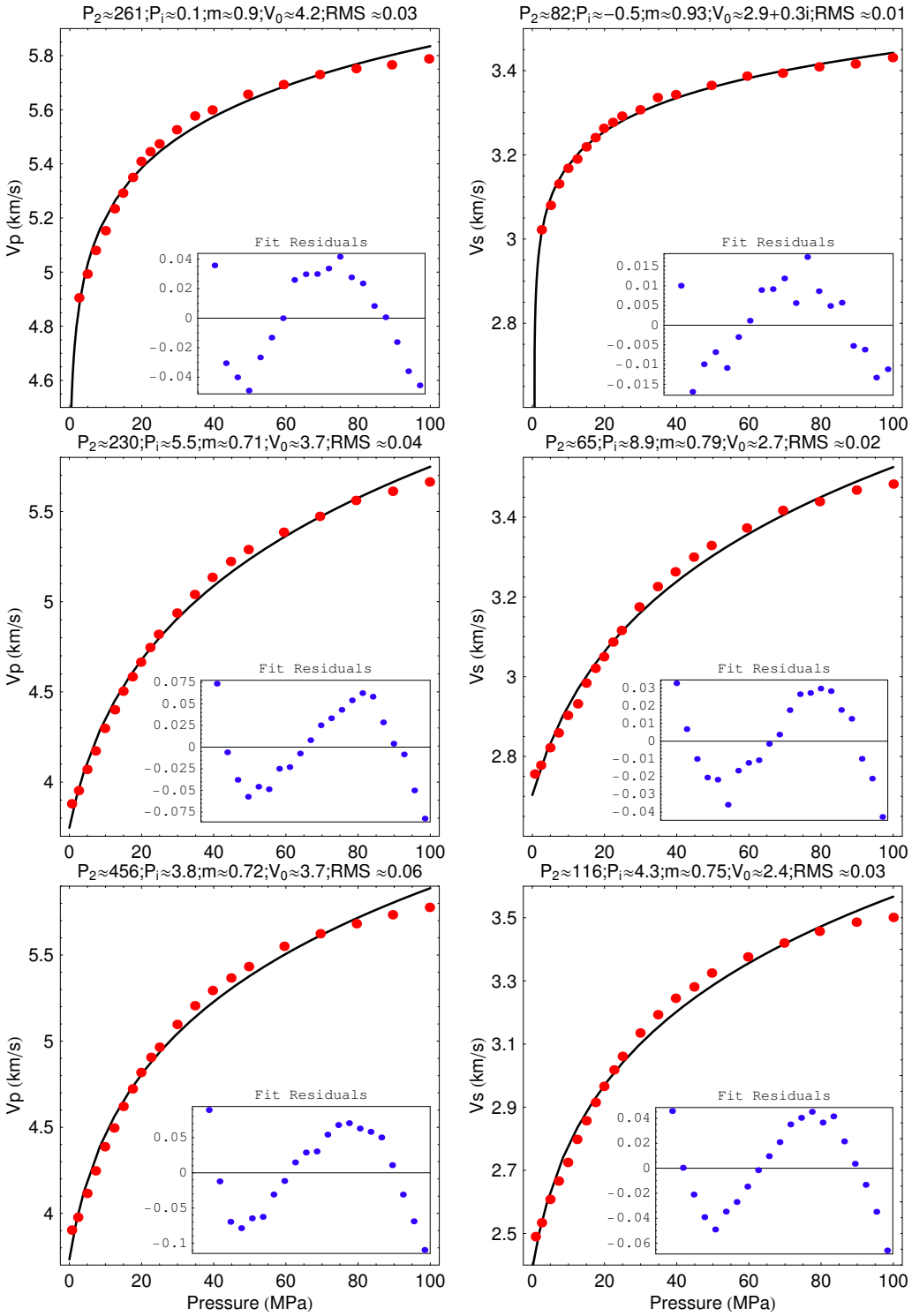

Fig. 3.4. Rigid-host fitting curve and residuals for Westerly (top), Barre (middle) and Chelmsford (bottom) granites from the Coyner (1984) data set.

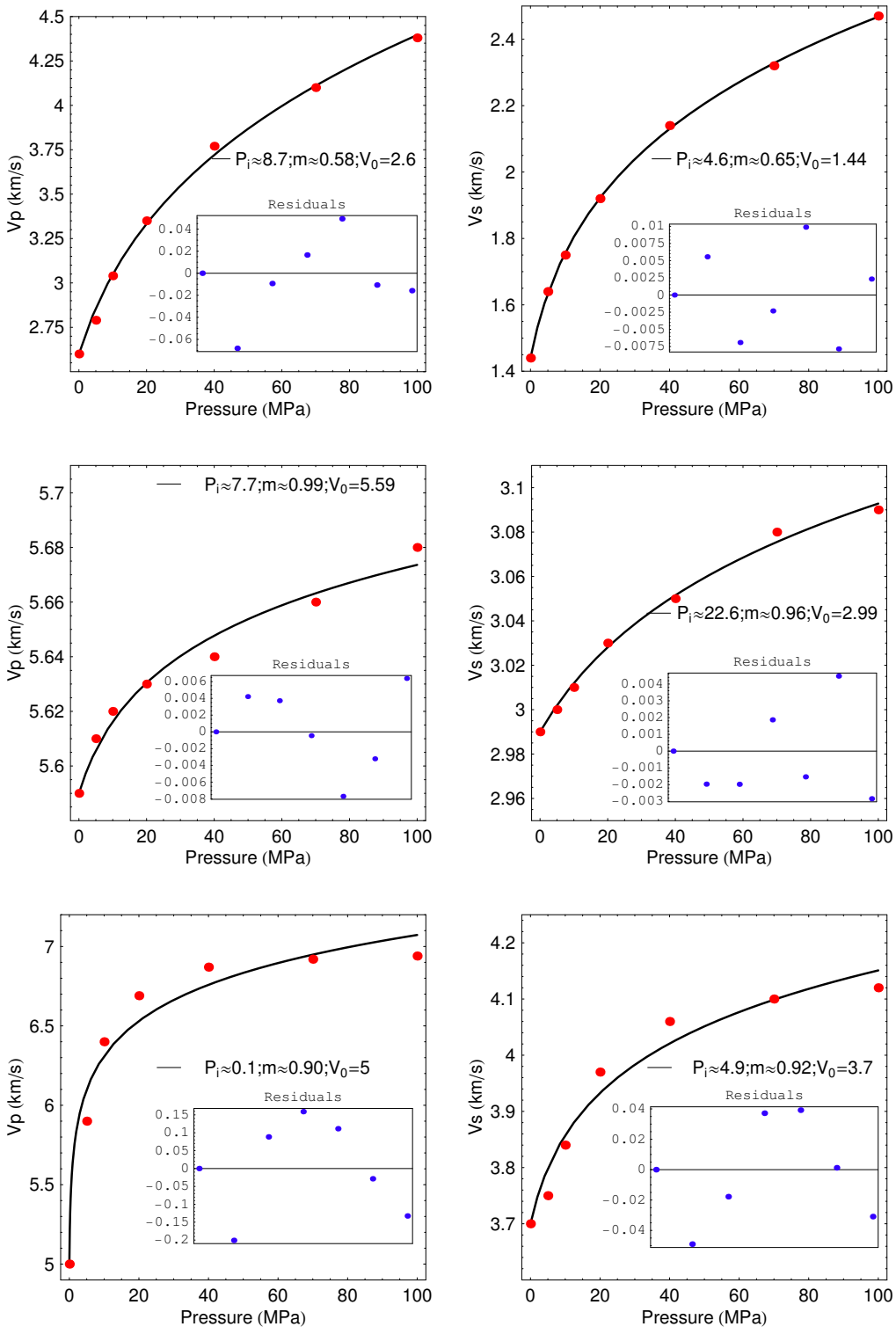

Fig. 3.5. Rigid-host fitting curve and residuals for Bedford (top), Solenhofen (middle) limestones and Webatuck dolomite (bottom) from Nur and Simmons (1969).

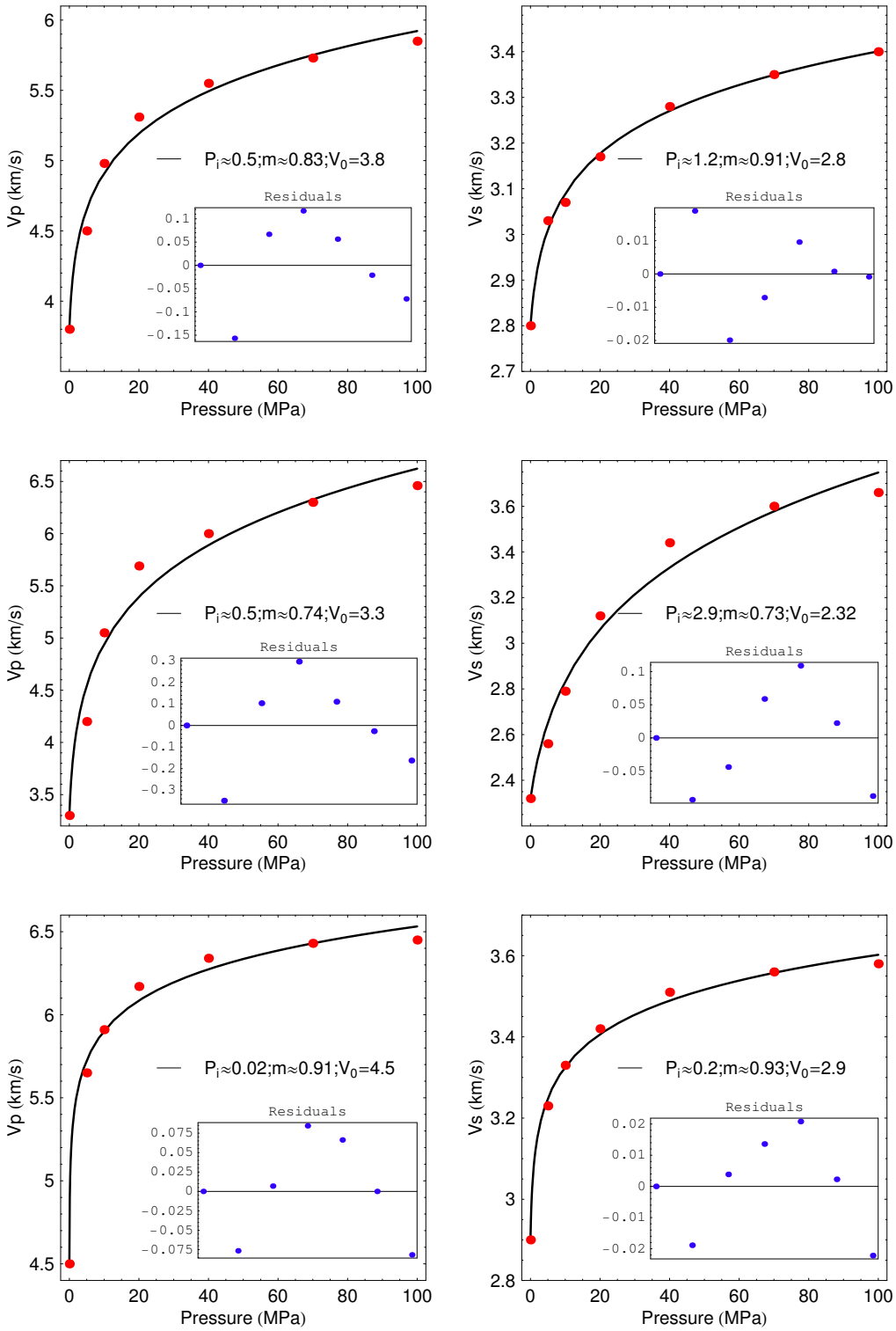

Fig. 3.6. Rigid-host fitting curve and residuals for Westerly (top), Casco (middle) and Troy (bottom) granites from the Nur and Simmons (1969) data set.

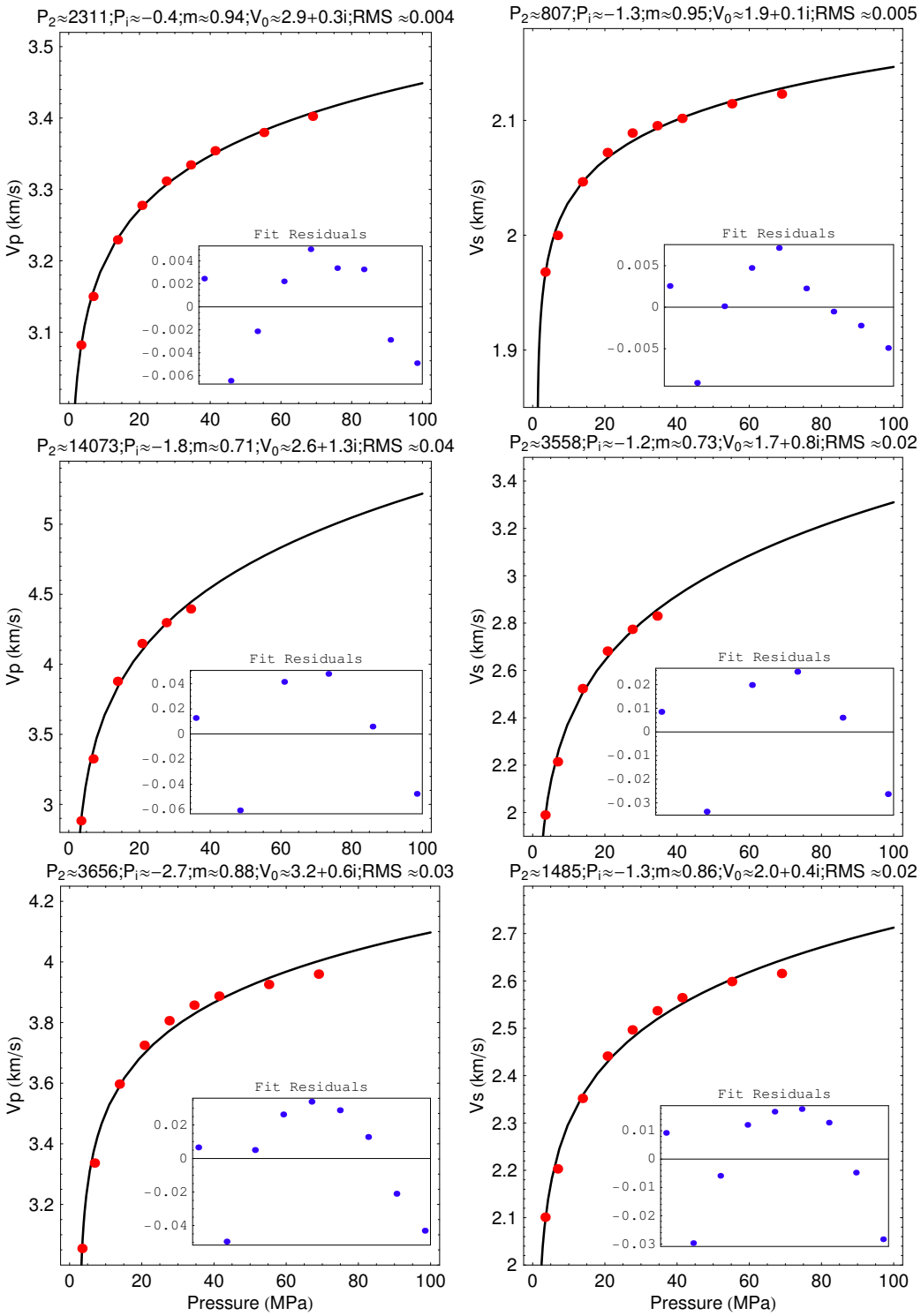

Fig. 3.7. Rigid-host fitting curve and residuals for Boise (top), St.Peter (middle) and Torpedo (bottom) sandstones from the King (1966) data set.

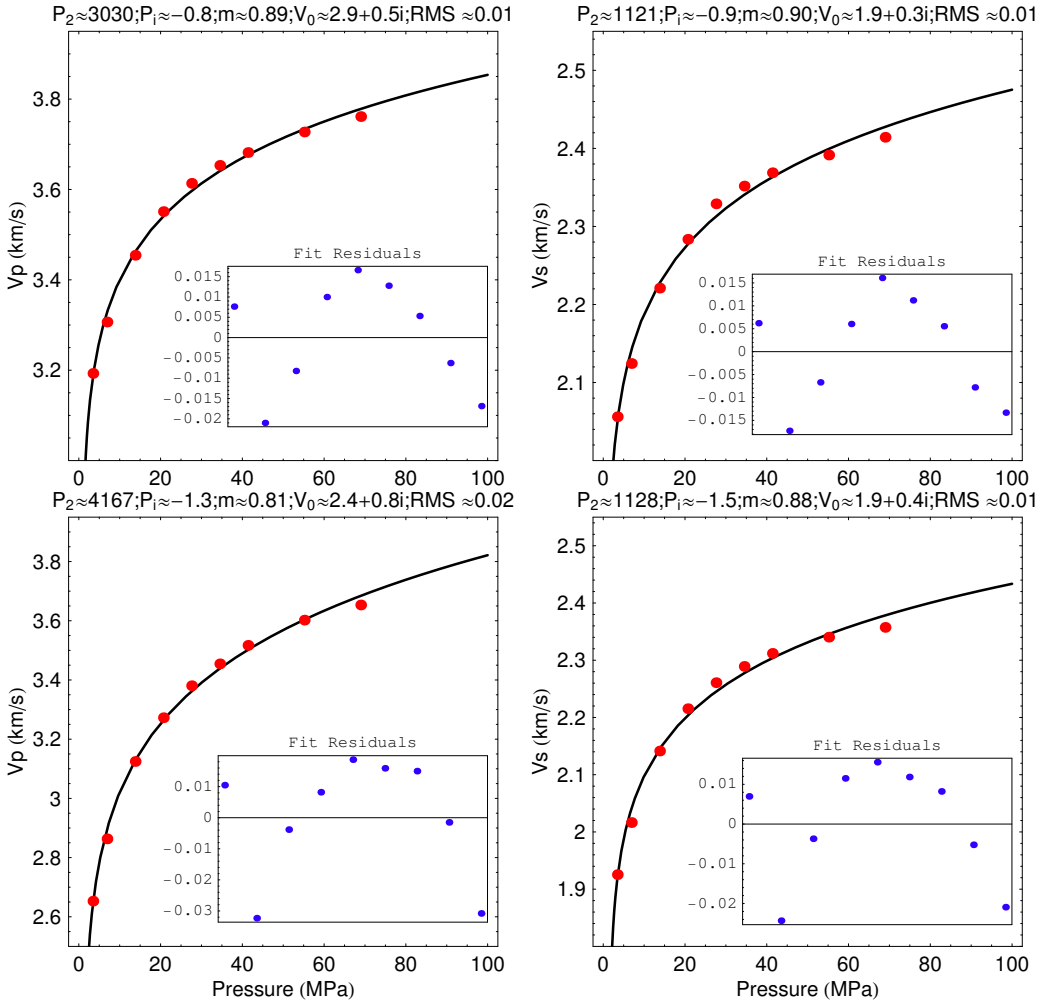

Fig. 3.8. Rigid-host fitting curve and residuals for Bandera sandstone, measurement direction is parallel (top) and perpendicular (bottom) to bedding, from the King (1966) data set.

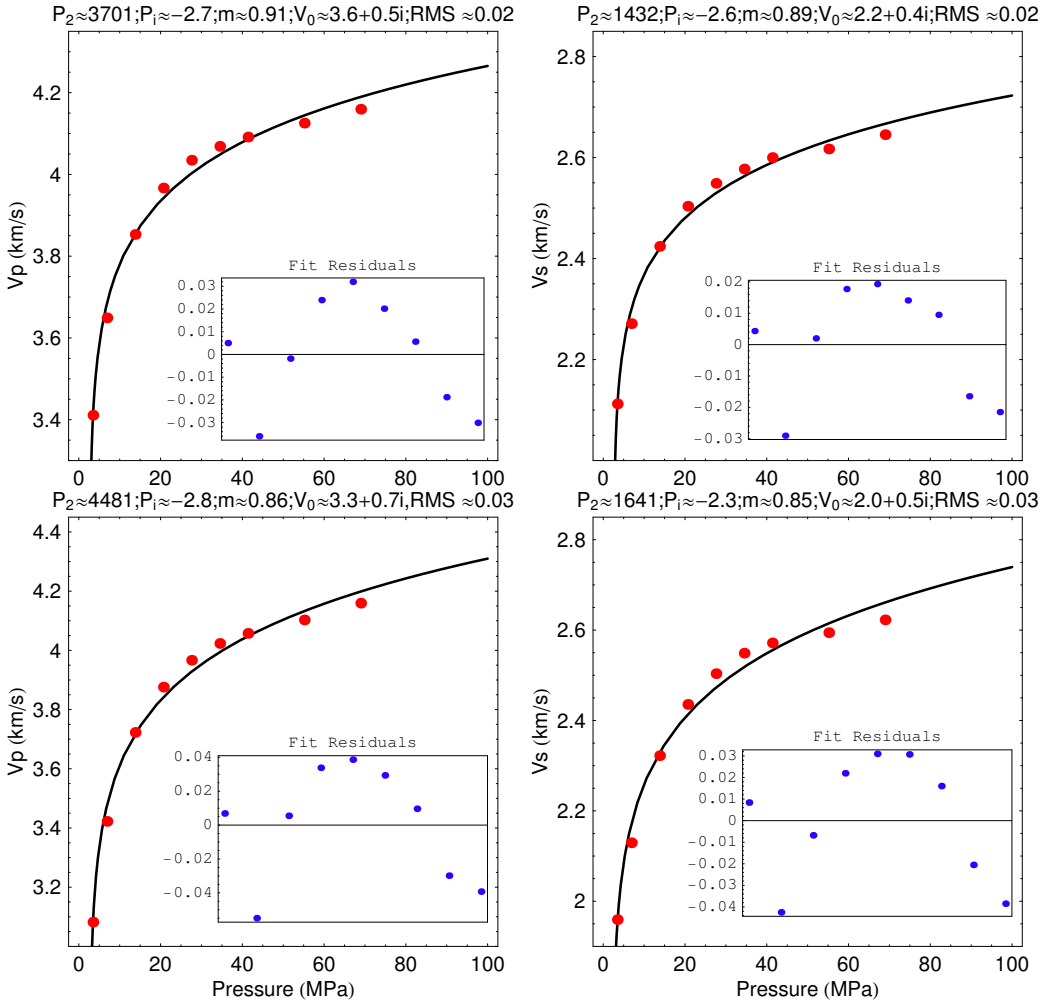

Fig. 3.9. Rigid-host fitting curve and residuals for Berea sandstone, measurement direction is parallel (top) and perpendicular (bottom) to bedding, from the King (1966) data set.

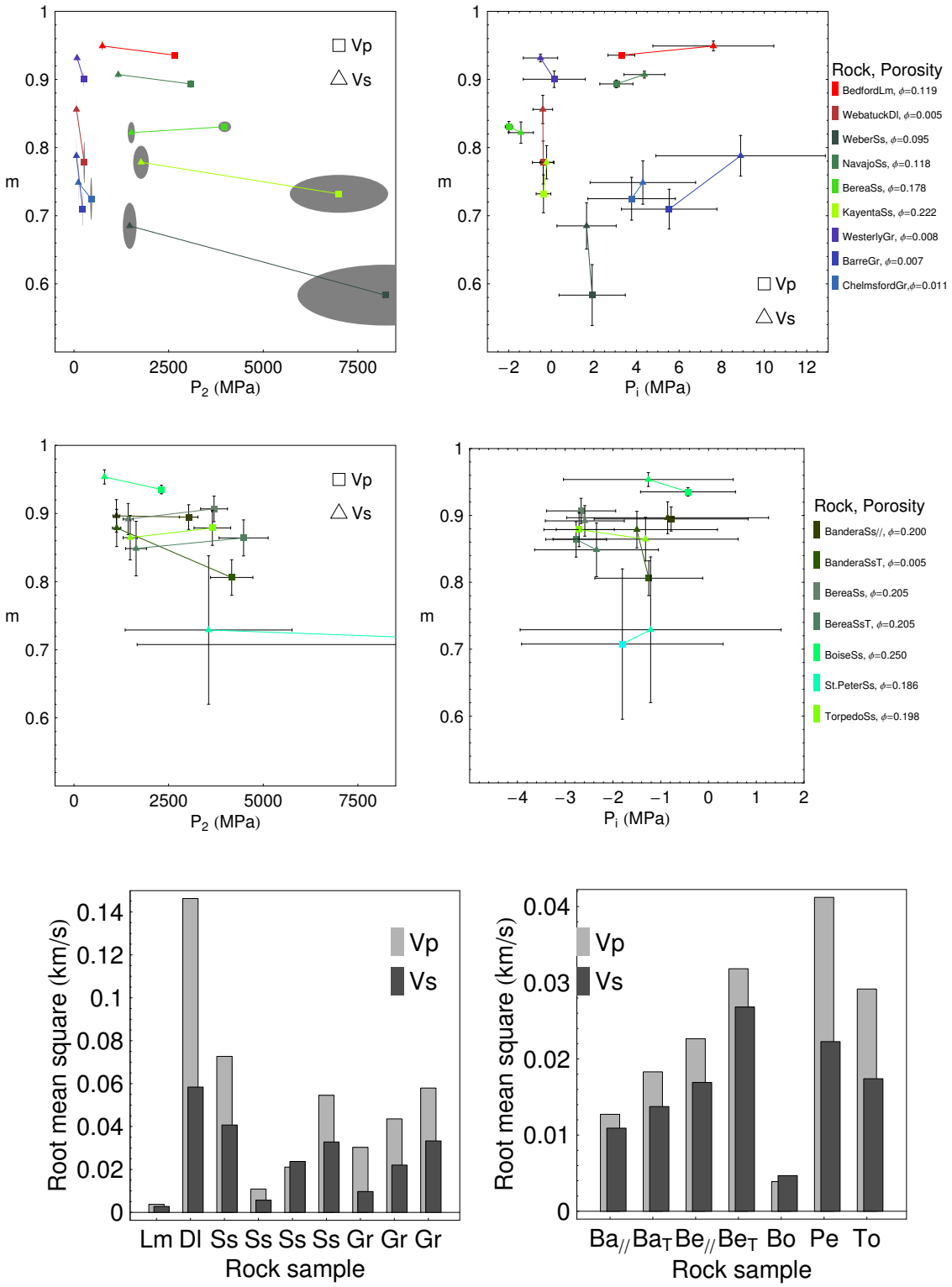

Fig. 3.10. Rigid-host best fit parameter estimates and RMS errors for rocks from the Coyner (1984) and King (1966) data sets.

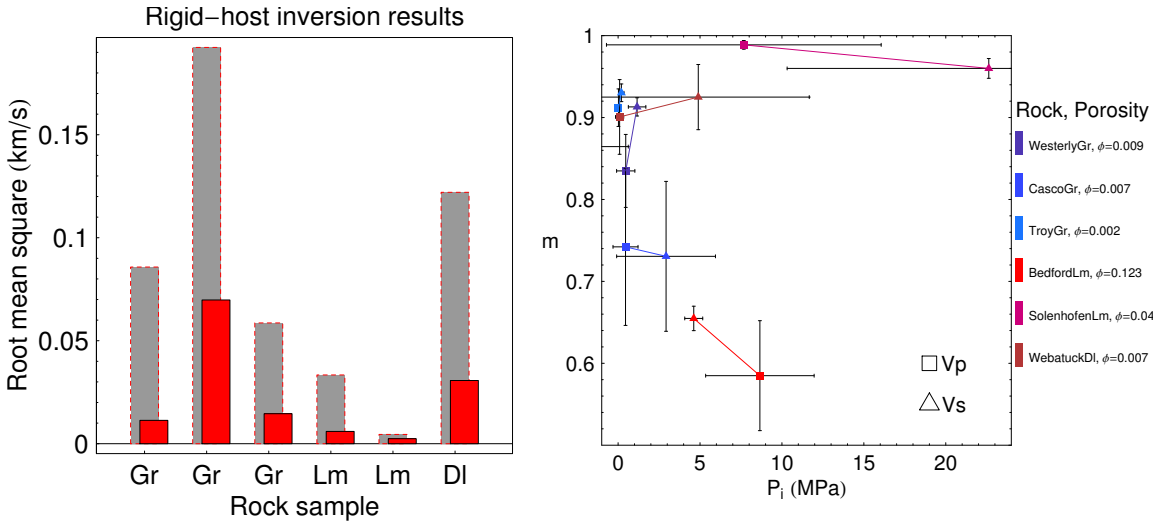

Fig. 3.11. Rigid-host best fit parameter estimates and RMS errors for rocks from the Nur and Simmons (1969) data set.

the inversion results in terms of the inverted parameters m, P_2 and P_i (see equations (2.9) and (2.11)). Notice that in general for V_p data or V_s data of each data set alone, a lower estimate value of m is typically associated with a larger confidence interval (and thus a larger uncertainty). This is an indication of a possible noise which has not been accounted for in the current rigid-host model (i.e. modeling error, as opposed to random error). Notice also that for each type of data (V_p or V_s), the estimate value of P_2 for sandstones tend to increase as the m estimate decreases.

The fact that V_s data result in systematically higher m and lower P_2 than V_p data suggests that S-wave velocity is less affected by pressure changes than P-wave velocity for the same rock. For instance, for the Bandera sandstone in the top panels of figure 3.8, the change in V_s is about 0.5 km/s for a value near 2 km/s, about 25 %, whereas for V_p, the change is about 1 km/s compared to a velocity of 3 km/s, about 33 %. The m and P_2 estimates are 0.9 and 1121 (MPa) for V_s data, and 0.89 and 3030 (MPa) for V_p data, respectively. Another example is, for the Chelmsford granite in the bottom panels of figure 3.4, the change in V_s is about 1.2 km/s for V_0 near 2.4 km/s, about 50 %, whereas for V_p, the change is about 2.2 km/s near 3.7 km/s, about 59 %. The m and P_2 estimates are 0.75 and 116 (MPa) for V_s data, and 0.72 and 456 (MPa) for V_p data, respectively. To explain this in terms of ADM, according to

equation (2.11), $dP/dx = P_2 x^{m^{-1}-1}$, a lower value of P_2 indicates a smaller envelope for deformation to take place, whereas a higher value of m between 0.5 and 1 indicates less variation in stiffness (i.e. more flat-lying, horizontal cumulative distribution) for the same deformation range.

For many rocks, the small confidence regions indicate that parameters can be reliably estimated using the velocity profile data from these rocks. Other rocks with large confidence regions have unreliable parameter estimates with large uncertainty. Note that although I inverted for values of m, P_2 and P_i because they are independent parameters, I have also done the inversion in terms of V_0, P_1 and P_i (Gangi, 1981) and converted them via equation (2.11) without change in the outcome.

From these results, several points emerge that draw attention. First, the rigid-host solution fits very well with the data from a few rocks, especially the Bedford and Solenhofen limestones (from both Coyner (1984) and Nur and Simmons (1969) data sets). Good fits can also be seen in stiff rocks such as the Navajo sandstone (which is listed by Coyner (1984) as having the "stiffest stress-strain relation"), or rocks that are subject to a smaller range of pressure such as the King (1966) high-porosity sandstones. Nevertheless, systematic misfits occur in the rest of rocks, comparatively larger than the measurement error ΔE, which is around 0.01 km/s or 10m/s in the Coyner (1984) data set. The fact that the fit residuals are lined up in a systematic pattern again suggests that there could be either modeling error or some coherent noise that can be modeled and corrected for. In that sense, the solution does a poorer job in several softer granites and the low-porosity rocks, while the worst fits are spotted in the Webatuck Dolomite with RMS error one order larger than ΔE. Note that the Webatuck Dolomite is also a very low-porosity rock (0.9%).

True to its assumption, the rigid-host solution applies well on rocks that are considerably stiff over the applied pressure range, such that the host rock compliance is negligible and deformation is approximately linear elastic. The stiffer rocks such as the limestones, the Westerly granite, or the Navajo sandstone, all have approximately linear stress-strain relationship over the range of applied pressure. However, the elastic region can be quiet short for a relatively soft and compliant rock such as can be seen on the Coyner (1984) graphs for stress-strain relationship for such rocks as the Weber sandstone or the Berea sandstone or a few other granites. In addition, the elastic region can also be short for a rock with very low, crack-like porosity such as the Webatuck Dolomite. This rock has $\phi = 0.5\%$ and is made up mostly from

the mineral dolomite which is indeed very stiff, so theoretically it should fit well with the rigid-host solution as does the other carbonate, Bedford Limestone. However, because the host is so stiff, the primary effect of pressure is to close the cracks, and that happens quickly due to the lack of porosity. Thus, presumably when pressure is increased up to some large enough value (approximately around 30 MPa), the majority of the cracks in this rock will have been closed, and there is very little deformation in the rest of the experiment. All responses afterwards are primarily those of the stiff mineral dolomite, making velocities look very "flat" over the rest of the applied pressure range. Therefore, depending on the rock, the applied pressure range is important for the application of the rigid-host solution. Generally, it should work better for a stiffer rock and a smaller range of pressure.

Because ADM is a 1-D model, either we apply its solutions to an isotropic rock to get one single set of inverted parameters, or else we will have different sets of parameters describing the velocity-versus-pressure relationship for different directions of measurement. Furthermore, because pressure affects V_p and V_s differently, we will also have two different sets of parameters describing the pressure dependence of V_p and V_s separately for each direction. Thus, it may be possible to infer for example that the Berea sandstone from the King (1966) data set is approximately isotropic because the measurements in two perpendicular directions (parallel and perpendicular to bedding) result in similar sets of parameter estimates; meanwhile, the Bandera sandstone from the same data set is anisotropic due to having different sets of inverted parameters in different measurement directions.

A sensitivity study allows us to assess the uncertainty and non-uniqueness in parameter estimates. This type of analysis helps determine the relationship between parameters and which ones are the most uncertain or insensitive to the model. Here I treat the rigid-host equation as a forward model and evaluate the objective function at different parameter values (equation (3.1)). It is easy to check that for each rock, the inverted parameter values (i.e. estimates) make up the global minimum which minimizes the value of the objective function. Plotting the objective function and its derivative with respect to a single parameter while keeping the other two at the global minimum shows that in all experimental rocks, the objective function is well-behaved with a well-defined global minimum. This means mathematically that the estimates are unique and the objective function is sensitive to each parameter. However, because the objective function is data-dependent (equation (3.1)) while the data can be noisy,

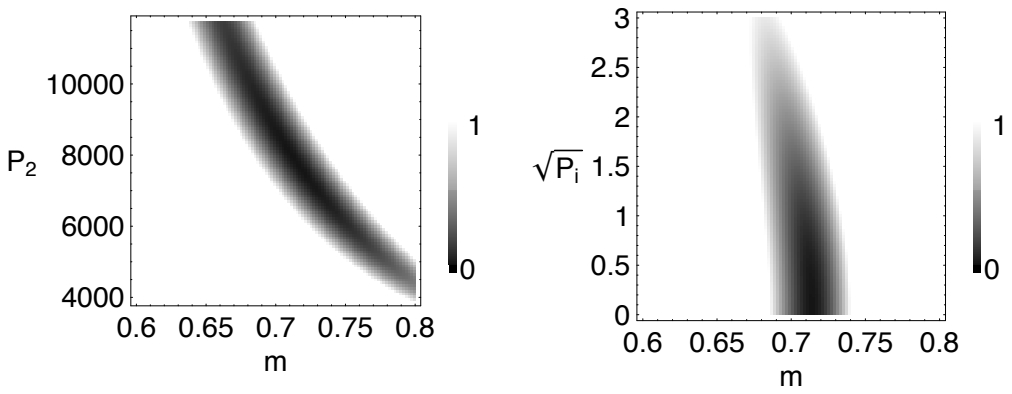

Fig. 3.12. Values of the objective function for the Berea sandstone from the Coyner (1984) data set showing the trade-off relationship between m and P_2 and the insensitivity with P_i.

parameter values near the minimum are also acceptable as inversion results. Thus, it is the noise (coherent or incoherent) that is responsible for the non-uniqueness of solution estimates and the insensitivity of the objective function to each parameter. If the objective function does not change too rapidly for values at and away from the minimum, we say that it is insensitive (or else, the least sensitive) to that parameter.

Plotting the objective function for two parameters while keeping one at the global minimum show that while there is a trade-off relationship between values of m and P_2, the forward rigid-host model is the least sensitive to values of P_i near the global minimum. This is illustrated on figure 3.12 for an example rock. This figure plots the value of the objective function which is the root-mean-square (RMS) of the differences between the model velocity prediction and the data values for the Berea sandstone, as the parameters are allowed to vary within their possible range of values (values above 1 km/s are cut off). As shown on the left panel, fixing P_i at the minimum, the values of the objective function are comparably similar as P_2 decreases and m increases and vice versa, while shown on the right panel, for a pair of values m and P_2 at the minimum, the objective function is similar for values of P_i near the minimum. My test results with other rocks and with synthetic data also show similar behaviors, indicating that these are properties of the rigid-host model solution. It further supports the non-uniqueness of the inverted solution we have seen as confidence regions.

3.4.2 Inversion results using the power-law compliant-host solution

Figures 3.13 to 3.20 show the compliant-host best fits and RMS errors for the V_p and V_s of all twenty rocks. Figures 3.21 and 3.22 summarize the compliant-host parameter estimates with the error bars showing the confidence regions of solution in terms of V_g, V_0, m, and P_i.

The first important remark is that compliant-host inversion does a much better job fitting the data in all rocks, compared to rigid-host inversion. The RMS errors using the compliant-host inversion is around an order better than those from rigid-host fit. Furthermore, the fit residuals are more random, proving that there is no coherent noise needed to be corrected for. This suggests that the equation used for inversion is the "correct" formula, which describes all pertinent physics involved.

However, notice right away that the inverted values for m are negative in many cases, and also not the same as the estimates from rigid-host inversion. The negative m values are uninterpretable using the current ADM. Secondly, the extremely large values of P_i also seem out of range regarding their physical meanings in the "bed-of-nails". This in turn suggests that the current ADM is not extensive enough to physically cover and interpret all real-life data. I postulate here that the reason for this is because of the initial presumption that the host rock moduli are pressure independent. In fact Carlson and Gangi (1985) mentioned that the m estimates are higher for the rigid-host than for the compliant-host solution because the rigid-host solution "includes the effect of the grain compressibility in the asperity-height distribution function" while the compliant-host solution does not, and thus the compliant-host estimate values for m are affected by the fact that "the grain velocity does not have an explicit pressure dependence." In chapter V, I will attempt to correct for this effect by extending the model to let the host rock depend on pressure.

Notice that in a few cases (e.g. V_s of Solenhofen limestone or V_p of Westerly Granite), the estimate of V_g is very large, indicating that the grain solid is much stiffer than the pores/cracks, hence its inverse, compliance, is negligible, and it points back to the rigid-host solution where we get the exact same set of parameters (m, P_2, and P_i). Thus, the compliant-host solution is indeed more general than the rigid-host solution, and should therefore be applicable to a broader variety of rocks.

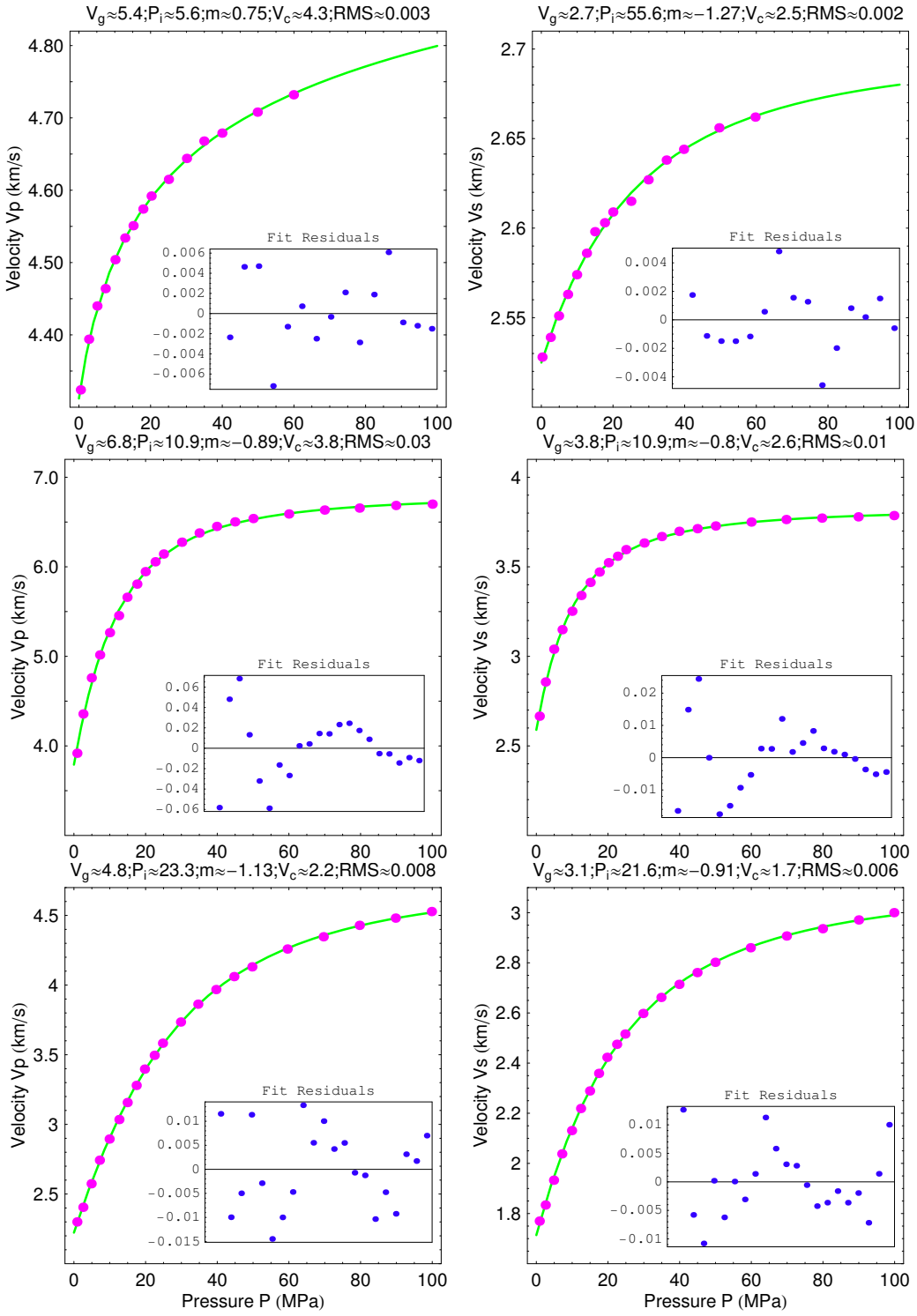

Fig. 3.13. Compliant-host fitting curve and residuals for Bedford limestone (top), Webatuck dolomite (middle) and Weber sandstone (bottom) from the Coyner (1984) data set.

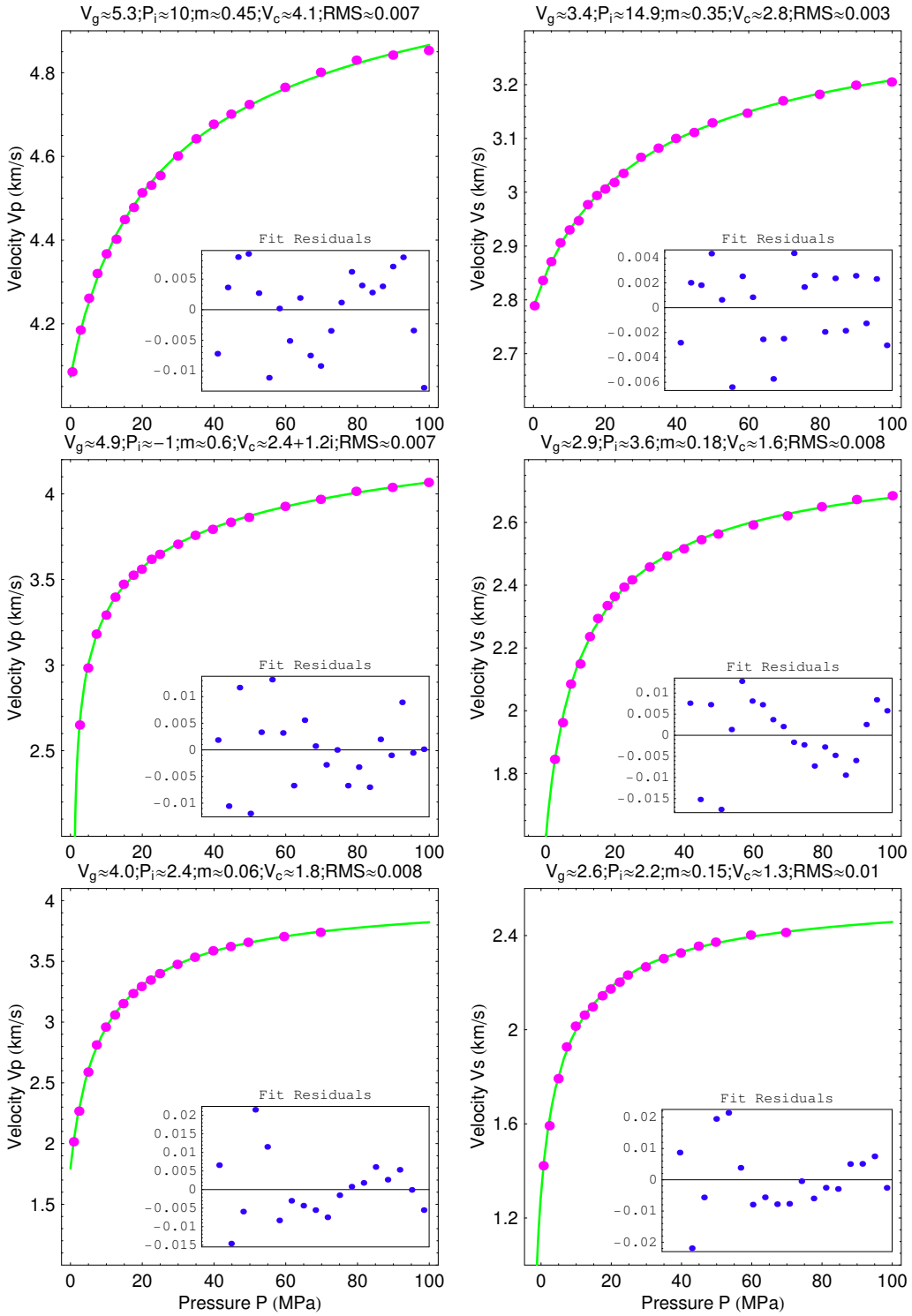

Fig. 3.14. Compliant-host fitting curve and residuals for Navajo (top), Berea (middle) and Kayenta (bottom) sandstones from the Coyner (1984) data set.

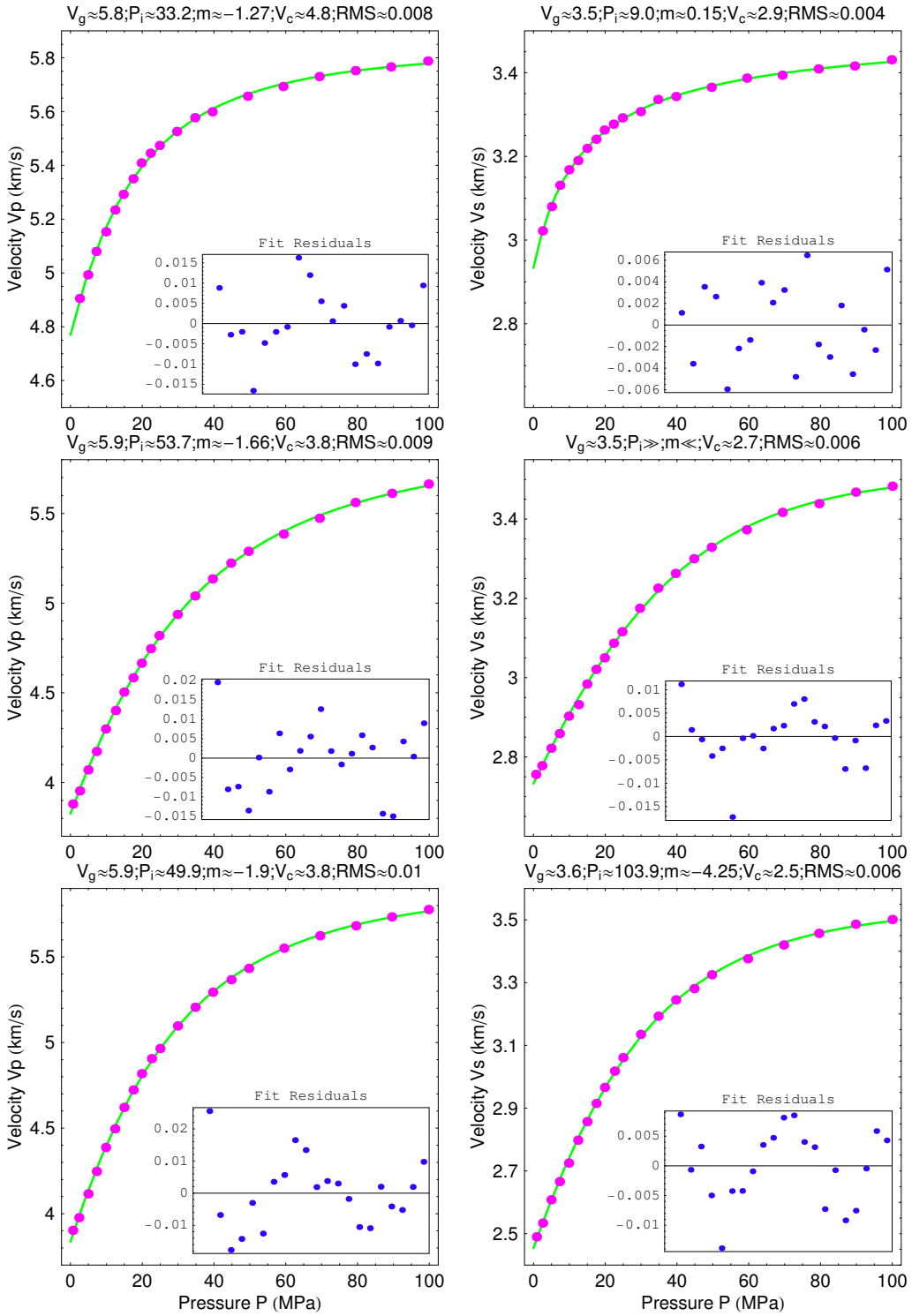

Fig. 3.15. Compliant-host fitting curve and residuals for Westerly (top), Barre (middle) and Chelmsford (bottom) granites from the Coyner (1984) data set.

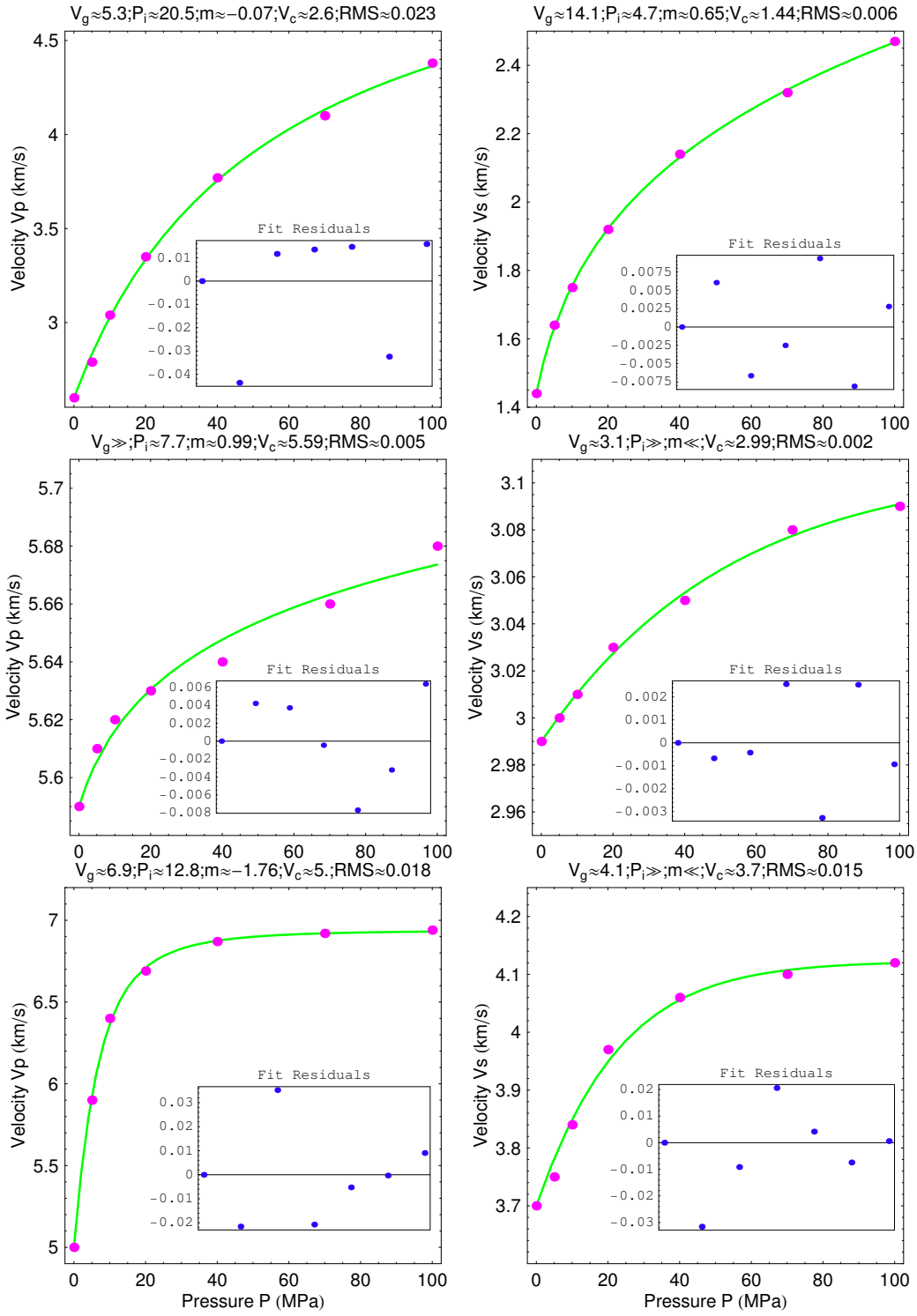

Fig. 3.16. Compliant-host fitting curve and residuals for Bedford (top), Solenhofen (middle) limestones and Webatuck dolomite (bottom) from the Nur and Simmons (1969) data set.

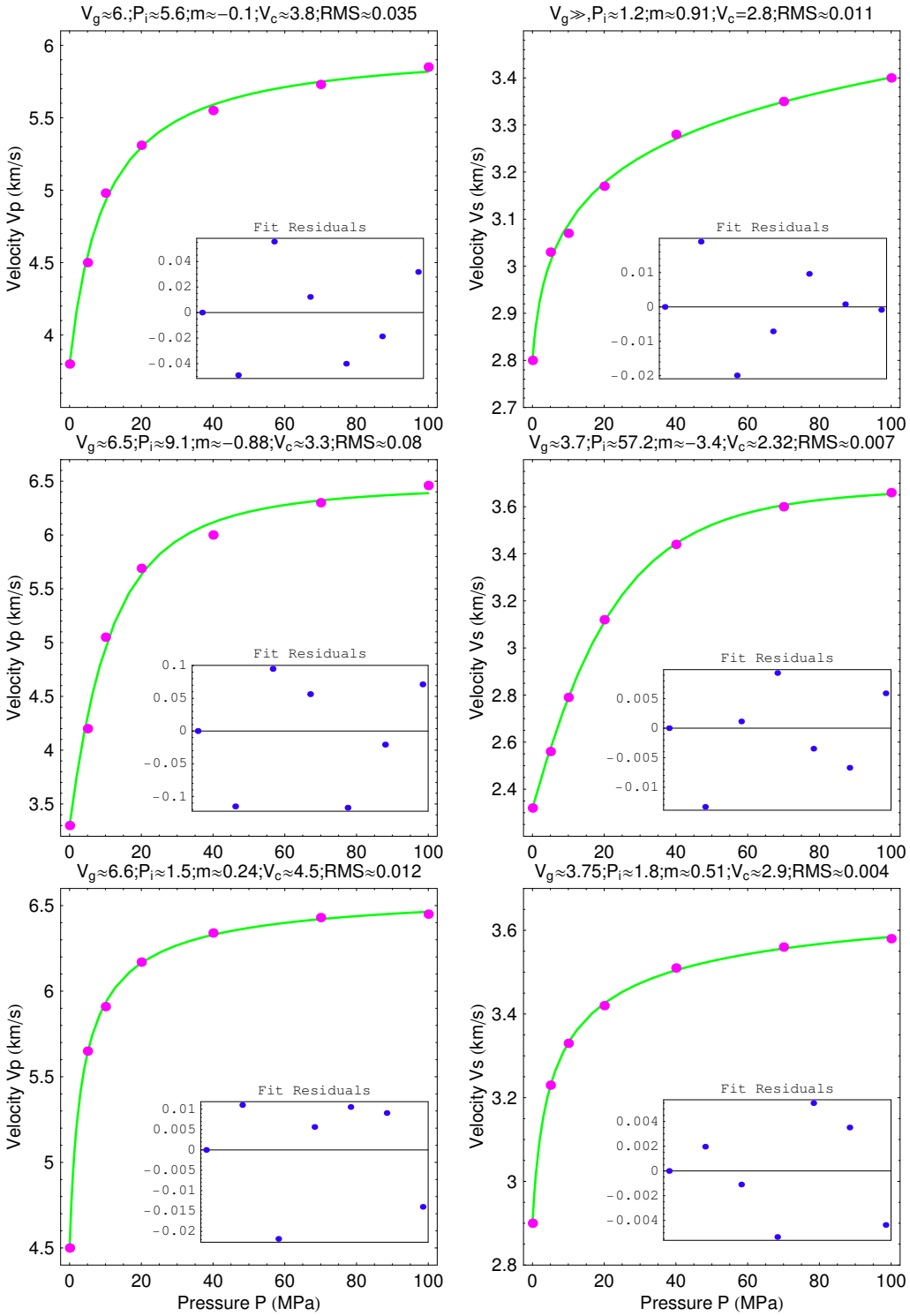

Fig. 3.17. Compliant-host fitting curve and residuals for Westerly (top), Casco (middle) and Troy (bottom) granites from the Nur and Simmons (1969) data set.

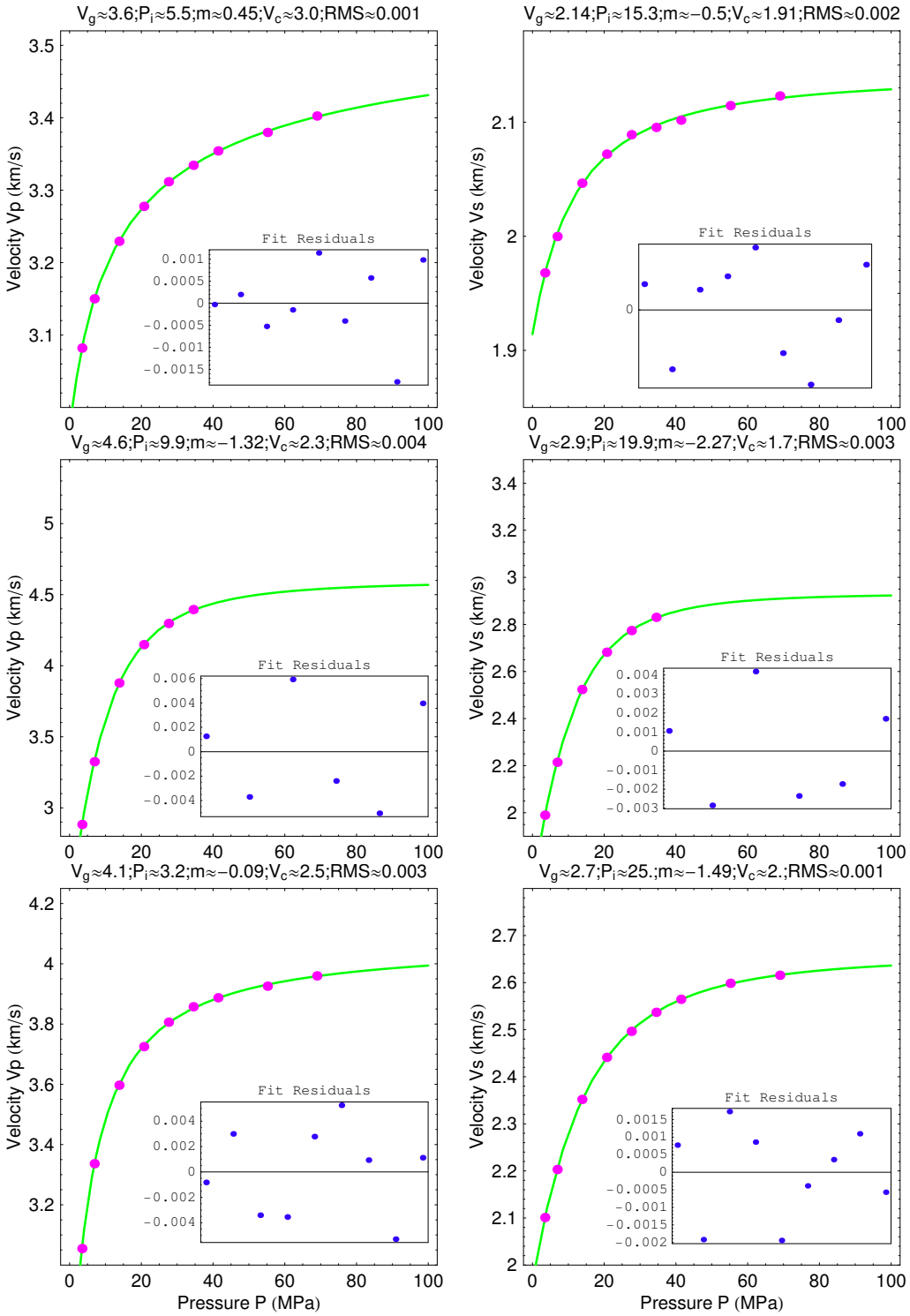

Fig. 3.18. Compliant-host fitting curve and residuals for Boise (top), St.Peter (middle) and Torpedo (bottom) sandstones from the King (1966) data set.

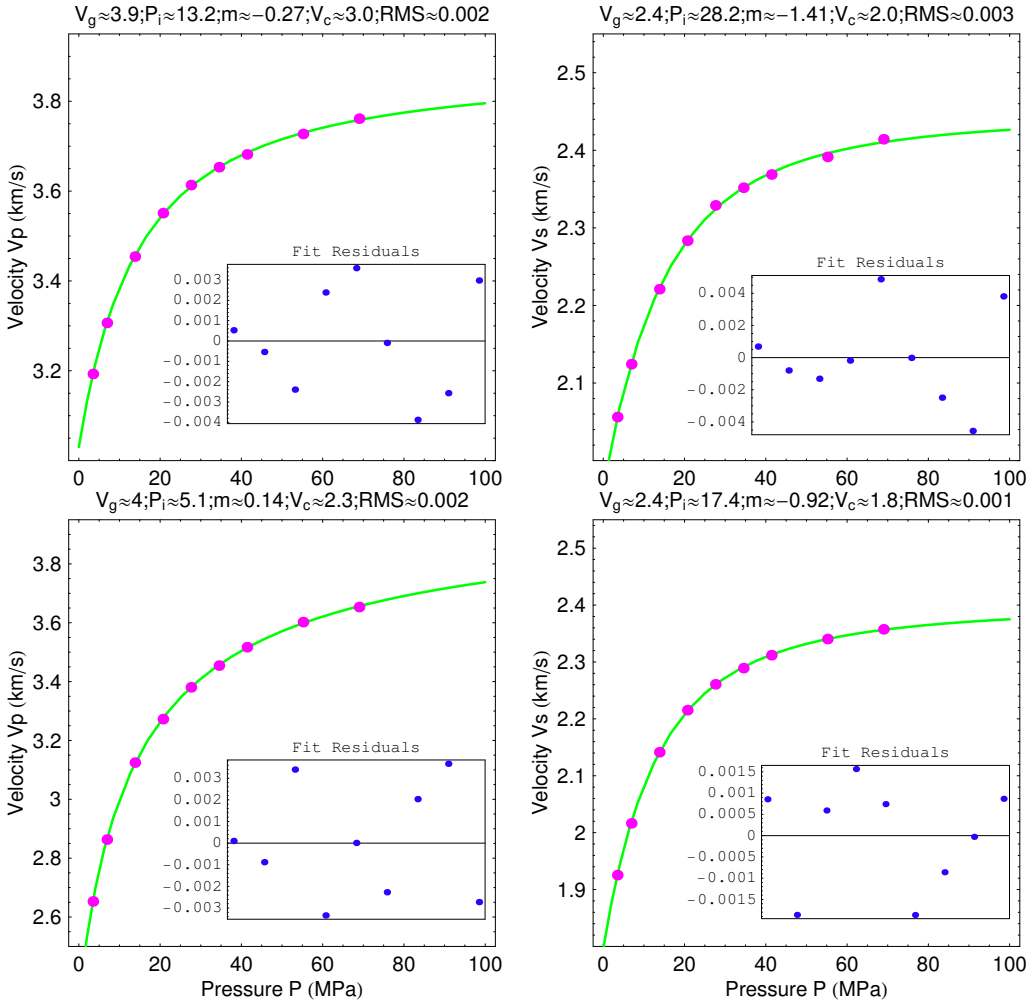

Fig. 3.19. Compliant-host fitting curve and residuals for Bandera sandstone, measurement direction is parallel (top) and perpendicular (bottom) to bedding, from the King (1966) data set.

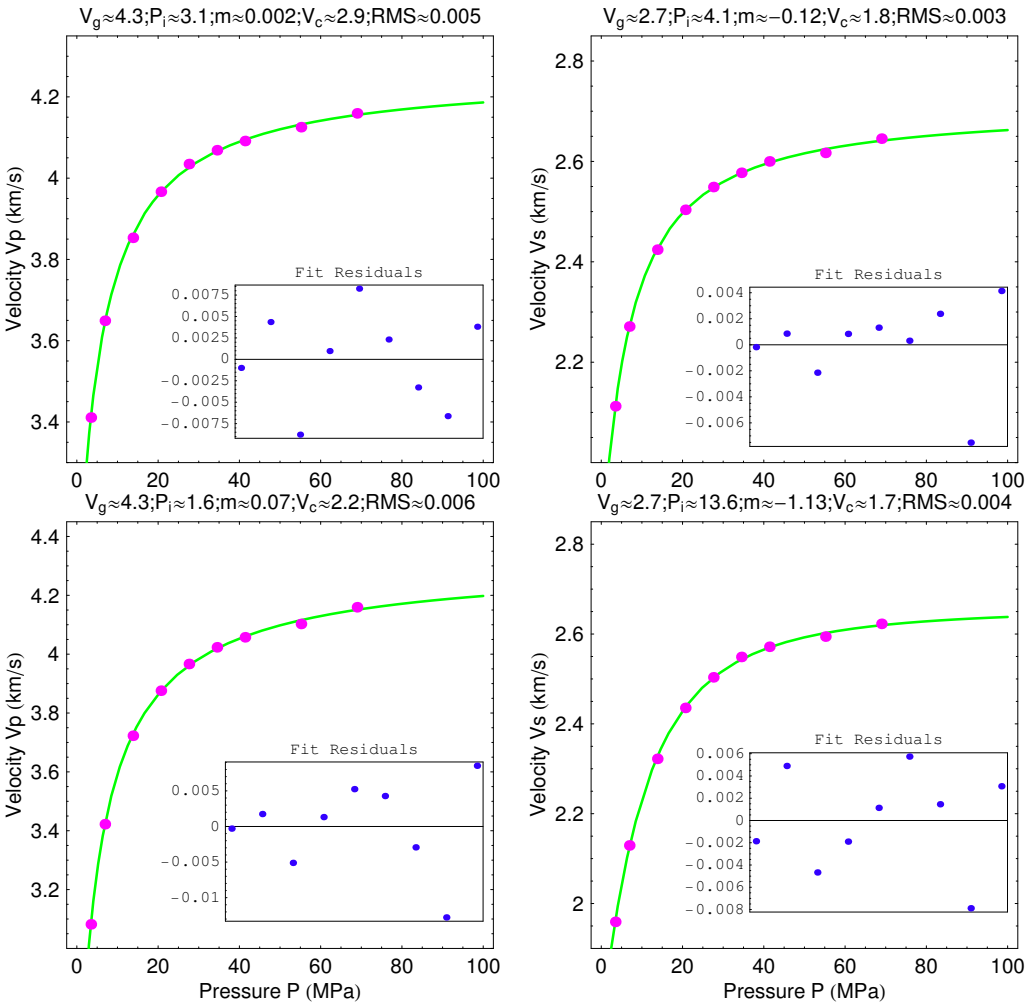

Fig. 3.20. Compliant-host fitting curve and residuals for Berea sandstone, measurement direction is parallel (top) and perpendicular (bottom) to bedding, from the King (1966) data set.

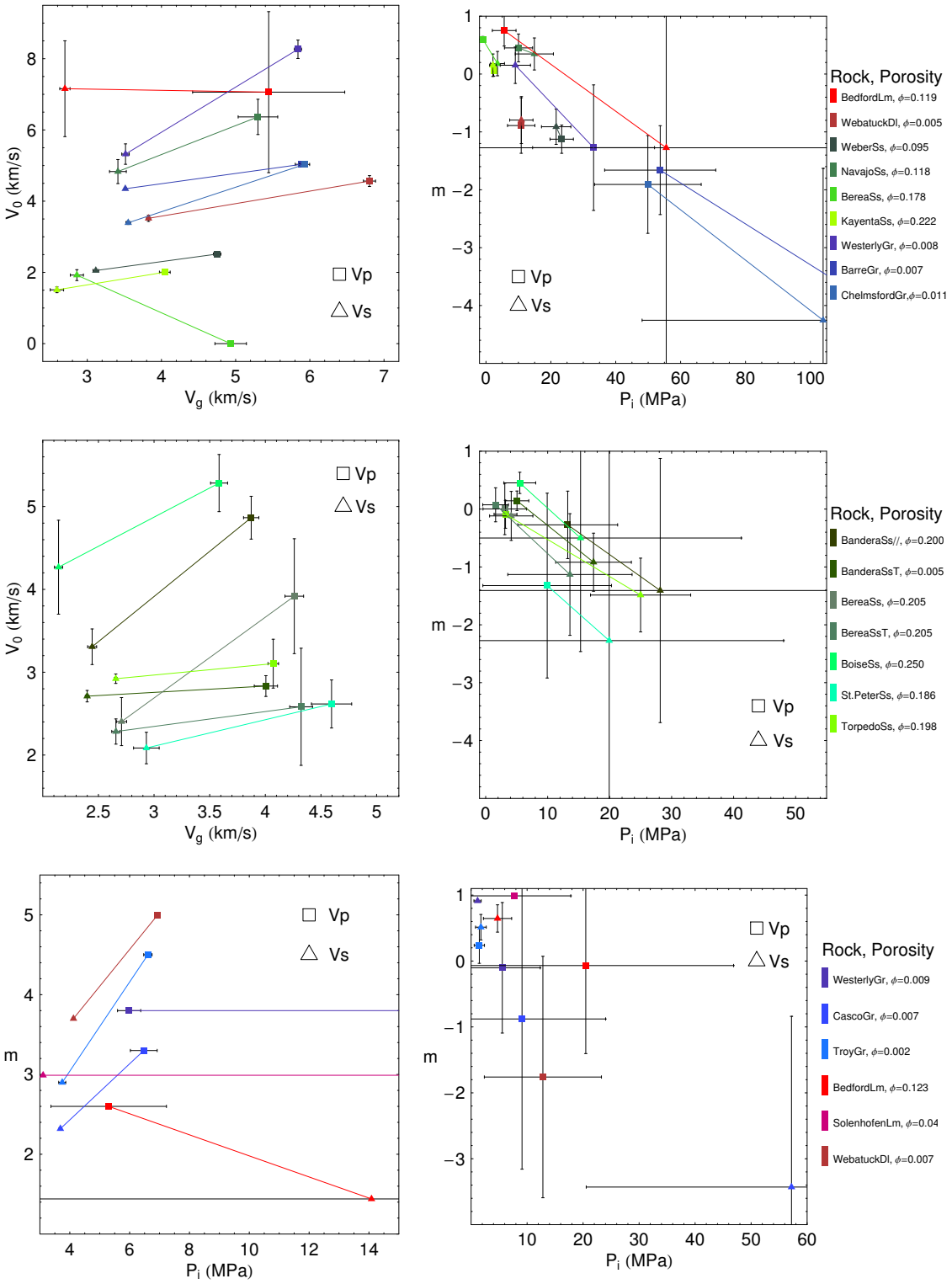

Fig. 3.21. Compliant-host best fit parameter estimates for rocks from the Coyner (1984) (top), King (1966) (middle), and Nur and Simmons (1969) (bottom) data sets.

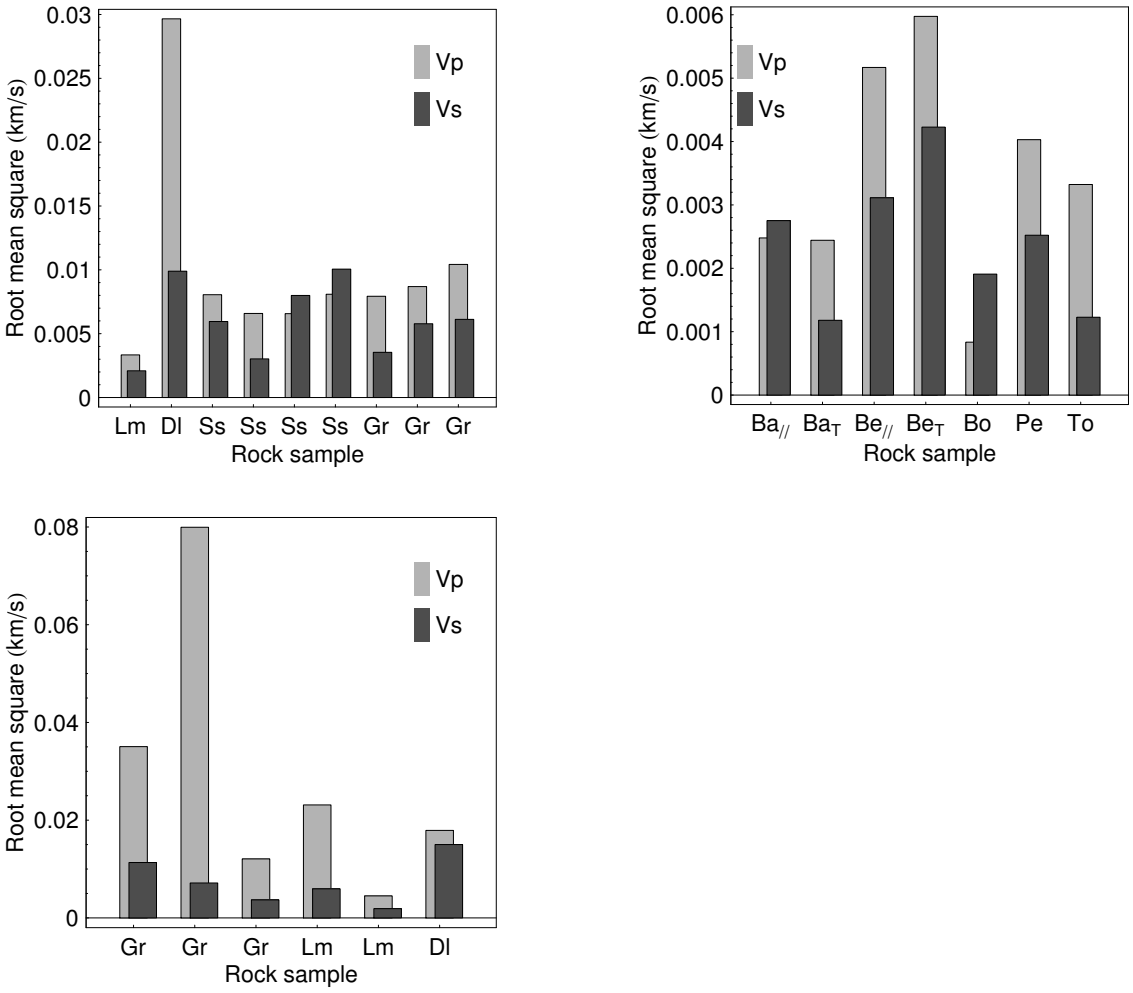

Fig. 3.22. RMS errors of compliant-host fit for rocks from the Coyner (1984) (left), King (1966) (right), and Nur and Simmons (1969) (bottom) data sets.

3.4.3 Discussions

It is noticeable that the sandstones, whether of low or high porosity, seem to all have high estimates of P_2 and a broad range of values for estimates of m in the rigid-host inversion (figure 3.10), while for the compliant-host inversion no such similarity can be seen (figure 3.21). For the rigid-host results, sandstones generally have estimates of P_2 higher than the carbonates and the granites, while their estimates of m are comparable. This is understandable regarding the physical meanings of these parameters. First, let us examine why the m estimates for almost all rocks are around 0.7 to 0.99. Note that m characterizes the shape of the power-law asperity-height distribution and the amount of asperities deformed increases with applied pressure. With intensity of applied pressure and reduction of fracturing, more and more originally tall asperities are deformed and brought into contact, and the asperities become more and more uniform in height (see equation (2.10) and figure 2.2 for the power-law distribution). Therefore, an inverted value of m closer to 0 means at that particular applied pressure, only a small number of (tall) asperities have been deformed and in contact while the rock is still dominated by asperities of contrasting heights (tall and short) which are subject to deformation and contact by pressure. Whereas, an inverted value of m closer to 1 means at that particular pressure most of the taller asperities have already been deformed and in contact, while the left-over asperities are all about equal in size and number. For the examined laboratory data sets, at high pressures (around 100 MPa) any tall isolated asperities will have been broken, so it makes sense that the estimates are larger than 0.5 and closer to 1.

On the other hand, sandstones have noticeably higher P_2 estimates than carbonates and granites (figure 3.10). Recall that in the "bed-of-nails" model, P_2 not only characterizes the asperity material but also the total number of asperities (equation (2.2)), thus its estimate should contain information about the host material as well as the maximum amount of possible contact in the studied rock when subjected to pressure. Hence, the high estimates of P_2 suggest that sandstones have more contact potential (i.e., larger N_T) thanks to the higher porosity, although not necessarily stiffer host-rock material (i.e., mineral composition) than compared to other types of rocks. From the ADM perspective, P_2 is constant in equation (2.1) indicates that the model assumes there is no deformation in the host, thus the host is rigid and does not depend on pressure. Because the solution imposes such rigid-host assumption which granular rocks like sandstones may not strictly follow, estimates for P_2 in sandstones

should also incorporate the host rock rigidity, which differs from more-obeying media such as igneous or hard carbonate rocks. While it makes sense to assume a constant value for P_2 in low-porosity, hard crystalline rocks (e.g. Gangi, 1981; Carlson and Gangi, 1985), granular media such as sandstones may not have the same host-rock rigidity and may be deformed much more easily. As discussed earlier, the large variety of variable parameters in sandstones (such as grain size, shape and sorting, porosity type, porosity, consolidation, etc...) greatly influence the variations and uncertainties in the contact potential and the characterized asperity material. Thus, it may be more valid to give P_2 some flexibility to represent the asperity material in sandstones (i.e. to let it vary with applied pressure). The bottom line is that the high estimate values for P_2 in sandstones may have been the consequence of an invalid rigid-host assumption. For the compliant-host solution, no such differentiation between rock types can be observed and this is believed to be the consequence of a more valid model.

Nevertheless, the rigid-host model solution has three physical parameters and it is still a good first-order approximation to laboratory data. The compliant-host model solution has four parameters and thus is expected to offer a more stable inversion as well as a much better fit to all rocks. However, we have also seen that the estimate values for the parameters using this solution, particularly for m and P_i, are not physically meaningful with respect to the original "bed-of-nails" physical model.

In any event, the estimate for P_i from both inversions has large uncertainties due to its sensitivity to low-pressure data measurements, agreeing with a previous study by Genova (2008). He concludes that the reason for the uncertainty of P_i is because of the lack of measurements near zero effective pressure. From the rigid-host equation (2.9), it is also deducible that changing the values of P_i affects the lower-pressure predictions more than it does to the higher-pressures. That means in the inversion, the low-pressure data points will affect the estimated values for P_i more than the high-pressure data points, and having a measure at zero pressure is the guarantee to have the most certain value of P_i, while not having that measure will introduce a degree of uncertainty into the estimate of P_i, and that degree of uncertainty increases with fewer low-pressure data points.

Figure 3.23 puts together a comparison between the two power-law inversion schemes for two example rocks from the Coyner (1984) data set. The onset shows fit residuals of only the compliant-host inversion, comparable in magnitude to the

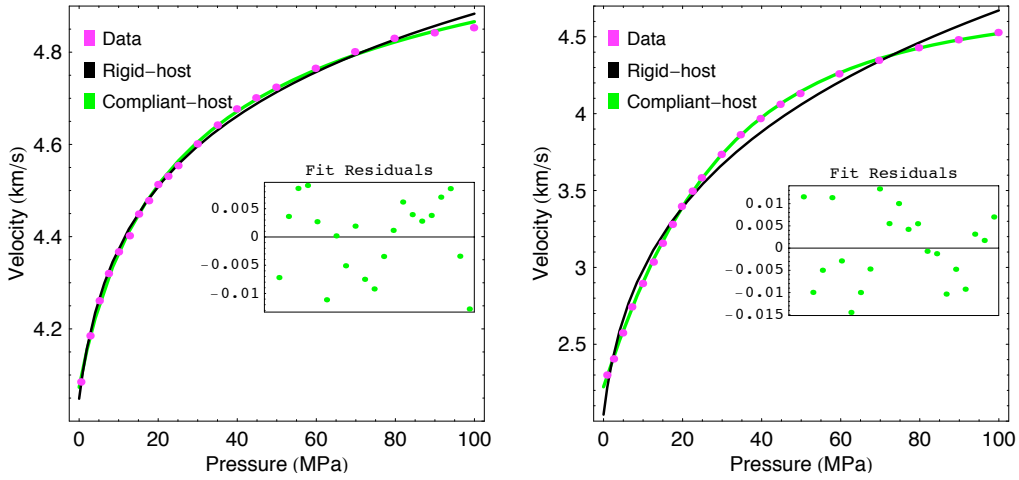

Fig. 3.23. Comparison between rigid-host and compliant-host inversion for two example rocks in the Coyner (1984) data set.

measurement error $\Delta E \approx 0.01$ km/s. For the Navajo sandstone, the rigid-host fits well to data but the compliant-host improves the fit even more. For the Weber sandstone, the rigid-host solution does a poor job while the compliant-host inversion maintains a good fit, with random fit residuals consistently less than ΔE. It is not coincidental that the Gangi (1981) solution works well in such rocks as the Bedford limestone and Navajo sandstone. Coyner (1984) graphically demonstrated that the pressure-versus-volumetric strain relationship is approximately linear in these rocks over the applied pressure range 0-100 MPa, whereas nonlinear in the rest of the rocks. Moreover, Navajo sandstone has "well-sorted grains," "the stiffest stress-strain relation and lowest crack porosity" (Coyner, 1984). A well-sorted sandstone would be more resistant to pressure as compared to a poorly sorted sandstone due to the pore geometry. A poorly sandstone would have more thinner crack-like pores while a well-sorted sandstone has less thinner cracks. thus deformation (i.e., porosity reduction) is more or less linear with pressure. Recall that ADM models pressure as directly proportional to the volumetric strain While the Weber sandstone is more dense ($\rho =$ 2.392 g/cc compared to 2.316 g/cc for Navajo) and more rigid (the bulk modulus of the grain solid is $K_b = 38.5$ GPa compared to 36 GPa for Navajo), it is less well-sorted, and its graphed porosity reduction with pressure is very nonlinear (Coyner, 1984). I have repeated the same analyses for all nine rocks from the Coyner (1984)data

set and came to the conclusion that the pore geometry influences pressure-induced deformation in rocks, predicting and determining the fit with the rigid-host solution (i.e. purely linear elasticity).

As demonstrated, rigid-host inversion using a power-law distribution of asperity heights) leads to some systematic and considerable misfits (compared to listed experiment error) for some experimental rocks. This indicates that the misfits are not random errors but "modeling errors" (Scales et al., 2001). In general, if the model accurately describes all the involved physics then the random errors should represent the random noise of the experiments, which is non-systematic and within the range of measurement error. Normally, every experiment will produce some random noise which can be large but is always highly variable and "cannot have any consistent patterns or effects across the data sample" (Trochim, 2000). Thus, the systematic and significant misfits indicate that these rocks do not match the assumptions of the rigid-host solution.

In general, the purpose of a theoretical model such as the "bed-of-nails" is to describe the true, natural physics that happen in real life. However, one physic that usually cannot be modeled well is the noise. Noise usually comes in two components: coherent and incoherent. The coherent part, if exist, is systematic and thus can be modeled and corrected for if we know what causes it. The incoherent part, or random noise, is what changes with every experiment and therefore non-systematic and cannot be modeled. Fortunately, it is possible to locate the source of random noise and thus quantify its limit range. For a laboratory experiment, the source of random noise is usually the precision of the measurements. The measurement error of an experiment envelopes the random noise. Thus, the quality of a data set is usually associated with the measurement error and how much noise is in it. Good-quality data is acquired when the experiments are precise and the measurement errors are negligible with no noise correction needed.

Good-quality data such as Coyner (1984) is important because it minimizes the effect of random noise, allowing the users to justify the usage of a model, i.e. how well it represents the actual physics, via the process of inversion. From the study of inverse theory, if the quality of the data is good, then the model accuracy in fitting data (i.e. the goodness of the fit) and physical interpretation (i.e. the consistency between physical meaning and interpretation) is what justifies its use (e.g., Scales et al., 2001). Thus, if the model accurately describes all the involved physics, then

the fit residuals should be comparable to the random noise in the data, and the physical interpretation should be consistent for parameter estimates. If either the model does not fit well with a good-quality data or there is a lack of consistency in the interpretation of the fit results, then there is a chance that some certain physics have been overlooked or underestimated in the model. In this case, it may be possible and of the user's interest to identify those physics and modify the model to include or re-model them. Mathematically, that would be equivalent to adding a new parameter with a new physical meaning in to the model solution, or changing certain parameters into variables, etc... So far, we have seen a lack of consistency, either in fit goodness or interpretation of results using current ADM solutions. In the next chapters, I will make attempts to modify ADM so as to simultaneously improve the fit as well as physically interpret inversion results.

3.5 Conclusions

Inversion results from this chapter show that although the rigid-host solution works well for several rocks fitting the data to within measurement error of 0.015 km/s (e.g. the RMS error for Bedford limestone is 0.004 km/s for V_p and 0.003 km/s for V_s and for Navajo sandstone is 0.01 km/s for V_p and 0.006 km/s for V_s), systematic misfits exists in other rocks, comparatively larger than the measurement error (e.g. in Webatuck dolomite the RMS error is 0.15 km/s for V_p and 0.06 km/s for V_s and in Weber sandstone it is 0.07 km/s for V_p and 0.04 km/s for V_s). In contrast, the compliant-host solution returns negligible and random errors in all rocks, for both V_p and V_s (e.g. for Webatuck dolomite the RMS error is 0.03 km/s for V_p and 0.01 km/s for V_s, while in Weber sandstone it is 0.008 km/s for V_p and 0.006 km/s for V_s. However, the inverted parameters fall uninterpretably out of their range as constrained by their physical meanings in the "bed-of-nails" model (e.g. negative m values and extremely large P_i values). Naturally, it poses questions about the applicability of the existing analytic solutions: *Are the solutions not accurate enough to model the data response, or is it something to do with the model? What causes such misfits and unphysical values? How can the model be modified so as to be consistent with the inversion results?* The following chapters will suggest an answer to these questions: the applied pressure range is too large for the rock deformation model either to assume a rigid host or to ignore the pressure dependence of the host modulus in these rocks.

Moreover, the results indicate that ADM allows the user to view a rock from two contrasting perspectives: either having a rigid frame and a flexible asperity-height distribution which dictates rock behaviors but should deviate from the approximate simple power-law, or having a compliant host with a power-law distribution of asperity heights. Using the power-law assumption, the first view leads to the rigid-host solution which is a good first-order approximation but can presumably be further improved (due to the systematic misfits). Thus, the power-law is a fit-for-purpose assumption and should only be used depending on the application. If the application requires only a simple and effective velocity-pressure relationship without emphasis on misfits and accuracy, the power-law should be used. However if it is important for the application to have an accurate prediction of velocity as a function of pressure, say for a particular rock, we can generalize the distribution of asperity shortnesses as not having to obey a simple power-law and invert for it from the rock. The second view allows for the development of the compliant-host solution (but still assuming a power-law distribution of asperity shortnesses) which improves the fit significantly compared to the first one, but returns unphysical parameter estimates, suggesting that the model has not adequately described the data. Here the model needs to be revised in order to be able to interpret these seemingly false values. Therefore, although ADM solutions are applicable to all rocks, in either view modifications of ADM are necessary for better data fitting and interpretation. For this purpose, I attempt to modify ADM from the rigid-host point of view in chapter IV and from the compliant-host perspective in chapter V.

As we know from chapter II, the good thing about the parameter P_2 is that it is independent of the distribution of asperity shortnesses. P_2 characterizes the asperity material, or the type of deformation that the asperities undergo. Thus, as long as it stays constant with pressure, the type of deformation is linear elasticity. So no matter the distribution (whether a power-law or some other type of distribution) is used to acquire an ADM-based solution for inversion purposes, the estimate of P_2 from inversion is unchanged. As a result, allowing for P_2 to change with pressure is equivalent to describing a nonlinear deformation. Thus, the demonstrated trade-off relationship between m and P_2 as influenced by the data (the objective function is the RMS of the differences between data and model, while P_2 and m are independent parameters in the model) suggests that P_2 is not independent of the distribution of asperity shortnesses, but instead decreases as pressure increases. The bottom line is

that the actual deformation occurred in these rocks are nonlinear, and in order to account for that we need to allow P_2 to decrease with pressure. This will be the goal of chapter V. On the other hand, from the ADM perspective, we can still view the rock as a "bed-of-nails" with a rigid host, while treating the distribution of asperity heights as a non-power-law. In chapter IV, I attempt to test this view and invert for the distribution of asperity shortnesses. Whether the modified model is self-consistent will verify this preconception.

CHAPTER IV

NUMERICAL INVERSION OF THE DISTRIBUTION OF ASPERITY HEIGHTS - MODEL IMPROVEMENTS FROM THE RIGID-HOST PERSPECTIVE

4.1 Introduction and summary

The (elastic) asperity-deformation bed-of-nails model (ADM, BNM), based on the idea of "rough surfaces in contact" or "imperfect interfacial contact" (e.g. Greenwood and Williamson, 1966; Greenwood and Tripp, 1967; Gangi, 1978; Walsh and Grosenbaugh, 1979; Brown and Scholz, 1985; Liu et al., 1996) is a notably useful model for describing the mechanical behaviors of fractures under external forces. The statistical approach of using distributions of asperity heights to describe the mechanism in which "random surfaces" come in contact has been used extensively in numerous applications in tribology and material science, to describe friction and wear (e.g. Kragelskii, 1965; Kotwal and Bhushan, 1996; Berthoud and Baumberger, 1998) and especially, elasticity theory and contact mechanics of materials (e.g. Pullen and Williamson, 1972; Bhushan, 1996; Bhushan, 1998; Yu and Polycarpou, 2004). Several good literature reviews on the history of contact theory and its applications include, for instance, Buczkowski and Kleiber (2000) and Bahrami et al. (2005). Particularly for rocks, Gangi (1978) first used BNM to study the effects of confining pressure on the permeability of rocks. Noting that a rock can be considered as a mixture of fractures and microfractures that include rough surfaces with contact points and open spaces, this model characterizes rock properties via "contact asperities." These asperities come in contact and deform under pressure, and the amount of deformation determines rock behaviors. On the other hand, other popular fracture/rock models tend to describe and categorize pressure dependence and elastic properties in terms of the void portion of the rock, such as the ellipsoidal crack model with pore-aspect ratios (PARs) (i.e. the aspect ratio, a fractional number, between the smallest and largest dimensions of the ellipsoid) representing the pore geometry (e.g. Walsh, 1965; Kuster and Toksöz, 1974; O'Connell and Budiansky, 1974; Hudson, 1980; Sun and Goldberg, 1997), where the amount of void space, represented by the concentrations

of PARs, determines the closure stress as well as rock properties.

Interestingly, the recent development of a new concept called "pore structure type" (Sun, 2004; Sun et al., 2006) seems to synthesize these two mainstreams. Sun (2004) combines all effects of pore structure, pore connectivity, grain contact, cementation, etc... into an universal parameter named "frame flexibility factor" used to quantify the pore structure effects on the elasticity of porous rocks. However, no correlation has yet been established between ADM and PAR. So far, ADM has mostly been applied in a few inversion studies (e.g. Gangi, 1981; Carlson and Gangi, 1985; Gangi and Carlson, 1996). Recently, Carcione et al. (2007) used ADM to determine the dilation factor for use in 4D monitoring. Meanwhile, PAR has been widely used in many topics of investigation, including effective properties of fractured media (e.g. Hudson et al., 1996; Pointer et al., 2000; Liu et al., 2000) and velocity inversion (e.g. Cheng and Toksöz, 1979; Burns et al., 1990; Sun and Goldberg, 1997). Effective medium theories (e.g. Kuster and Toksöz, 1974; O'Connell and Budiansky, 1974; Bruner, 1976; Hudson, 1980; Xu and White, 1995) and their applications in time-lapse studies of porous and fractured media tend to prefer the use of ellipsoidal pores parameterized by aspect ratio to model elastic moduli (and thus, seismic velocities). Nevertheless, the use of PAR has often led to complications that require trading off between simplification and accuracy (e.g. Keys and Xu, 2002). Naturally, it poses a question about how suitable ADM is in such applications. Therefore, in this chapter I specifically compare ADM with PAR in terms of physical meaning and applicability in order to see if a link exists between them.

Using existing analytic ADM solutions (Gangi, 1981; Carlson and Gangi, 1985), I perform nonlinear regression to estimate velocity curves that best fit the laboratory data measured by Coyner (1984), King (1966), and Nur and Simmons (1969), and show results in chapter III. I then examine the feasibility of the solutions by analyzing the inversion statistics such as sensitivity, uncertainty and nonuniqueness of the parameter estimates. From chapter II, the analytic "rigid-host" solution assumes that the rock frame is much stiffer than the cracks, while the analytic "compliant-host" solution assumes that the rigidity of the rock frame is comparable to that of the fractures. Both solutions assume linear elastic deformation of asperities and a power-law distribution of asperity shortnesses. My inversion results from chapter III have shown that the power-law set of solutions can reproduce velocity-versus-pressure data quite well, though systematic and significant misfits with the rigid-host solution

are recorded in rocks that exhibit nonlinear behaviors, whereas the compliant-host solution offers a better fit but with physically uninterpretable parameter values.

Because the rigid-host solution returns systematic and significant misfits in many experimental rocks, it may be possible to improve on its fit capability as well as the overall applicability of ADM. Generally in a mathematical solution of a physical model, each parameter or variable describes an involved physic, while the equations describe the interactions and/or interrelations between these physical quantities as the variable is allowed to change while the parameters are held constant. Thus, from the mathematical point of view, there might be two possible accounts for the (significant and systematic) rigid-host misfits: either (a) a missing parameter in the model equation, or (b) certain parameters could (and should) be made variables that change as pressure increases instead of applying pressure independent values. From the inverse theory point of view, certain "a priori" assumptions may have limited the ability of this solution, as a forward model, to describe certain physics in certain rocks. For instance, while the assumption of rocks having an infinitely rigid host and a power-law distribution of asperity heights may be true for some rocks, such assumption may not always be true for all rocks, as the asperity distribution may differ from one rock to another.

In this chapter, I implement a numerical method similar to the differential effective medium (DEM) technique (e.g. Cheng and Toksöz, 1979; Tran et al., 2008; which inverts for a PAR spectrum), but instead I invert for the generalized distribution of asperity heights. This numerical implementation improves the goodness of fit at the expense of increasing the number of describing parameters and computation time. I discretize the deformation axis at a number of sample points and invert for the value of the cumulative distribution function (CDF) of the asperity-height distribution at each of the sample points by perturbing its value vertically around the analytically inverted power law. As a result, our numerical inversion does a better job of fitting the data compared to the analytic solution, but at the expense of using more parameters to describe the distribution function, as well as computation time. However, the results justify our initial postulation of a generalized asperity-height distribution of arbitrary form. By comparing asperity-height inversion results to a linearized method for pore-aspect ratio inversion (e.g. Cheng and Toksöz, 1979), we hope to bring out the link between ADM and PAR, an established standard in the industry. The comparison indicates that two models describe the same physical

phenomenon: the general increase in contact area due to pressure, highlighting the potentials of ADM-based solutions as suitable for ease of implementation.

4.2 Rigid-host rock model without the power-law assumption - Method and application of numerical generalization and inversion of the asperity-height distribution

An elastic property of a rock is an average between the property of the inclusion pores/cracks with that of the host rock. The contribution of the host rock property to the overall rock property is either significant or negligible depending on how it compares to that of the fractures. Nevertheless, ADM allows the users to assume that the host rock is always much more rigid and thus its compliance is negligible compared to the cracks, equating the rock elastic moduli to those of the fractures and attributing all natural rock physics to the linear elastic deformation of the asperities as they come into contact in the "bed-of-nails". Using ADM as a rock model, we can view a rock as having a rigid host while the fractures portion is controlled by a distribution of asperities whose heights may or may not follow a power-law (although the power-law is a good estimate). Thus, in order to more accurately predict subtle variations in velocity with pressure, in this chapter I employ a new implementation to test the idea of allowing the distribution of asperity shortnesses (which supposedly accounts for all physics involved in the change of pressure) to have an arbitrary shape that deviates from the simple power-law, and invert for it using the velocity-versus-pressure data.

From the rigid-host perspective, asperity deformation x is linear elastic, and the distribution of asperity shortnesses, represented by the CDF $N(x)$, also the number of asperities in contact (at deformation or shortness x), dictates rock behaviors. While the distribution of asperity shortnesses does not have to obey a simple power law such as assumed by Gangi (1978; 1981) and subsequent papers, the power law is indeed a useful choice for analytic results because not only it allows for a direct relation between velocity and pressure but it is also a fairly good approximation of natural behaviors of real rocks. However, as the rock is exposed to large-enough values of pressure, the power-law is no longer a good approximation (and we have seen examples of which in chapter III). In order to demonstrate that the power-law is fit-for-purpose

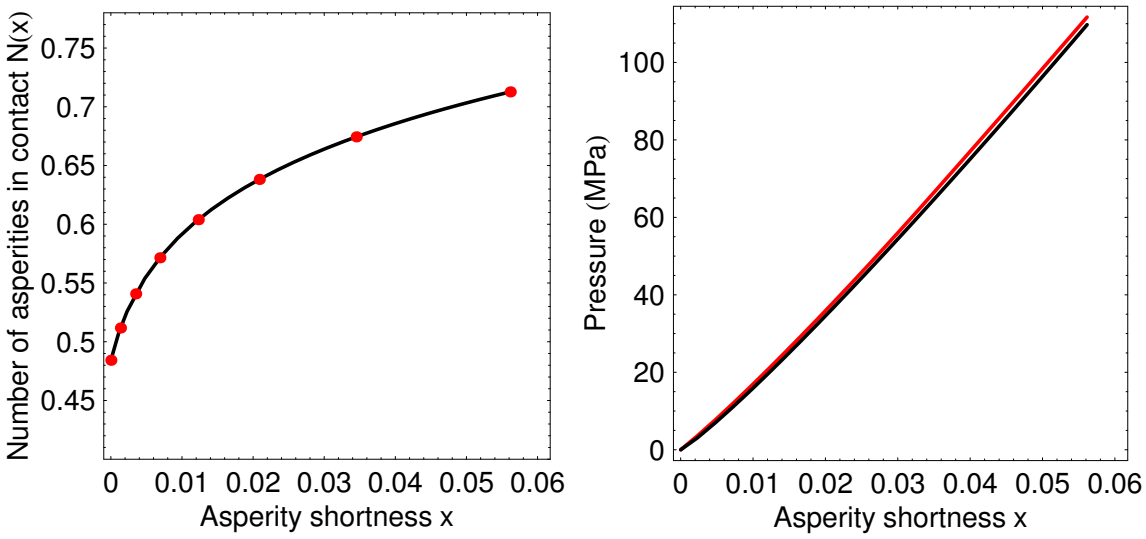

Fig. 4.1. Illustrations of a logarithmic sampling scheme of the distribution function and resulting numerical calculation of pressure. The example rock is the Navajo sandstone.

from this perspective, I generalize the distribution of asperity shortnesses $N(s)$ in equation (2.3), allowing it to have an arbitrary form instead of the power-law such as in equation (2.10), and numerically invert for it from real rock data.

The parameters to be inverted for in a rigid-host ADM would be P_2 and the cumulative distribution function (CDF) $N(s)$. However, because P_2 is independent of the distribution, we can elect to fix the value of P_2 as estimated from the power-law rigid-host fit. Thus, the only parameter left to be inverted for is the distribution function $N(s)$. Here I employ a numerical method to generalize and invert for the distribution of asperity heights in each experimental rock. I divide the deformation axis (x) into bins at a number of samples x_i, and invert for the value of the CDF $N(x)$ of the asperity-height distribution at each sample $N_i = N(x_i)$ by searching over a grid of its possible range of values, while linearly interpolating in between these points (x_i, N_i). For an illustration, on the left panel of figure 4.1, the red dots indicate such sample points. Pressure and velocity are evaluated numerically corresponding to the interpolated distribution function $N(x)$ using equations 2.5 and 2.11, and matched with the data for the best fit in a least-square sense. Similar to velocity changing rapidly at low pressures, the distribution $N(x)$ also has a high

curvature at x near zero. Using a non-uniform sampling scheme such as logarithmic sampling helps to catch the rapid changes of the function at small values of x. For all numerical results in this chapter, I use a logarithmic sampling scheme and a linear function to interpolate among the sample points.

In figure 4.1, I show an example of the sampling scheme as well as the starting search model. The rock is the Navajo sandstone from the Coyner (1984) data set. First, the asperity shortnesses corresponding to the minimum input pressure (0.5 MPa, from the data) and an assigned maximum pressure (115 MPa) are calculated. Then this range of asperity shortness is converted into logarithmic scale and uniformly sampled (with 8 samples in this case). Next, shown on the left panel, the power-law distribution function of the best power-law rigid-host fit $N(x)$ (black curve) is sampled with the above logarithmic scheme (red dots). Then, a linear interpolation function is applied (among the red dots) to create the starting distribution function. Again, note that this starting search model samples the black curve (i.e. the best power-law rigid-host fit) at the red sample points. Finally, pressure is calculated as proportional to the numerical integration of the (starting) distribution function. The right panel of figure 4.1 shows the calculated pressure (in red) in comparison with the power-law rigid-host pressure calculation (black curve). Note that the red model is not an analytic curve, but made up of linear segments.

In this method of numerically approximating the distribution function, the non-uniqueness of the solution is apparent because for instance, the interpolating function affects the evaluation of related quantities. In addition, the choice of value for the parameter P_2 also has an uncertainty degree of its own, from power-law rigid-host inversion. Despite this non-uniqueness, however, the overall fluctuating behavior of the fit solution is constrained by the input velocity profile, and should not change along with the different choices of parameters. Because our goal is to predict the subtle changes in the velocity profile in order to test the idea of an arbitrary, non-power-law distribution function, we want to (discretely) invert for the distribution function from measured data and see if doing that improves the overall fit, compared to the power-law solution. The goodness of the numerical fit depends on the number of samples (i.e., parameters or bins describing the distribution function $N(s)$) as well as the fineness of the search grid ΔN. This has an implication on the expense of computing time: the finer the grid, the better the fit, but also the longer the search. Fortunately, we have known in advance that the actual distribution function in all

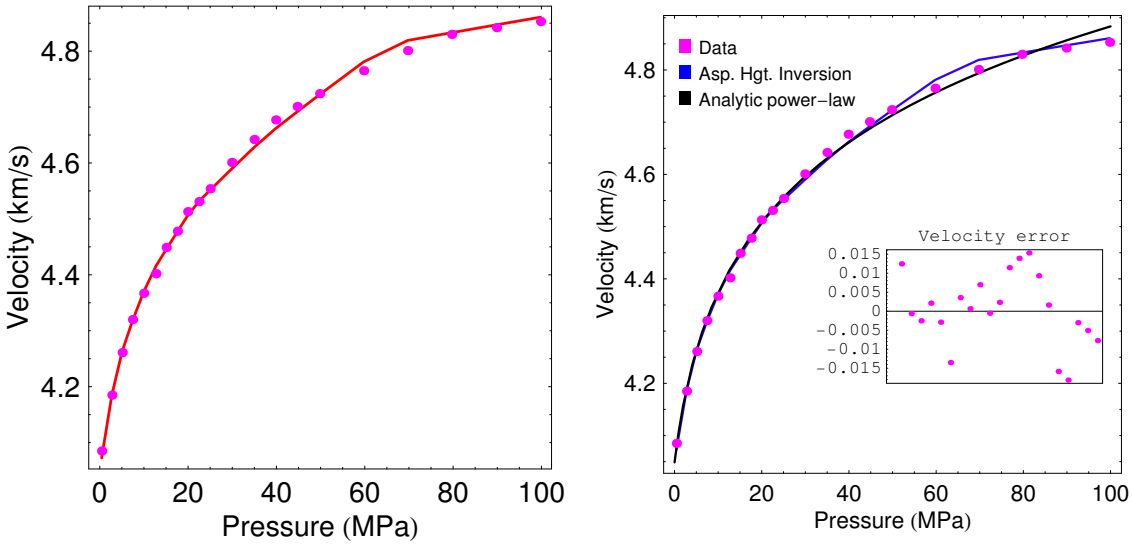

Fig. 4.2. Comparison of velocity profiles of the initial model (red), numerically inverted model (blue), and analytic power-law rigid-host best fit (black). The data is shown as magenta dots. The example rock is the Navajo sandstone.

rocks more or less follow a power-law, and that knowledge provides good starting guesses for our numerical inversion. Thus, here I apply the perturbation method of modifying the values of the pre-inverted power-law distribution function at the pre-fixed sample points, and grid-search over a large enough range of values at those samples to find the best match with the data in terms of pressure and velocity.

Despite the apparent non-uniqueness associated with the interpolation function, this numerical implementation should not change the general behavior of the final inverted distribution. That means, the inverted CDF $N(s)$ should always show the predicted fluctuating-while-monotonically-increasing behavior regardless whether a linear, parabolic, or cubic spline interpolation is used. For the sake of simplicity, I have used linear interpolation for all of my numerical inversion results. Moreover, beside such non-uniqueness of solution, another limitation of this method is the indirect relation between pressure and velocity. Both quantities are related through the deformation x and the distribution function $N(s)$ on the interval $[0, x]$. This adds to the cost of computing time for the generalized inversion. Here we can notice again the advantage of the power-law assumption, as it allows for a direct, straightforward one-on-one mapping between pressure and velocity.

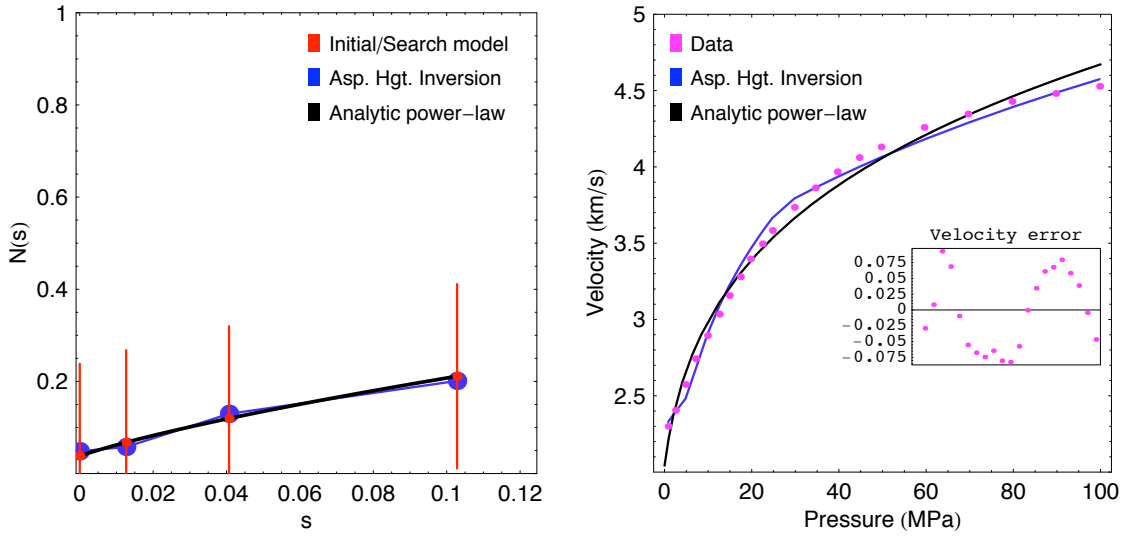

Fig. 4.3. Results of a 3-bin (4-point) grid-search inversion for Weber sandstone.

Figure 4.2 shows a plot of data measurements and a comparison of velocity profiles for the initial search model, the analytic power-law rigid-host best fit, and the numerically inverted model. Notice that since the analytic power-law rigid-host best fit has already fitted so well with the data from this rock, numerical inversion causes no significant improvement of errors. I have systematically performed numerical inversion for all rocks from the Coyner (1984) data set, and in the below section I present results from a few example rocks.

4.3 Results of numerical implementation of the generalized rigid-host rock model

Figure 4.3 shows the numerical inversion results for an example rock, the Weber sandstone from the Coyner (1984) data set, whose data originally do not fit well with the power-law rigid-host solution. On the left panel shows a comparison of distribution models: the distribution function of the best power-law fit displayed in black, the numerical models before (displayed in red, which samples the analytic power-law function at the 4 sample points) and after numerical inversion (displayed

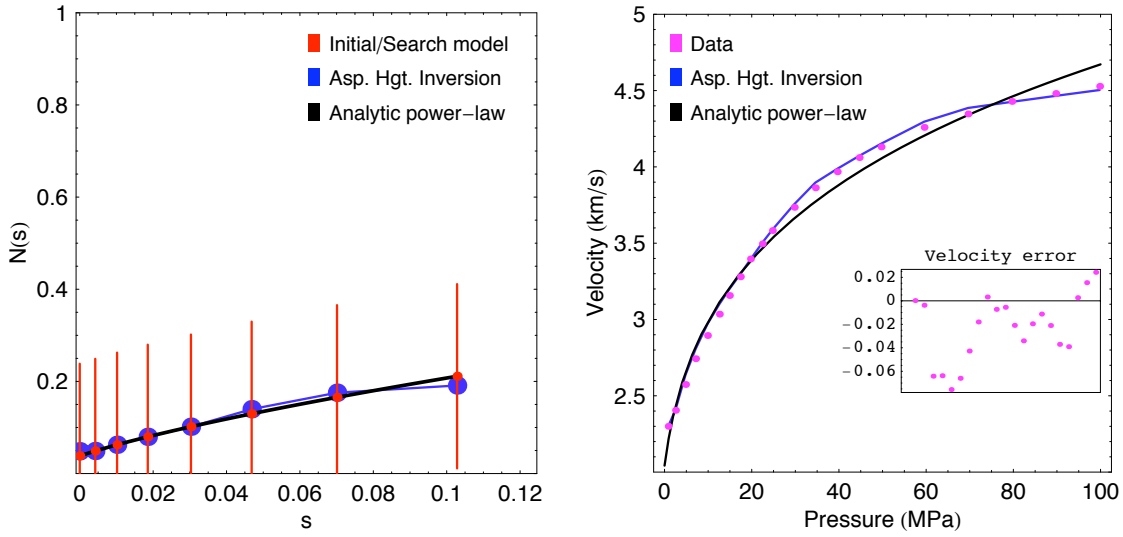

Fig. 4.4. Results of a 7-bin (8-point) grid-search inversion for Weber sandstone.

in blue). Here I use a 3-bin (4-point) logarithmic sampling scheme to sample the x-axis and a linear interpolation scheme for the discrete models. The red vertical bars show the search range at each sample point along which I perturb the distribution function $N(s)$ and compute the relevant pressure and velocity. I first use a coarse (vertical) grid of $\Delta N = 0.05$ then later refine the search by reducing it to $\Delta N = 0.01$. The panel on the right shows the original velocity data (magenta dots) together with the velocity profiles back-calculated from power-law rigid-host inversion (black curve) and a 3-bin grid-search inversion result (blue curve). The onset shows the remaining misfits after the grid-search inversion (i.e. the residuals of the blue curve). The RMS errors are (approximately) 0.073, 0.076, and 0.058 km/s, respectively for the best analytic power-law rigid-host fit (black), numerical power-law initial guess with a linear interpolation (red), and numerical 3-bin grid-search inversion result with a linear interpolation (blue).

Figure 4.4 shows the results of a 7-bin (8-point) grid-search inversion for the Weber sandstone, using the same (vertical) grid and (horizontal) logarithmic sampling scheme. Similar to figure 4.3, the left panel shows a comparison of models for the (cumulative) distribution function $N(s)$: the CDF of the best power-law fit displayed in black, the numerical models before numerical inversion in red (which

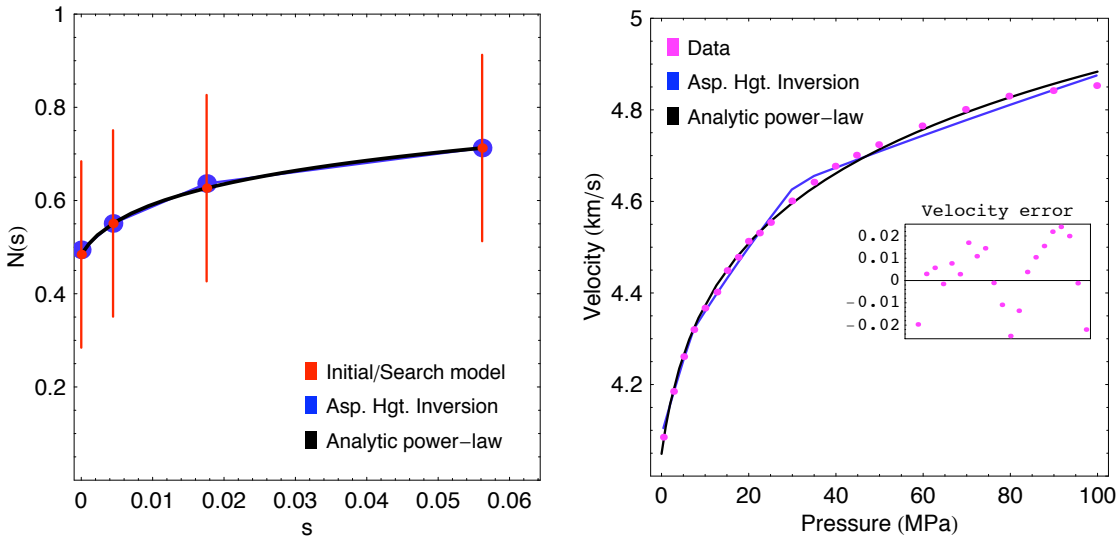

Fig. 4.5. Results of a 3-bin grid-search inversion from the rigid-host perspective for Navajo sandstone.

samples the analytic power-law function at the 8 sample points) and after numerical inversion in blue. Again the vertical red bars show the search range at each sample point, and discrete models use linear interpolation. The panel on the right shows the velocity profiles associated with the best power-law fit (in black) and with the numerical inversion result (in blue). The original velocity input data is also shown as magenta dots on this panel figure while the onset shows the remaining misfits after inversion. Velocity RMS errors associated with the black, red, and blue models are approximately 0.073, 0.073, and 0.038 km/s, respectively. Notice that the final model (blue) using 7-bin sampling improves fit by ≈50% compared to using only 3 bins. Thus, increasing the number of sample points (bins) improves fit significantly, but at the expense of computation time. The actual amount of time difference depends on the grid being used, the speed of the computer and how much memory is free for use in the calculation. For an estimate, the 3-bin case is faster by about one order (10 times). The results show that the numerical implementation indeed improves fit and velocity prediction in this rock, while the inverted distribution function deviates slightly from the power-law.

For the Navajo sandstone whose data already fit well with the analytic power-law rigid-host solution (RMS error of ≈ 0.011km/s with the best power-law fit), a 3-bin

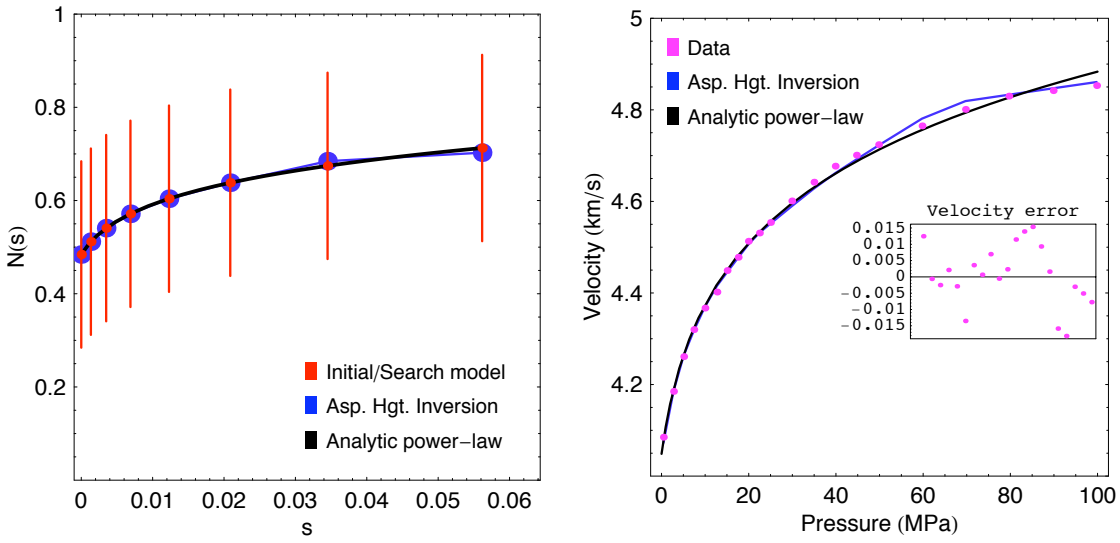

Fig. 4.6. Results of a 7-bin grid-search inversion from the rigid-host perspective for Navajo sandstone.

grid-search inversion slightly increases the RMS error (≈ 0.014km/s) due to the coarse sampling of the deformation axis (see figure 4.5); however, an 7-bin sampling scheme is dense enough for numerical inversion to improve the velocity RMS error further (≈ 0.009km/s) compared to the analytic power-law case (see figure 4.6). Figure 4.7 summarizes the RMS errors remain after a 3-bin grid-search inversion for the set of rocks from the Coyner (1984) experiments. It shows a general improvement of about 20%-50% velocity compared to the analytic power-law best fit. Again, these RMS errors can be improved further by increasing the number of sample points, or using a finer grid. However, there is a trade-off between fit improvement and computational cost. Increasing the number of control points improves the fit (as shown in figure 4.4 for the Weber sandstone) but could also be inefficient as the distribution takes many parameters to describe, while the computation time increases exponentially. In order to be computationally efficient, I recommend using a larger search range for the sample points x near zero and a smaller range for those at large x (because velocity does not change as rapidly at high pressures or large deformations as compared to low pressures or small deformations). It is also more efficient to use a coarser grid at first to find and close in the "proper" search range, then repeat the search with half the grid, and so on. In any event, numerical inversion results confirm our initial

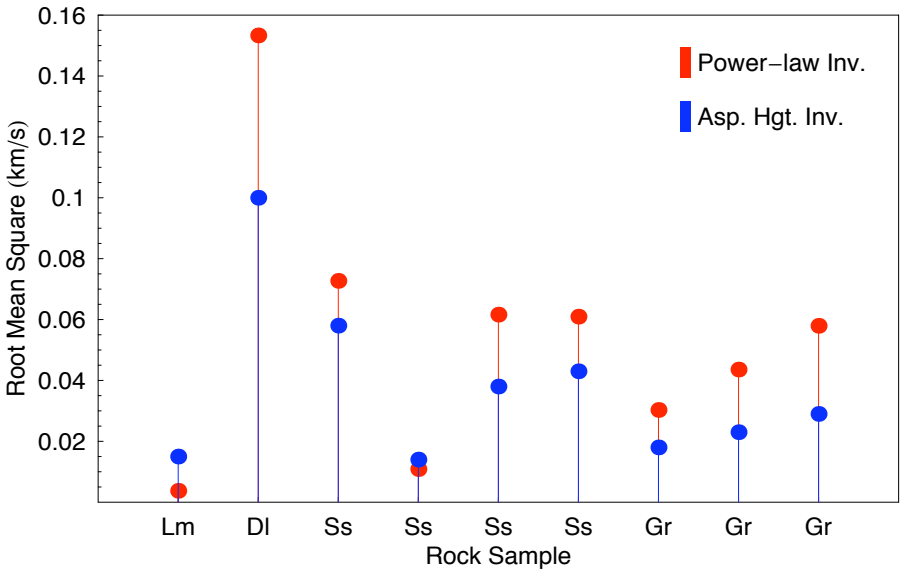

Fig. 4.7. RMS errors of a 3-bin grid-search AHI compared to those of the analytic power-law rigid-host best fit for the V_p of all experimental rocks in the Coyner (1984) data set.

postulation that the true distribution of asperity heights is arbitrary depending on the rock and does not have an universal form (particularly, a simple power-law), but it does deviate slightly from a simple power-law, and a perturbation of the best fit power-law can lead to a solution that better predicts velocity data.

4.4 Discussion - Comparison with pore-aspect ratio (PAR) inversion

To justify our work, we compare our inversion results (both analytic and numerical) with a well-known linearized inversion scheme made popular by Cheng and Toksöz (1979). The concept of a pore-aspect ratio (PAR) has been widely used, especially in describing the microstructure of the rocks as well as specifying an effective medium for time-lapse seismic modeling. This method inverts for a PAR spectrum from the V_p and V_s pressure profiles of the rock, assuming the properties of the grain solid are known. The spectrum contains discrete concentrations of the porosity for different bins of aspect-ratios. An increase in pressure closes the porosity made up by all elliptical cracks having ratios in between the bin boundaries. Pressure is related

to PAR using the (Walsh, 1965) formula for closure stress while velocities are related to PAR using the differential effective medium (DEM) model (Kuster and Toksöz, 1974). The inversion can be linearized by applying a "self-consistent" method (e.g. O'Connell and Budiansky, 1974) to solve an over-determined system of linear equations, such as shown by Tran et al. (2008).

The complications involved in the concept and applications of PAR have led to a general awareness about the trade-off between simplification and accuracy in the practice of PAR methods. For example, the DEM model associated with the scattering theory by Kuster and Toksöz (1974) has always been considered numerically intensive. Several authors have attempted to improve on the efficiency of this method, including Xu and White (1995), Keys and Xu (2002). However, the reason the PAR method is still used very frequently in the industry is because of its strength in fluid substitution. Because this model models rock properties via the void portion of the rock, it is easy to replace such void with any fluid whose properties are known. Once the model is set and all parameters defined, replacing the fluid content of the rock can be easily done by just including a fluid term into the equations. Thus, it is understandable that PAR has been used extensively and a common concept in the literature.

Intuitively, we postulate that the inverted distribution of asperity heights, which determines the fracture and rock behaviors according to ADM, will bear some resemblance to the PAR spectrum from "linearized inversion" (Cheng and Toksöz, 1979), because they both describe a single physical phenomenon: the pressure-induced change in contact area among the fractures. As pressure is introduced into the rock, which otherwise is in equilibrium, some of the thinner cracks are closed, reducing the total porosity (technically), bringing the stand-alone asperities into contact, generally increasing the total area of contact among asperities in the rock. Imaginatively as the pressure increases, longer asperities are brought into contact and deformed before the shorter ones, while thinner ellipsoidal cracks with smaller pore-aspect ratio are closed before the more spherical ones. When pressure closes cracks of a certain aspect ratio, it has also brought a certain number of asperities into contact and deformed those asperities. Note that although the linearized inversion method (Cheng and Toksöz, 1979) requires that the PAR spectrum be discrete, the nature of this spectrum is that it is a distribution of PARs (recall that a PAR is a fractional number), thus it should be continuous. Because of such reasons, the popular concept of a PAR α should be

analogous and somehow connected to that of the deformation x from the BNM. Thus, a comparison of inversion results together with their physical meanings is in order to see if such connection is visible.

Here we postulate that because both methods, ADM and PAR, attempt to describe the same physics (i.e., the effects of pressure on elastic rock properties, particularly velocities) by relating both quantities (pressure and velocity) to a responsible distribution in terms of deformation (i.e., the closure of aspect ratios is also a type of deformation), the two distributions should look similar. The difference in the models is that one describes it via compressing elastic springs, the other via stiffening and closing ellipsoidal pores. Nonetheless, the distribution of asperities which determines the rock behaviors should bear some resemblance to the PAR spectrum, although not totally because of their physical meaning, the non-uniqueness of inversion solutions as well as the method and data used. The comparison can be found in both the indirect relation of pressure and velocity through a third variable (either asperity height or PAR), and in the physical meaning of that variable (i.e. deformation). Under the same pressure influence, longer asperities are first-in-line to be brought into contact and deformed just like the thinner ellipsoidal cracks with smaller pore-aspect ratio getting closed before the more spherical ones do. The end result is an increase in contact area which both models include. Due to the non-uniqueness of the sampling scheme and of the bin-interpolation function, it is necessary to relate both distributions to the responsible pressure. Here I compare the two methods in terms of accuracy and computing resource.

Note that the result of the numerical inversion implementation is similar to the differential effective medium (DEM) technique (e.g. Cheng and Toksöz, 1979; Tran et al., 2008) of discretely describing a distribution. Both implementations samples the axis of the independent variable (i.e. deformation x or pore-aspect ratio α) using non-uniform binning, and invert for the value of the distribution function at the bin locations. In the case of PAR, it is the pore-aspect ratio spectrum, or the porosity concentrations as the distribution of aspect ratios. However, much of the rest is different between the two implementations, and in order to compare them we need to map from pore-aspect ratio to asperity shortness (or deformation) through pressure. The difference is in the method used for inversion. Cheng and Toksöz (1979) use a linearized inversion, solving an over-determined linear system of equations and find an estimate best fit. This adaptive method makes it a "self-consistent" way to estimate

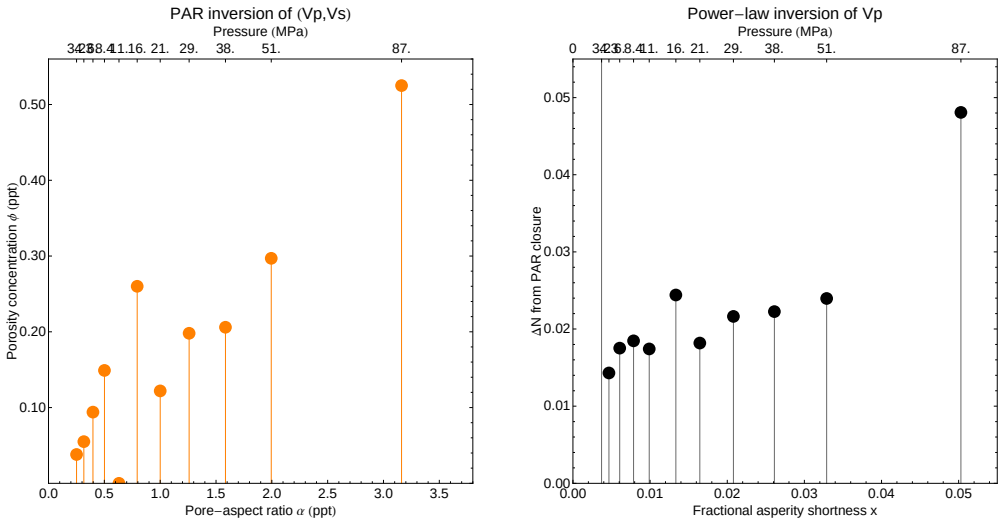

Fig. 4.8. Comparison of inverted distributions using PAR with that from rigid-host inversion

a fit to velocity profiles, but it can only reproduce velocities to a maximum of 3%-5% of the original velocity values (Tran et al., 2008). Examples of results for data considered in this dissertation suggest that because it combines input data from both V_p and V_s, the back-calculated velocities are usually "compensated" between V_p and V_s. PAR inversion often over-predicts the back-calculated V_p while under-predicts V_s in order to compensate the errors.

Figure 4.8 shows an example of the comparison of the two inverted distributions on the Berea sandstone. The result for PAR inversion was run from the same code as was used in the paper by Tran et al. (2008), and provided to me through personal communication by Tran (2008). We map the observed pressures to pore closure using the Walsh (1965) formula

$$\alpha = \frac{4(1-\nu)P_c}{\pi E} \tag{4.1}$$

and the back-calculated effective moduli as inputs. Here α is the aspect ratio that will be closed at closure pressure P_c, E is the Young's modulus and ν is the Poisson's ratio of the effective material. On this graph of pressure versus closure, we linear interpolate to find the closure pressure that would close those ratios on the inverted spectrum. Such closure pressure are displayed on the top of the frames. Using these pressure values as inputs, we find the corresponding asperity shortness on the back-calculated

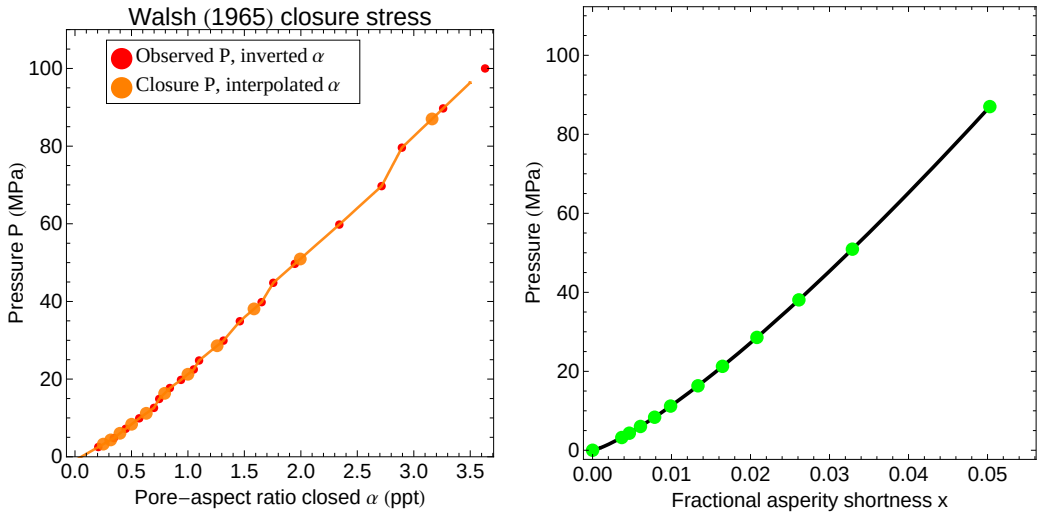

Fig. 4.9. Pore-aspect ratios are mapped and interpolated to find corresponding closure pressure (left panel) and then mapped to corresponding asperity shortness (right panel).

pressure versus asperity shortness, and then map them on to the distribution of asperity shortnesses. Figuring that each closure pressure would close all the PARs within one bin, we make the analogy that the same closure pressure would bring a number of asperities into contact, so the corresponding effect of pressure on the number of asperities in contact is the difference of two adjacent asperity bins. This mapping process is illustrated on figure 4.9.

Similar features can be seen on both distributions. The general behavior is that the influence of pressure (i.e. the change in number of asperities in contact, or the crack porosity closed) increases with the deformation. Although not displayed here, similar features and general behavior are also seen on the inverted asperity-height distribution for V_s. However, when we go to the numerical results (figure 4.10), we cannot see such features, as the distributions look very different compared to those in figure 4.9. There is still, however, an agreement between the spectrums for V_p and V_s.

The interpretation is in the order of match among velocity profiles. Figure 4.11 shows the superposition of V_p (left panel) and V_s (right panel) profiles calculated from PAR (blue dots), rigid-host (black) and the data (red dots) Note from above that the numerical inversion result has the best match with the data due to its flexible form of

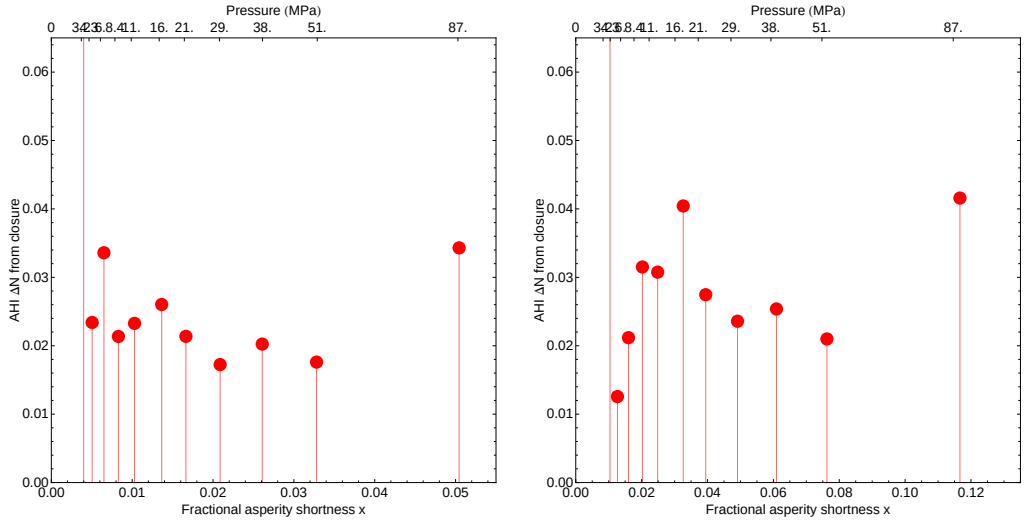

Fig. 4.10. Comparison of inverted distributions using numerical inversion for V_p (left panel) and V_s (right panel)

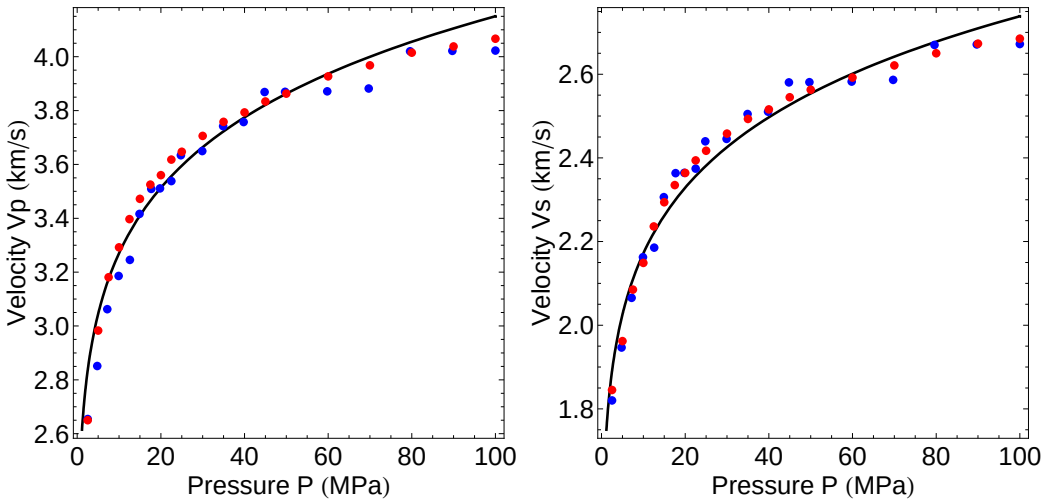

Fig. 4.11. Comparison of velocity profiles for Berea sandstone. Red dots are the Coyner (1984) measurements, blue dots are the PAR inversion back-calculated velocities, and the black curve represents the power-law rigid-host best fit.

the distribution function. The RMS errors of the numerical inverison back-calculated velocities with the data are around 0.007 km/s. Whereas, both the PAR and rigid-host back-calculated velocities have around an order larger of mismatch with the data, 0.07 km/s and 0.06 km/s respectively for V_p and 0.02 km/s and 0.03 km/s respectively for V_s. Thus, the two distribution are comparable only when they have the same match with the data. The features associated with the numerical inversion is more representative of the real microstructures of the rock, however, because it allows the best match with measured velocities. Note that the tall spike at the beginning of the asperity-height distribution is due to the gradual change in velocity within the fist bin. The PAR spectrum does not have the same feature because it assumes constant velocity within each bin.

4.5 Conclusions

We implement a numerical method similar to the differential effective medium (DEM) technique (e.g. Cheng and Toksöz, 1979; Tran et al., 2008; which inverts for a PAR spectrum), but instead we invert for the generalized distribution of asperity heights. This numerical implementation improves the goodness of fit at the expense of increasing the number of describing parameters and computation time. As a result, our numerical inversion does a better job of fitting the data compared to the rigid-host analytic solution, but at the expense of using more parameters to describe the distribution function, as well as computation time. The results confirms our initial postulation that from the rigid-host point of view, the asperity-height distribution is arbitrary from rock to rock, and does not have an universal form (such as a simple power-law).

By relating both distributions to the closure stress (or pressure), we have been able to demonstrate the link that exists between two methods of pore-aspect ratio and asperity deformation, and justify the use of asperity-deformation model by showing a complete comparison between inversion results as well as their physical meanings. Our comparison between asperity-height inversion and pore-aspect-ratio inversion suggest that two models describe the same physical phenomenon, which is the general increase in contact area due to pressure. While the pore-aspect ratio model is complicated yet more widely used, with the same goal of inverting velocity to within reasonable errors, ADM-based solutions is much more suitable for ease of implementation.

CHAPTER V

NONLINEAR DEFORMATION AND THE PRESSURE DEPENDENCE OF THE HOST ROCK - MODEL EXTENSION FROM THE COMPLIANT-HOST PERSPECTIVE

5.1 Introduction and summary

As shown in chapter III, an overall assessment of my inversion results shows that although the analytic rigid-host solution (with a power-law distribution of asperity heights) fits the data quite well for several stiff rocks, systematic and considerable misfits exist in many other rocks. On the contrary, inversion results for the same laboratory rocks using the analytic compliant-host solution (also with a power-law distribution of asperity heights) show random and relatively small misfits (compared to listed measurement error) for all studied rocks. This comparison suggests that the latter solution has the "correct" mathematical formula. However, the parameter estimates acquired from inversion fall out of their model-constrained range, indicating that they are not physically meaningful, or hypothetically, they represent, reflect or include a physical phenomenon that has not yet been taken into account by the asperity-deformation model (i.e. ADM). In other words, there exists a chance that the model may have over-constrained some physics that may actually be negligible in the model assumptions domain but become significant over a larger application domain. Particularly in this case, the original ADM assumes that the range of applied stress (or pressure) is small enough such that strain is infinitesimal and asperity deformation remains linear elastic; however in real life, such a range of applied pressure as large as 100 MPa could bring out the nonlinearity of (still elastic) deformation, making the original assumption fall short.

Although it may seem at first that the parameter estimates from the analytic power-law compliant-host inversion do not make physical sense (by falling out of their constrained ranges), that is only true in terms of a purely (linear) elastic "bed-of-nails" model. Because in reality "most rocks are nonlinear solids" (Coyner, 1984), it may be possible that those (compliant-host) inversion estimates actually describe the nonlinear behavior in natural rock deformation while their "unphysical" negative

values reflect the possibility of such physic not being included in the model. Because the ADM rigid-host and compliant-host rock models have already been good first-order approximations to natural rock behaviors under the influence of pressure (as seen from inversion results), the only physic that has not been and needs to be accounted for is the pressure dependence of the host-rock compliance. Note that Carlson and Gangi (1985) mentioned this physical phenomenon without including it in their (compliant-host) solution, which further supports the hypothesis (from the model perspective) that the host pressure dependence is responsible for the observed nonlinear behavior of rock deformation. Following this thought process, I postulate that such nonlinearity of deformation can be conveniently built into the "bed-of-nails" model via the asperity material, since the "bed-of-nails" model assumes rigid fracture faces and constant porosity (i.e. all deformation goes into the asperities). Therefore in this chapter, I propose an extension of the "bed-of-nails" model that has the potential to explain the negative values from compliant-host inversion. By letting the material constant P_2 vary as a nonlinear function of the deformation x (and thus, of applied pressure P), I modify several equations in the process but derive the exact same final equation as the compliant-host solution, but with a new parameter representing a new physic, regarding the original ADM assumptions: nonlinear deformation of asperities. In terms of a rock model, the new parameter represents the dependence of the host rock to applied pressure.

In reality, natural rock deformation can indeed be nonlinear, - so it makes sense that the analytic power-law rigid-host solution returns systematic error in many cases, especially for such a large applied pressure range as 0-100 MPa. Because the original, analytic rigid-host solution assumes that linear-elastic asperity deformation and a power-law distribution of asperity heights govern the behaviors of the fracture (and thus, of the rock) model, changing the type of asperity deformation (from linear to nonlinear) while keeping the (asperity-height) distribution intact is one approach towards improving the model's ability to fit and interpret laboratory data. The other approach which involves allowing the distribution to change while maintaining linear-elastic deformation of asperities has been addressed in chapter IV.

5.2 Proposed extension of ADM - Theoretical approach

5.2.1 The modified compliant-host "bed-of-nails" model

As seen in chapter III, inversion using the analytic power-law compliant-host solution (equation (2.12)) results in small and random residual errors but uninterpretable parameter estimates. Particularly, negative values of m and large estimate values of P_i are reported for the laboratory data sets from Coyner (1984), King (1966), and Nur and Simmons (1969). Because a power-law distribution of asperity heights constrains m to be between 0 and 1 (see equation (2.10)), it may seem that these estimates *do not make physical sense*. A possible, hypothetical reason for this can be found in chapter I, where I have noted that allowing for the pressure dependence of the rock frame might be able to improve the solution. In their derivation of the compliant-host solution, Carlson and Gangi (1985) mention correctly that the variation of the host matrix modulus with pressure is small in single crystals and low-porosity crystalline rocks, so the variation of velocity with pressure (below 1000 MPa) depends largely on the linear porosity and modulus of the cracks. However, there are two other important points that need to be further considered. First, it is not necessary that this observation can be generalized for other rock types, porosity, and rigidity. Second, Carlson and Gangi (1985) only consider the rate of change $\frac{\partial V}{\partial P}$, so the significance of this assumption depends on how big the range of applied pressure ΔP is. Therefore, the dependence of the host rock moduli to applied pressure may become significant over a large deformation, and thus needs to be accounted for in the model.

In the original ADM, the distribution of asperity shortnesses is modeled so as to account for all physics occurring as effects of pressure, yet the deformation of the asperities is assumed purely linear elastic. As many stress-versus-strain analyses from rock mechanics studies reveal, the linearity assumption is only approximately true for small stages of deformation, but usually not the entire (large-enough) range of deformation (or applied pressure). For large deformations, the host rock becomes pressure-dependent, strain no longer infinitesimal, making deformation nonlinear (but still elastic). Because the "bed-of-nails" model assumes two rigid faces and constant porosity, and attributes deformation and all changes to the asperities in contact, the part of deformation resulting from the pressure dependence of the host could (and should) also be built into the asperity model. Because of the random and small misfits to data measurements in all of the experimental rocks, I postulate that the

compliant-host solution has the correct mathematical form, and that the power law is still a good, natural approximation to pressure-induced contact deformation. Thus, I attempt to extend the model such that the same equation can be derived, but with a different parameter (modifying m, which describes the distribution of linear-elastic asperities) that describes a new physics: the involvement of the pressure dependence of the host rock.

5.2.2 Mathematical representations

In order for the host rock to comply to and depend on pressure, I choose to build the pressure dependence of the host into the asperity model (i.e. the "nails"). Note that the host compliance can be described adequately by a parameter V_g (such as in the compliant-host solution), while the host pressure dependence is what needs to be included in the model. Although this dependence can also be built into V_g, I choose to instead modify the constant P_2 (see equations 2.2 and 2.3) which is representative of the asperity material in the "bed-of-nails" model (see section 2.2.1.2, chapter II), because it leads to the exact same equation as the compliant-host solution, thus helps me explain the inversion results (i.e. negative values), as demonstrated below. When the "bed-of-nails" model is used to represent a rock, because the fracture faces are considered to be infinitely rigid, the asperity material characterizes the actual rock-frame material. In the original "bed-of-nails", P_2 is a constant because the asperity material is modeled as linear elastic. Here I modify P_2 by allowing it to change nonlinearly with pressure (and thus, deformation).

In order to characterize the pressure dependence of the host, I propose that the asperity material property P_2 be decreasing with the elastic strain x as the fracture closes under the influence of pressure, while simultaneously the asperities deform elastically according to the distribution of asperity heights. That is, as pressure increases, the asperities in contact remain following the power-law due to their height distribution, but the strength of the asperity material reduces, i.e. the asperities become weaker during the process (meaning the spring constant decreases). I postulate that this decrease on the strength of the asperity material is also in the form of a power-law:

$$P_2 = P_2(x) = P_3 x^{-a} \tag{5.1}$$

where x is the elastic deformation (strain) induced by pressure, and $a \geqslant 0$ char-

acterizes the power-law deformation of the host. When $a > 0$, the deformation is nonlinear elastic. When $a = 0$ the deformation is fully linear elastic. P_3 is a constant that describes the initial pressure at zero strain (i.e. the yield stress of the original undeformed material).

Just like in the original model, the asperities deform elastically, following a power-law distribution of heights characterized by the parameter m:

$$P(x) = P_2 \int_0^x N(s)ds = P_3 m x^{-a} x^{m^{-1}} = P_3 m x^{m^{-1}-a} \tag{5.2}$$

In other words, the model asperities simultaneously undergo a combination of linear elastic deformation and strain weakening, each process obeying a power-law of its own. This concept of strain weakening should only be understood abstractly in terms of the model (i.e. a strain weakening "bed-of-nails" is unrealistic). The other process, linear elastic deformation of asperities, represents and approximates the true contact regime in natural rocks. Here, the power-law distribution of asperity shortnesses is:

$$N(s) = s^{m^{-1}-1} \tag{5.3}$$

with the constraint $0 < m \leqslant 1$, naturally as in the original "bed-of-nails".

The elastic modulus is:

$$M(x) = \frac{dP}{dx} = P_3(1 - ma)x^{m^{-1}-a-1}. \tag{5.4}$$

The value of $M(x)$ can be positive or negative depending on whether pressure $P(x)$ increases or decreases with the elastic strain x, and eventually depending on values of m and a. Here the two mechanisms of deformation work their way opposite of each other under the effect of pressure. If $m^{-1} > a$, contact deformation is dominant, so it requires an increasing amount of energy ΔP to deform the same strain increment Δx, so $P(x)$ increases with x and $M(x) > 0$. If $m^{-1} < a$, the host deformation is dominant, so it requires less and less amount of energy ΔP to deform the same strain increment Δx, so $P(x)$ decreases with x and $M(x) < 0$. When $m^{-1} = a$, each deformation process requires the same amount of energy, so $M(x) = 0$. so a specific pressure large enough will automatically deform the whole rock, as the rock has no resistance to deformation at all. However the stiffness of the rock, being equal to the magnitude of the elastic modulus, is required to increase with elastic strain, so the only constraint in this model is $m^{-1} - a - 1 \geqslant 0$ or $b = 1/(m^{-1} - a) \leqslant 1$. Here b is

the parameter that describes the power-law manner of the total deformation which is a combination of contact asperity and host deformations.

Now if we go through the same derivations as by Carlson and Gangi (1985) to account for the asymptotic grain-matrix velocity and porosity reduction, the final equation relates between pressure and velocity:

$$\frac{1}{[V(P)]^2} = \left(\frac{1}{V_c^2} - \frac{1}{V_g^2}\right)\left(1 + \frac{P}{P_i}\right)^{(b-1)} + \frac{1}{V_g^2} \tag{5.5}$$

with the constraint $b \leqslant 1$ (b can be negative). Note that the mathematics regarding letting P_2 (or equivalently, k, etc..) change with P are similar and lead to identical final equations. Hence, this extension of ADM has incorporated the pressure dependence of the host rock, which accounts for visco-elasticity and for nonlinear rock deformation.

5.2.3 Consistency with inversion results

Because the final equation is the same, the extended model returns exactly the same parameter estimates as with the Carlson and Gangi (1985) compliant-host solution. With the extended model however, the parameter estimates now make physical sense. In this model, b is one of the parameter estimates (in lieu of the parameter m as compared to the Carlson and Gangi (1985) solution), and is consistent with the inversion results shown in figures 3.21 and 3.22 as the only constraint on its value is $b \leqslant 1$. It accounts for the (power-law) shape of the total deformation including contact asperity and host-rock deformations. While the inverted parameter b only takes into account the combined effect, there is obviously a trade-off between the two deformation mechanisms and it is not possible to know the correct value of each.

In addition, $P_i = P_3 m x_i^{1-b}$ accounts for the total pre-stress deformation (expressed in terms of the pre-stress elastic deformation x_i). Thus, the value of P_i can be large depending on how much deformation the rock has undergone prior to experimental pressure application (such as the cycling of rocks in the experiments by Coyner (1984) to get rid of hysteresis effects - i.e. the pressure cycling must have permanently deformed some of the asperities).

5.3 Supporting evidence

In this section I present all supporting evidence that points toward the necessity of extending ADM as above. My main postulation is that when undergoing a large deformation (such as rocks subject to effective pressures as large as 100MPa), the rock material exhibits nonlinear behaviors. Only when the material can be considered very stiff over the applied pressure range (i.e. brittle deformation), then the behaviors is approximately linear elastic (which is exactly the assumption of the original ADM). When any material undergoes a small deformation (i.e. low pressures), linear elasticity is a good approximation, but for a large (enough) deformation (i.e. high pressures), the process will be nonlinear. In other words, the rigid-host rock model becomes more and more invalid as the applied pressure increases.

5.3.1 Linearity vs. nonlinearity rock behaviors

Figure 5.1 shows the volumetric strain versus stress curves of the Coyner (1984) rocks on the left panel and my calculation of the slopes of these curves on the right. The curves on the stress-strain profile are not actually curves but a linear interpolation of digitized values taken from separate profiles for different rocks from the dissertation of Coyner (1984). It explains the blocky slope calculation on the right. Notice the linearity in the profiles for Bedford limestone and the nonlinearity in curves associated with other rocks over their experiment range of applied pressure. In fact, there is a strong agreement between the degree of linearity (i.e. how close slope profile is to being a constant) and the rigid-host RMS errors seen in figure 3.10. Bedford limestone, Navajo sandstone and two granites whose data fit quite well with the rigid-host equation all have stiff and linear (more or less) stress-strain behavior. Meanwhile, the other rocks show very nonlinear behavior and that agrees with the relatively large misfits with the rigid-host equation seen in figure 3.10.

5.3.2 Inversion application for progressively increasing pressure inputs

One way to verify our postulation is to see how well the rigid-host solution does with data of progressively increasing pressure inputs. Generally, inversion results have less error with fewer data points; however, that should not be the case if the error is monotonically increasing for all rocks with one data point added at a time, which indicates

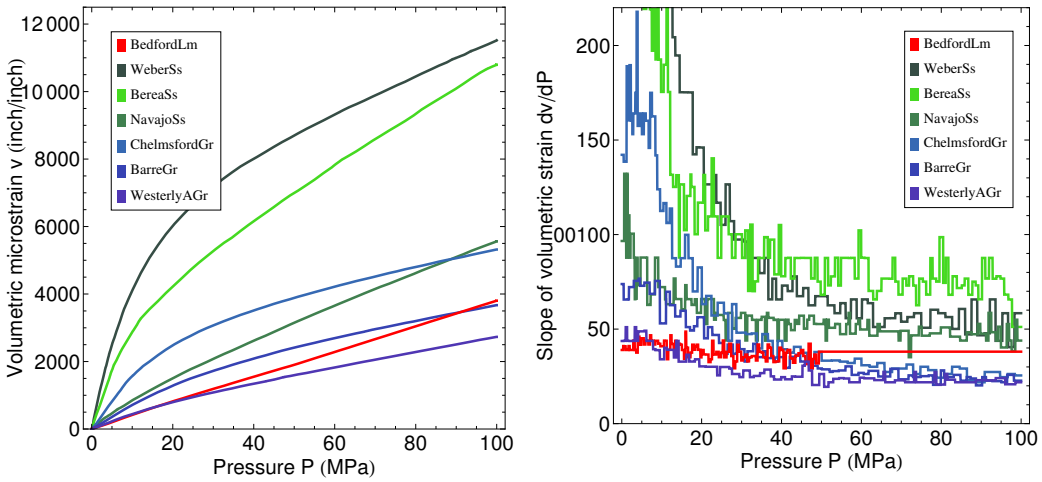

Fig. 5.1. Rocks with linear and nonlinear behavior over the applied pressure range. The left panel shows the stress-strain curve, digitized and reproduced from Coyner (1984). The right panel shows the slope of strain with respect to stress, calculated using the data on the left panel.

modeling error instead. Thus, if our postulation is correct, the rigid-host solution should return larger and larger RMS error when fitting to these data. That is, the rigid-host solution should work very well (for all rocks) for low-pressure measurements and return larger and larger error when higher-pressure measurements are included in the analysis. Note that we can do this only because the data is of good quality and the noise is considerably small (measurement error is approximately 0.015 km/s or 15 m/s for the Coyner (1984) rocks). Figure 5.2 shows a summary of rigid-host inversion results from this study. For most rocks, RMS error systematically increases with increasing pressure above 25 MPa and this even begins at zero pressure for several rocks. Notice that the rigid-host does quiet a good job fitting data less than about 25 MPa for most rocks, indicating that indeed the range of applied pressure should have something to do with the fit. On the other hand, the compliant-host solution fits well with all data and RMS errors are mostly within measurement error while the errors are randomly (i.e. non-systematically) varied (see figure 5.3). Therefore, extending the model to interpret the compliant-host inversion results is meaningful.

More evidence can be seen when we look at the inverted parameter values from rigid-host inversion. Figures 5.4 and 5.5 show the inverted parameter values for m

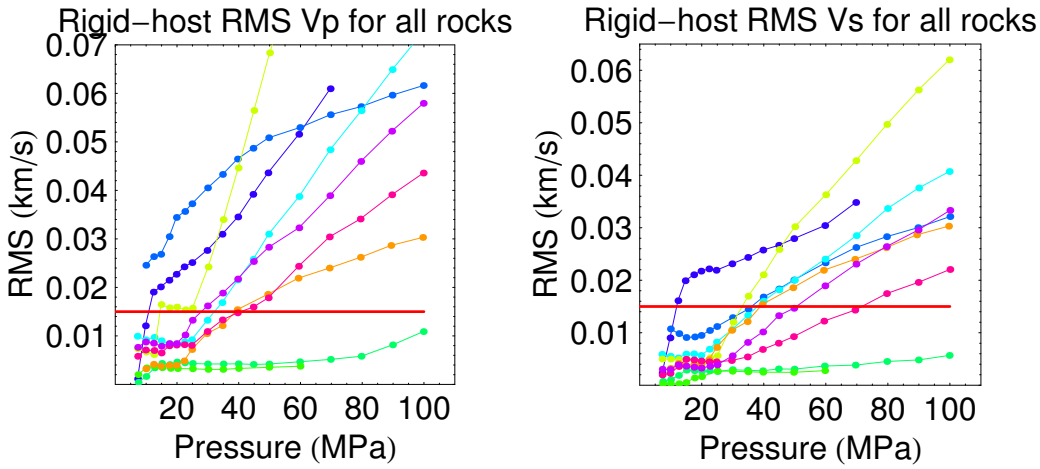

Fig. 5.2. RMS errors for V_p (left panel) and V_s (right panel) from rigid-host inversion with progressively increasing pressure inputs. The red bar indicates estimated measurement error.

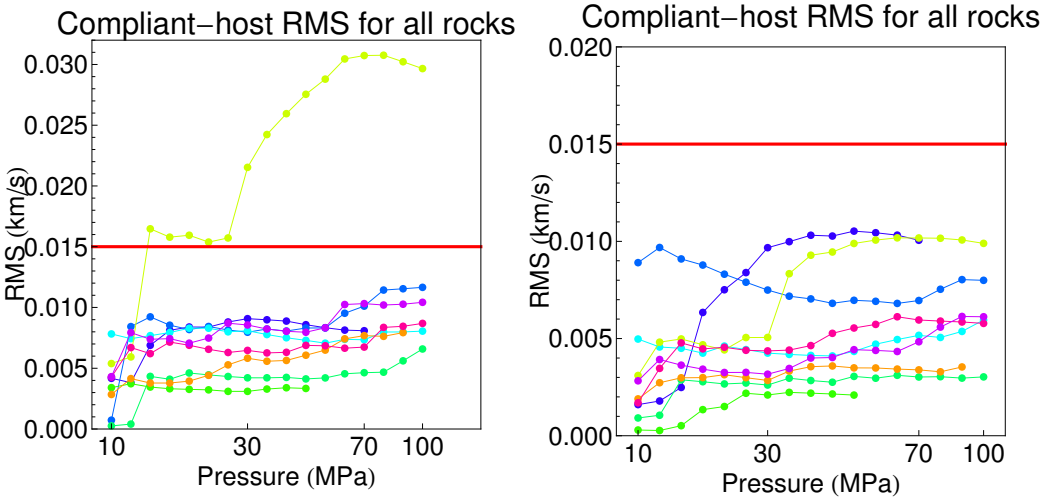

Fig. 5.3. RMS errors for V_p (left panel) and V_s (right panel) from compliant-host inversion with progressively increasing pressure inputs. The red bar indicates estimated measurement error.

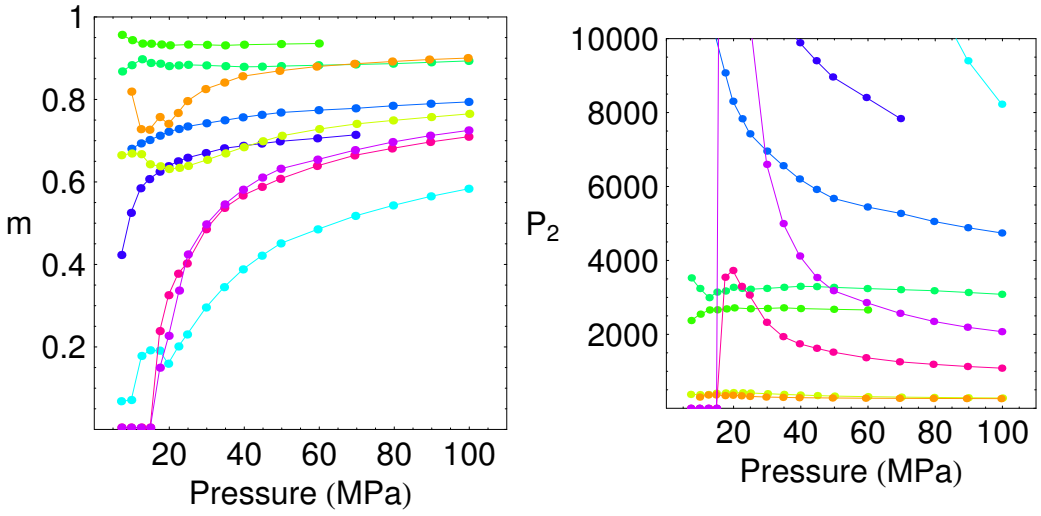

Fig. 5.4. Inverted m (left panel) and P_2 (right panel) values for V_p of the Coyner (1984) rocks, from rigid-host-host inversion with progressively increasing pressure inputs.

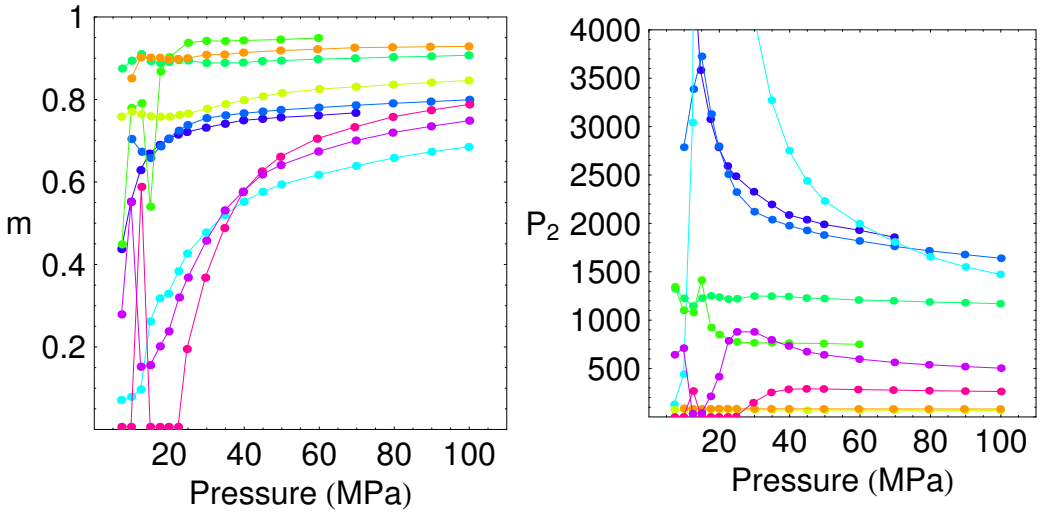

Fig. 5.5. Inverted m (left panel) and P_2 (right panel) values for V_s of the Coyner (1984) rocks, from rigid-host-host inversion with progressively increasing pressure inputs.

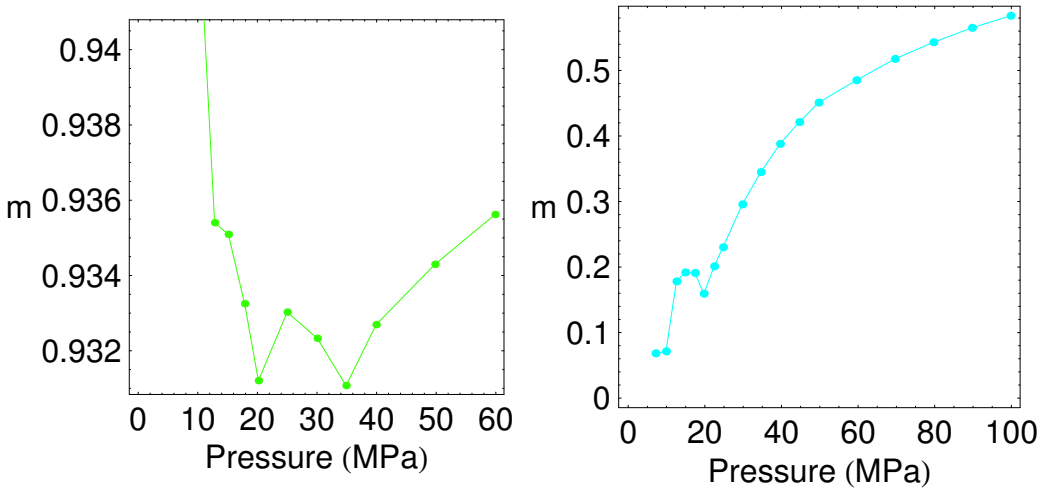

Fig. 5.6. Inverted m values for V_p of Bedford limestone (left panel) and Weber sandstone (right panel) in the Coyner (1984) data set, from rigid-host-host inversion with progressively increasing pressure inputs.

and P_2 from rigid-host inversion with progressively increasing pressure inputs. The figures suggest the idea of why letting P_2 change with P or x in the extended model. As shown, the inverted values for P_2 and m change with pressure in rocks whose data do not fit well with the rigid-host solution. Thus the deformation should be described as nonlinear over this pressure range. The value of m increases while the value of P_2 decreases with increasing pressure. Hence, in order to improve misfits from the rigid-host inversion, we can choose to either fix P_2 and let m change or fix m and let P_2 change with P (or x). The former has been addressed by a numerical implementation in chapter IV, while the latter is the motivation to the extension of ADM in this chapter.

From chapter III, observe that all rigid-host inverted values of m are between 0.5 and 1. The value of m does not change much for Bedford limestone whose data fits well with the rigid-host solution, as I include only the low-pressure measurements or the high-pressure measurements as well (see figure 5.6). My synthetic data test also confirms the fact that if the data agrees well with the fitting model, the parameter estimates do not change as we have more or less data. I interpret this as because Bedford is dominated by equant pores, so the effect of pressure tends to be linearly proportional to the volumetric strain which fits the description of ADM and the

rigid-host solution (see equation 2.4). Also, the rock grain solid is stiff so deformation occurs mostly on the asperity contacts while reducing porosity. However, for a rock such as the Weber sandstone (whose data the rigid-host solution does not fit well), the value of m increases from close to 0 to close to 0.6 (see figure 5.6), while the value of P_2 decreases (recall the trade-off relationship between m and P_2), as I increase the pressure inputs. My interpretation of this observation is as follow:

The Bedford limestone has equant-pores while the Weber sandstone has cracks-like pores. As pressure is increased, it affects the pores in Bedford limestone equally in all directions, and there is a very small, linear reduction of porosity (Coyner, 1984). The Weber sandstone is different. As pressure is increased, it closes the crack-like pores at low-pressure, and going into high pressures most cracks have been closed and the pores kick in. There is a nonlinear, big reduction of porosity in Weber sandstone where the curve is the most nonlinear at low pressure range and becomes increasingly linear (Coyner, 1984). I interpret this as the ranges of applied pressure are high enough to close most of the cracks. If I include the high-pressure data, the value of m gets larger and approaches 1 as pressure increases. Thus, there is a transition from crack-like to pores in Weber sandstone (this also agrees with what Coyner wrote in his dissertation) which makes the rigid-host solution not fit the data. In other words, the solution will fit well only if the porosity is dominated by either all cracks or all pores whereas a transition will increase the value of m but the fit gets poorer as pressure increases. The conclusion is that for rocks in which transition of pore geometry occurs under influence of pressure from crack-like to pore-like, or equally, pore-aspect ratio increasing (i.e. nonlinear deformation), the rigid-host solution does not apply well. Also, for rocks that are soft the solution does not apply well either (i.e. host rock compliance). The compliant-host solution however applies well because the parameter b actually accounts for both deformation in the host as well as in the pores.

5.3.3 Fluid substitution

Gangi and Carlson (1996) have developed formulae for the substitution of fluid using ADM:

$$M_{ru} \approx \frac{1}{\rho V_p^2} = \frac{\phi/3}{(1 - P_p A'_f) M_a(P) + [1 - A_f] M_f(P_p)} + \frac{1 - \phi/3}{M_g} \tag{5.6}$$

$$\mu_{ru} \approx \frac{1}{\rho V_s^2} = \frac{\phi/3}{(1 - P_p A'_f)\mu_a(P)} + \frac{1 - \phi/3}{\mu_g} \tag{5.7}$$

where

M_{ru} and μ_{ru} are the elastic moduli of the (undrained) rock, respectively;

V_p and V_s are the P- and S- wave velocity of the rock, respectively;

ρ and ϕ are the density and porosity of the rock (assumed constant with pressure), respectively;

$A_f(P) = A_f(P_c, P_p)$ is the fractional asperity contact area, which is a function of the effective pressure P or (equivalent) pressures P_c and P_p, and A'_f is its derivative.

P_p, P_c, P_d and P are the pore, confining, differential and effective pressure, respectively. These are related via

$$\begin{cases} P = P_c - nP_p \\ n = 1 - A_f(P_d) \\ P_d = P_c - P_p \end{cases} \tag{5.8}$$

M_a, M_f, M_g are the P-wave moduli of the asperities, fluid and the grain matrix, respectively. μ_a, μ_g are the shear moduli of the asperities and the grain matrix, respectively. The methods are described more completely in the appendix.

The above formulae are based on the compliant-host solution with the use of the parameter m representing linear elasticity. The advantage of the compliant-host solution is easily understood: it allows a better match with the dry data compared to the rigid-host. However, the calculations only work for values of m between 0 and 1, because for a negative m value the calculated velocities return complex values. Based on the compliant-host inversion results in chapter III, I have tried the fluid substitution for several rocks whose inversion returns a positive value of m, and an example velocity prediction is shown in figure 5.7 for the Navajo sandstone with the fluid being benzene. The fact that their calculation is off by a pattern indicates that the change in contact area by asperity deformation has not been correctly estimated due to the presence of the host-rock deformation parameter a (see equation 5.1).

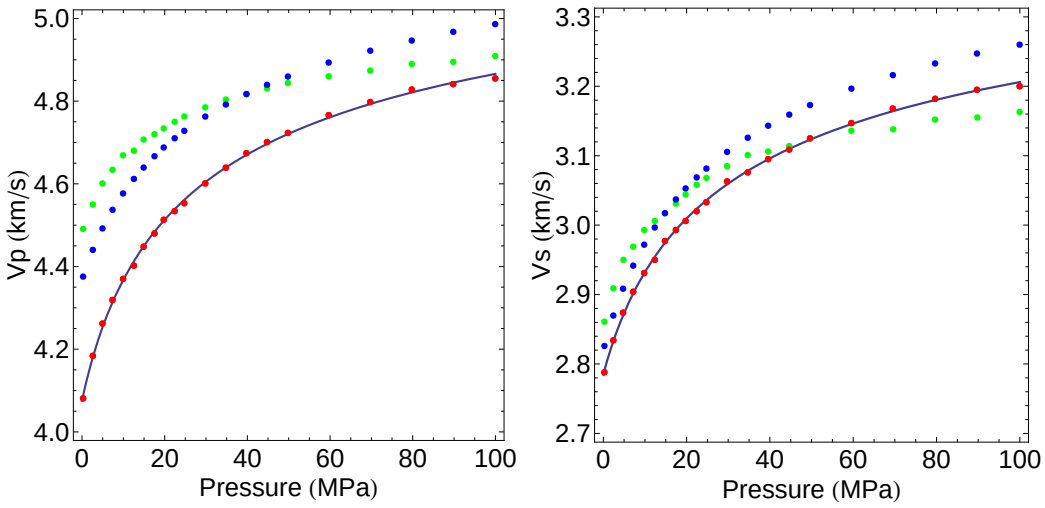

Fig. 5.7. Fluid substitution on Navajo sandstone for V_p (left panel) and V_s (right panel) using Gangi and Carlson (1996) ADM-based formulae. Red dots are the dry data measurements. The black curve represents the best compliant-host fit. The blue dots are the predicted values for fluid (benzene) substituted velocity. The green dots are the measured fluid-saturated data.

5.4 Conclusions

In this chapter I propose to extend the original ADM to account for a new physical phenomenon, the pressure dependence of the host rock which causes nonlinear visco-elastic deformation, so that the parameter estimates using the compliant-host equation make physical sense. This involves allowing the material constant P_2 to change with the elastic deformation x (or pressure P), which can simultaneously account for nonlinear visco-elasticity as well as the host rock pressure dependence. The extended model contains exactly the same final equation as the compliant-host solution, but with a new parameter b whose only constrain is $b \leqslant 1$ accounting for the total rock deformation including contact asperity and host rock deformations. The pre-pressure P_i also has a new physical meaning, as it accounts for the total pre-stress deformation which include both elastic and plastic deformation. Since the fit using the compliant-host equation is exceptionally good (i.e. random and small misfits), and due to its simple formula and ease of implementation, it has the potential to become the universal model used for data fitting and interpretation.

Because it is possible to derive the current ADM solutions using the extended

model, (e.g. fixing P_2 constant) it can be concluded that this model is more generalized than the original model. Supported by a list of evidence, the extended model explains well the "unphysical values" from compliant-host inversion and interpret all other physical phenomena happen under the influence of pressure, thus has the potential to become the universal model for use in all rocks.

In comparison to the rigid-host perspective, this model extension is obviously an equally unrealistic representation of the actual physics that occur under the influence of pressure, but in terms of fitting data and consistency of interpretation, it is comparable to the numerical implementation from the rigid-host perspective in chapter IV. Its advantage is the ease of implementation as well as the ability to fit and interpret laboratory data. Its limitation, however, is the non-uniqueness in specifying the contact asperities, so applications involving dimensions other than the measurement direction, such as the calculation of contact area, are also non-uniquely determined. This leads to difficulties in the practice of fluid substitution, such as one listed in the appendix.

CHAPTER VI

CONCLUSIONS AND FUTURE WORK

6.1 Conclusions

I first describe the "bed-of-nails" model in chapter II and demonstrate its applications in chapter III by presenting inversion results for the laboratory data sets, using the power-law solutions, i.e. the power-law rigid-host and compliant-host rock models. A comparison between the two results reveals systematic and considerable misfits for many of the studied rocks if only the rigid-host solution is used, whereas a much better fit with more random residuals, mostly within the range of measurement error, is obtained in all of the studied rocks when the compliant-host solution is used. Nevertheless, since the parameter estimates from inversion using the compliant-host solution do not make physical sense (by falling out of their constrained ranges) in terms of a linear-elastic "bed-of-nails" model, I propose a non-linear elastic "bed-of-nails" model that has the potential to explain these values. Because the original, analytic rigid-host solution assumes that linear-elastic asperity deformation and a power-law distribution of asperity heights govern the behaviors of the fracture (and thus, of the rock) model, changing the type of asperity deformation while keeping the (asperity-height) distribution intact is one approach towards improving the model's ability to fit and interpret laboratory data. The second approach involves allowing the distribution to change while maintaining linear-elastic deformation of asperities. This asperity-height inversion also shows significant reduction in residual errors. Overall, both revised model solutions improve fits and help explain the microstructures and behaviors of the rock, as well as the reason for misfits and unphysical values associated with the original solutions.

This dissertation investigates two different ways to improve misfits and interpret laboratory data by undoing some of the initial assumptions made in the rigid-host solution: (a) non-linear inversion using the analytic compliant-host solution with a power-law asperity-height distribution, and (b)a generalized inversion using the rigid-host model with an arbitrary asperity-height distribution. These are step-by-step efforts in order to understand why significant misfits still exist for the rigid-host solution

even with excellent-quality data. The compliant-host solution attempts to analytically solve the case when the modulus of the fracture is comparable to that of the host rock (i.e. the rock frame and the cracks have similar stiffness). Mathematically, it adds one more parameter to the list of parameters from the Gangi (1981) solution. The generalized inversion is a discrete, numerical method that allows for the discretization and perturbation of the distribution of asperity heights in order to find one that allows a good match of modeled and measured velocity. The method has the ability to locate the source of error in the original solution and improve the accuracy of velocity prediction. Compare to an existing method of pore-aspect ratio spectrum inversion, this method is much more suitable for ease of implementation as well as accuracy. Finally, I have developed an extension of ADM which explains for nonlinear deformation, and provide evidence to support the theory.

6.2 Future work

The link between the velocity inversion methods of pore-aspect ratio spectrum and asperity-height distribution can be better established via the relation to the contact area, which should be proportional to both porosity and the number of asperities in contact. Finding these constants of proportionality will thus probably unite all methods of velocity inversion as well as demonstrate the connection between mechanical and physical behaviors of the rock. It will also help in fluid substitution applications which in turn supports a better prediction of the pressure influence on rock properties. The next stage of the research should focus on trying to update and combine these ADM-based rock-physics models with the current theoretical solutions (e.g. Pointer et al., 2000; Liu et al., 2000) and study effects of pressure changes on the time-lapse seismic of fractured media.

REFERENCES

Aki, K. I., and Richards, P. G., 1980, Quantitative seismology: Theory and methods: W.H. Freeman and Co.

Anderson, T. L., 1995, Fracture mechanics: Fundamentals and applications: CRC Press.

Angerer, E., 2002, Processing, modeling and predicting time-lapse effects of overpressured fluid-injection in a fractured reservoir: Geophys. J. Int., **149**, 267–280.

Bahrami, M., Yovanovich, M. M., and Culham, J. R., 2005, A compact model for spherical rough contacts: Journal of Tribology, **127**, 884–889.

Barton, N., 2006, Rock quality, seismic velocity, attenuation and anisotropy: CRC Press.

Berryman, J. G., 1980, Long wavelength propagation in composite elastic media: J. Acoust. Soc. Am., **68**, 1809–1831.

Berthoud, P., and Baumberger, T., 1998, Shear stiffness of a solid-solid multicontacts interface: Proceedings: Mathematical, Physical and Engineering Science, **454**, no. 1974, 1615–1634.

Bhushan, B., 1996, Contact mechanics fo rough surfaces in tribology: Single asperity contact: ASME J. of Appl. Mech. Rev., **49**, 275–298.

——— 1998, Contact mechanics fo rough surfaces in tribology: Multiple asperity contact: Tribol. Lett., **4**, 1–35.

Bortfeld, R., 1961, Approximations to the reflection and transmission coefficients of plane longitudinal and transverse waves: Geophys. Prosp., **92**, 485–502.

Brown, S. R., and Bruhn, R. L., 1998, Fluid permeability of deformable fracture networks: Journal of Geophysical Research, **103**, no. B2, 2489–2500.

Brown, S. R., and Scholz, C. H., 1985, Closure of random elastic surfaces in contact: Journal of Geophysical Research, **90**, no. B7, 5531–5545.

Brown, S. R., and Scholz, C. H., 1986, Closure of rock joints: Journal of Geophysical Research, **91**, 4939–4948.

Brown, S. R., 1987, Fluid flow through rock joints: The effect of surface roughness: Journal of Geophysical Research, **92**, no. B2, 1337–1347.

——— 1995, Simple mathematical model of a rough fracture: Journal of Geophysical Research, **100**, no. B4, 5941–5952.

Bruner, W. M., 1976, Comment on 'Seismic velocities in dry and saturated cracked solids' by Richard J. O'Connell and Bernard Budiansky: Journal of Geophysical Research, **81**, no. 14, 2573–2578.

Buczkowski, R., and Kleiber, M., 2000, Statistical model of strongly anisotropic rough surfaces for finite element contact analysis: Int. J. Numer. Meth. Engng, **49**, 1169–1189.

Burns, D. R., Cheng, C. H., and Wilkens, R. H., 1990, Sandstone pore aspect ratio spectra from direct observations and velocity inversion: International Journal of Rock Mechanics and Mining Science and Geomechanics Abstracts, **27**, no. 4, 315–323.

Carcione, J. M., Landro, M., Gangi, A. F., and Cavallani, F., 2007, Determining the dilation factor in 4D monitoring of compacting reservoirs by rock-physics models: Geophys. Prosp., **55**, no. 6, 793–804.

Carlson, R. L., and Gangi, A. F., 1985, Effect of cracks on the pressure dependence of P wave velocities in crystalline rocks: Journal of Geophysical Research, **90**, no. B10, 8675–8684.

Castagna, J. P., and Backus, M. M., 1993, Offset dependent reflectivity - Theory and practice of AVO analysis: Society of Exploration Geophysicists.

Castagna, J. P., Swan, H. W., and Foster, D. J., 1998, Framework for AVO gradient and intercept interpretation: Geophysics, **63**, no. 3, 948–956.

Chapman, M., 2003, Frequency-dependent anisotropy due to meso-scale fractures in the presence of equant porosity: Geophys. Prosp., **51**, 369–379.

Cheng, C. H., and Toksöz, M. N., 1979, Inversion of seismic velocities for the pore aspect-ratio spectrum of a rock: Journal of Geophysical Research, **84**, 7533–7543.

Coyner, K. B., 1984, Effects of stress, pore pressure, and pore fluids on bulk strain, velocity, and permeability in rocks: Ph.D. dissertation, Massachusetts Institute of Technology.

Crampin, S., and Zatsepin, S. V., 1997, Modelling the compliance of crustal rock – II. response to temporal changes before earthquakes: Geophys. J. Int., **129**, 495–506.

Crampin, S., 1981, A review of wave motion in anisotropic and cracked elastic media: Wave Motion, **3**, 343–391.

Dieterich, J. H., and Kilgore, B. D., 1996, Imaging surface contacts: power law contact distributions and contact stresses in quartz, calcite, glass and acrylic plastic: Tectonophysics, **256**, 219–239.

Dvorkin, J., and Nur, A., 1996, Elasticity of high-porosity sandstones: Theory for two North Sea data sets: Geophysics, **61**, no. 5, 1363–1370.

Eberhart-Phillips, D., Han, D.-H., and Zoback, M. D., 1989, Empirical relationships among seismic velocity, effective pressure, porosity, and clay content in sandstone: Geophysics, **54**, no. 1, 82–89.

Endres, A. L., and Knight, R. J., 1997, Incorporating pore geometry and fluid pressure communication into modeling the elastic behavior of porous rocks: Geophysics, **62**, no. 1, 106–117.

Fehler, M., 1982, Interaction of seismic waves with a viscous liquid layer: Bulletin of the Seismological Society of America, **72**, no. 1, 55–72.

Gangi, A. F., and Carlson, R. L., 1996, An asperity-deformation model for effective pressure: Tectonophysics, **256**, 241–251.

Gangi, A. F., 1978, Variation of whole and fractured porous rock permeability with confining pressure: Int. J. Rock. Mech. Min. Sci., **15**, 249–257.

——— 1981, The variation of mechanical and transport properties of cracked rock with pressure: Proceedings of Symposium on Rock Mechanics, **22**, 369–379.

Gardner, G. H. F., and Harris, M. H., 1968, Velocity and attenuation of elastic waves in sands: SPWLA Logging Symposium, 9th Ann., Trans., M1–M19.

Gassmann, F., 1951, Über die elastizität poröser medien: Vier. der Natur. Gesellschaft in Zürich, **96**, 1–23.

Gdoutos, E. E., 2005, Fracture mechanics: An introduction: Springer, 2nd edition.

Genova, E., 2008, Stochastic modeling of the variation of velocity and permeability as a function of effective pressure using the bed-of-nails asperity-deformation model: M.S. thesis, Texas A&M University.

Gibson, R. L., and Toksöz, M. N., 1990, Permeability estimation from velocity anisotropy in fractured rock: Journal of Geophysical Research, **95**, no. B10, 15643–15655.

Goodman, R. E., 1976, Methods of geological engineering in discontinuous rocks: West Publishing.

Greenwood, J. A., and Tripp, J. H., 1967, The elastic contact of rough spheres: J. Appl. Mech., **89**, 153–159.

Greenwood, J. A., and Williamson, J., 1966, Contact of nominally flat surfaces: Proc. Roy. Soc. London. Ser. A, **295**, 300–319.

Ha-Duong, M., and Keith, D. W., 2003, Carbon storage: the economic efficiency of storing CO_2 in leaky reservoirs: Clean Technology and Environmental Policy, **5**, 181–189.

Hadley, K., 1976, Comparison of calculated and observed crack densities and seismic velocities in westerly granite: Journal of Geophysical Research, **81**, no. 20, 3484–3494.

Han, D.-H., and Batzle, M., 2006, Velocities of deepwater reservoir sands: The Leading Edge, **25**, no. 4, 460–466.

Hepple, R. P., and Benson, S. M., 2005, Geologic storage of carbon dioxide as a climate change mitigation strategy: performance requirements and the implications of surface seepage: Environmental Geology, **47**, 576–585.

Hudson, J. A., Liu, E., and Crampin, S., 1996, The mechanical properties of materials with interconnected cracks and pores: Geophys. J. Int., **124**, 105–112.

Hudson, J. A., 1980, Overall properties of a cracked solid: Math. Proc. Camb. Phil. Soc., **88**, 371–384.

Jack, I., 1997, Time-lapse seismic in reservoir management: Society of Exploration Geophysicists.

Jiang, Y., Li, B., and Tanabashi, Y., 2006, Estimating the relation between surface roughness and mechanical properties of rock joints: Int. J. Rock. Mech. Min. Sci., **43**, 837–846.

Keys, R. G., and Xu, S., 2002, An approximation for the xu-white velocity model: Geophysics, **67**, no. 5, 1406–1414.

King, M. S., 1966, Wave velocities in rocks as a function of changes in overburden pressure and pore fluid saturants: Geophysics, **31**, no. 1, 50–73.

Koefoed, O., 1955, On the effect of Poisson's ratios of rock strata on the reflection coefficients of plane waves: Geophys. Prosp., **30**, no. 4, 381–387.

Kotwal, C. A., and Bhushan, B., 1996, Contact analysis of non-gaussian surfaces for minimum static and kinetic friction and wear: STLE Tribol. Trans., **39**, 890–898.

Kragelskii, V. I., 1965, Friction and wear: Butterworth.

Kumar, A., Datta-Gupta, A., Shekhar, R., and Gibson, R. L., 2008, Modeling time lapse seismic monitoring of CO_2 sequestration in hydrocarbon reservoirs including compositional and geochemical effects: Petroleum Science and Technology, **26**, 887–911.

Kuster, G. T., and Toksöz, M. N., 1974, Velocity and attenuation of seismic waves in tow-phase media: Part I. theoretical formulations: Geophysics, **39**, 587–606.

Kwon, O., Kronenberg, A. K., Gangi, A. F., and Johnson, B., 2001, Permeability of wilcox shale and its effective pressure law: J. Geophys. Res., **106**, 19339–19353.

Lin, R. P., and Phair, S. M., 1993, AVO tuning: 63rd SEG Expanded Abstract, **12**, 727–730.

Liu, E., MacBeth, C. D., Pointer, T., Hudson, J. A., and Crampin, S., 1996, The effective elastic compliance of fractured rock: SEG Technical Program Expanded Abstracts, **15**, no. 1, 1842–1845.

Liu, E., Hudson, J. A., and Pointer, T., 2000, Equivalent medium representation of fractured rock: Journal of Geophysical Research, **105**, no. B2, 2981–3000.

Liu, E., Vlastos, S., Li, X., Main, I. G., and Schoenberg, M., 2004, Modeling seismic wave propagation during fluid injection in a fractured network: Effects of pore fluid pressure on time-lapse seismic signatures: The Leading Edge, **23**, 778–783.

Mavko, G., and Nur, A., 1978, The effect of nonelliptical cracks on the compressiblity of rocks: Journal of Geophysical Research, **83**, 4459–4468.

Mukerji, T., Berryman, J. G., Mavko, G., and Berge, P. A., 1995, Differential effective medium modeling of rock elastic moduli with critical porosity constraints: Geophys. Res. Lett., **22**, 555–558.

Norris, A. N., 1985, A differential scheme for the effective moduli of composites: Mechanics of Materials, **4**, 1–16.

Nur, A., and Simmons, G., 1969, The effect of saturation on velocity in low porosity rocks: Earth and Planetary Science Letters, **7**, no. 2, 183–193.

O'Connell, R. J., and Budiansky, B., 1974, Seismic velocities in dry and saturated cracked solids: Journal of Geophysical Research, **79**, no. 35, 5412–5426.

Oda, M., 1986, An equivalent continuum model for coupled stress and fluid flow analysis in joined rock masses: Water Resour. Res., **22**, 1845–1856.

Ostrander, W. J., 1984, Plane-wave reflection coefficients for gas sands at nonnormal angles of incidence: Geophysics, **49**, no. 10, 1637–1648.

Parrish, D. K., and Gangi, A. F., 1981, A nonlinear least squares technique for determining multiple-mechanism, high-temperature creep flow laws: Geophys. Monogr. Ser., **24**, 287–298.

Pointer, T., Liu, E., and Hudson, J. A., 2000, Seismic wave propagation in cracked porous media: Geophys. Prosp., **49**, 509–522.

Pullen, J., and Williamson, J. B. P., 1972, On the plastic contact of rough surfaces: Proc. Roy. Soc. London. Ser. A, **327**, 159–173.

Pyrak-Nolte, L. J., 1996, The seismic response of fractures and the interrelations among fracture properties: Int. J. Rock Mech. Min. Ser. & Geomech. Abstr., **33**, no. 8, 787–802.

Richards, P. G., and Frasier, C. W., 1976, Scattering of elastic waves from depth-dependent inhomogeneities: Geophysics, **41**, no. 3, 441–458.

Rutherford, S. R., and Williams, R. H., 1989, Amplitude-versus-offset variations in gas sands: Geophysics, **54**, no. 6, 680–688.

Scales, J. A., Smith, M. L., and Treitel, S., 2001, Introductory geophysical inverse theory: Samizdat Press.

Schlueter, E. M., Zimmerman, R. W., Witherspoon, P. A., and Cook, N. G. W., 1997, The fractal dimention of pores in sedimentary rocks and its influence on permeability: Engineering Geology, **48**, 199–215.

Schoenberg, M., 1980, Elastic wave behavior across linear slip interfaces: J. Acoust. Soc. Am., **68**, no. 5, 1516–1521.

Shekhar, R., and Gibson, R. L., 2005, Fractured reservoir characterization using seismics: SEG Technical Program Expanded Abstracts, **24**, no. 1, 1445–1448.

Shekhar, R., Gibson, R. L., Kumar, A., and Datta-Gupta, A., 2006, Seismic modeling of compositional and geochemical effects in CO_2 sequestration: SEG Technical Program Expanded Abstracts, **25**, no. 1, 2176–2180.

Sheriff, R. E., 1991, Encyclopedic dictionary of exploration geophysics: Society of Exploration Geophysicists, 3rd edition.

Shuey, R. T., 1985, A simplification of the Zoeppritz equations: Geophysics, **50**, no. 4, 609–614.

Smith, G. C., and Gidlow, P. M., 1987, Weighted stacking for rock property estimation and detection of gas: Geophys. Prosp., **35**, no. 9, 993–1014.

Sun, Y. F., and Goldberg, D., 1997, Effects of aspect ratio on wave velocities in fractured rocks: SEG Technical Program Expanded Abstracts, **16**, no. 1, 925–928.

Sun, Y. F., Berteussen, K., Vega, S., Eberli, G. P., Baechle, G. T., Weger, R. J., Massaferro, J. L., Gartner, G. L. B., and Wagner, P. D., 2006, Effects of pore structure on 4d seismic signals in carbonate reservoirs: SEG Technical Program Expanded Abstracts, **25**, no. 1, 3260–3264.

Sun, Y. F., 2004, Pore structure effects on elastic wave propagation in rocks: Avo modelling: Journal of Geophysics and Engineering, **1**, no. 4, 268–276.

Swan, G., 1981, Tribology and the characterization of rock joints: Proc. U. S. Symp. Rock Mech., **22**, 402–407.

Toksöz, M. N., Cheng, C. H., and Timur, A., 1976, Velocities of seismic waves in porous rocks: Geophysics, **41**, 621–645.

Tran, D. T., Rai, C. S., and Sondergeld, C. H., 2008, Changes in crack aspect-ratio concentration from heat treatment: A comparison between velocity inversion and experimental data: Geophysics, **73**, no. 4, E123–E132.

Trochim, W., 2000, The research methods knowledge base: Atomic Dog Publishing, 2nd edition.

Vlastos, S., Liu, E., Main, I. G., Schoenberg, M., Narteau, C., Li, X. Y., and Maillot, B., 2006, Dual simulations of fluid flow and seismic wave propagation in a fractured network: effects of pore pressure on seismic signature: Geophys. J. Int., **166**, no. 2, 825–838.

Walsh, J. B., and Grosenbaugh, M. A., 1979, A new model for analyzing the effect of fractures on compressibility: J. Geophys. Res., **84**, 3532–3536.

Walsh, J. B., Brown, S. R., and Durham, W. B., 1997, Effective media theory with spatial correlation for flow in a fracture: Journal of Geophysical Research, **102**, no. B10, 22,587–22,594.

Walsh, J. B., 1965, The effects of cracks on the compressibility of rock: J. Geophys. Res., **70**, no. 2, 381–389.

Xia, C. C., Yue, Z. Q., Tham, L. G., Lee, C. F., and Sun, Z. Q., 2003, Quantifying topography and closure deformation of rock joints: Int. J. Rock. Mech. Min. Sci., **40**, 197–220.

Xu, S., and White, R. E., 1995, A new velocity model for clay-sand mixtures: Geophys. Prosp., **43**, 91–118.

Yu, N., and Polycarpou, A., 2004, Combining and contacting of two rough surfaces with asymmetric distribution of asperity heights: Journal of Tribology, **126**, 225–232.

Yuh, S. H., 2004, Time-lapse seismic monitoring of subsurface fluid flow: Ph.D. dissertation, Texas A&M University.

Zamora-Castro, S. A., Oleschko, K., Flores, L., Ventura, E., and Parrot, J. F., 2008, Fractal mapping of pore and solid attributes: Vadose Zone Journal, **7**, 473–492.

Zatsepin, S. V., and Crampin, S., 1997, Modelling the compliance of crustal rock – I. response of shear-wave splitting to differential stress: Geophys. J. Int., **129**, 495–506.

APPENDIX A

LITERATURE REVIEW AND APPLICATION OF FLUID SUBSTITUTION USING THE ASPERITY-DEFORMATION MODEL

Fluid substitution by Gangi and Carlson (1996)

Gangi and Carlson (1996) modeled the fluid and pressure effects on seismic velocities of a fractured rock using the Gangi (1978) "bed-of-nails" model as such:

$$M_{ru} \approx \frac{1}{\rho V_p^2} = \frac{\phi/3}{(1 - P_p A_f')M_a(P) + [1 - A_f]M_f(P_p)} + \frac{1 - \phi/3}{M_g} \tag{A.1}$$

$$\mu_{ru} \approx \frac{1}{\rho V_s^2} = \frac{\phi/3}{(1 - P_p A_f')\mu_a(P)} + \frac{1 - \phi/3}{\mu_g} \tag{A.2}$$

where

M_{ru} and μ_{ru} are the elastic moduli of the (undrained) rock, respectively;

V_p and V_s are the P- and S- wave velocity of the rock, respectively;

ρ and ϕ are the density and porosity of the rock (assumed constant with pressure), respectively;

$A_f(P) = A_f(P_c, P_p)$ is the fractional asperity contact area, which is a function of the effective pressure P or (equivalent) pressures P_c and P_p, and A_f' is its derivative.

P_p, P_c, P_d and P are the pore, confining, differential and effective pressure, respectively. These are related via

$$\begin{cases} P = P_c - nP_p \\ n = 1 - A_f(P_d) \\ P_d = P_c - P_p \end{cases} \tag{A.3}$$

M_a, M_f, M_g are the P-wave moduli of the asperities, fluid and the grain matrix, respectively. μ_a, μ_g are the shear moduli of the asperities and the grain matrix, respectively.

Available information

The available information from the Coyner (1984)experiments are:

- The fluid (e.g water, $M_f \approx 2.25GPa$, benzen, $M_f \approx 1.21GPa$)
- Pore pressure $P_p = 10MPa$ and increasing values of confining pressure P_c.

- Velocities V_p and V_s vs. differential pressure $P_d = P_c - P_p$ (up to 100 MPa) for five water-saturated rocks.

- Density ρ and porosity ϕ of the five rocks.

- M_a and M_g can be estimated from the inversion of the dry-rock data using the Carlson and Gangi (1985) compliant-host solution as such:

$$\frac{1}{[V_{dry}(P)]^2} = \left(\frac{1}{V_c^2} - \frac{1}{V_g^2}\right)\left(1 + \frac{P_c}{P_i}\right)^{(m-1)} + \frac{1}{V_g^2} \tag{A.4}$$

The inverted parameters in this solution are m, P_i, V_g, and V_c, from which M_g and M_a can be computed:

$$M_g = \frac{1}{\rho V_g^2} \tag{A.5}$$

$$M_a(P) = \frac{1}{\rho V_{crack}(P)^2} = \left(\frac{1}{V_c^2} - \frac{1}{V_g^2}\right)\left(1 + \frac{P}{P_i}\right)^{(m-1)} \tag{A.6}$$

Note a relation among the parameters in this solution:

$$V_0^2 = 1/\left(\frac{1}{V_c^2} - \frac{1}{V_g^2}\right) = \frac{(P_1/P_i)^m P_i}{m\rho\phi/3} \tag{A.7}$$

where the parameter P_1 is related to the "well-known" parameter P_2:

$$P_1 = mP_2 \tag{A.8}$$

Unknown quantities

We do not know the effective pressure P, but it can be calculated from the known P_c and P_p if we also know the fractional asperity contact area A_f at that specific differential pressure $P_d = P_c - P_p$ (see equation 5.8). Hence, the only remaining unknown quantity is the functional fractional asperity contact area $A_f(P_d)$. (Its derivative A_f' can be inferred from its functional form.)

Calculation of contact area by Gangi and Carlson (1996)

The asperity contact area $A_c(h)$ is related to the distribution of asperities $N(l)$ and the cross-sectional area of the asperities $a(l)$ in contact as such (Gangi and Carlson, 1996):

$$A_c(h) = \int_h^L a(l)dN(l). \tag{A.9}$$

The "bed-of-nails" model assumes $a(l)$ proportional to l so equation A.9 leads to (Gangi and Carlson, 1996):

$$A_c(P) \approx \frac{A_0}{m}\left(\frac{P+P_i}{P_1}\right)^{1-m}. \tag{A.10}$$

and the fluid contact area is

$$A_f(P) = \frac{A_c(P)}{A_0} = \frac{1}{m}\left(\frac{P+P_i}{P_1}\right)^{1-m}. \tag{A.11}$$

and as a function of the differential pressure:

$$A_f(P_d) = \frac{1}{m}\left(\frac{P_d+P_i}{P_1}\right)^{1-m}. \tag{A.12}$$

The derivative is:

$$A'_f(P) = \frac{1}{mP_1}\left(\frac{P+P_i}{P_1}\right)^{m}. \tag{A.13}$$

From the available P_c and P_p we can use the above equations to try to predict velocities and compare to the actual measurements. Below are the steps in the recipe for fluid substitution.

Recipe

Follow the below steps to practice fluid substitution as shown by Gangi and Carlson (1996):

1- Invert the dry data to estimate values for the parameters m, P_i, V_g, and V_c using the compliant-host equation A.4.

2- Calculate M_g, V_0 and P_1 using equations A.5 and A.7.

3- Calculate the effective pressure P at specific pressures P_c and P_p using equation A.3.

4- For each calculated effective pressure, calculate the fractional asperity contact area $A_f(P)$ and its derivative $A'_f(P)$ using equations A.11 and A.13.

5- Plug all available and calculated information into equations A.6, A.1 and A.2 to predict velocities at those confining and pore pressures.

Limitation of the method

At step 1 above, several of the Coyner (1984) rocks result in a negative value for m. At step 2, the calculation of P_1 (using equation A.7) returns a complex number because m is negative. If instead, we consider the extended model above, these

inverted values would be for the parameter b, and a negative value of b means the host deforms faster than the contact asperities. Due to the non-uniqueness (between m and a) in specifying the physical asperities, we do not yet have a way to estimate the correct contact area in this case.

In short, the calculation of the fluid-induced modulus involves contact area which involves the power-law distribution of asperities represented by the parameter m whose inverted value is either negative (using the compliant-host equation), or cannot be separated from the combined effect with the host pressure-dependence (using the extended model).

VITA

Hoa Quang Bui was born in Hanoi, Vietnam. After receiving his B.S. (in 2001) and M.S. (in 2004) degrees in geophysics at the University of Oklahoma, he attended Texas A&M University to work on his Ph.D. program in exploration geophysics, under Dr. Richard L. Gibson Jr. His research interests are seismic imaging and interpretation, AVO, rock properties and fracture reservoir characterization. He successfully defended his Ph.D. thesis in October 2008, and is now working for BP America Inc. as a geophysicist. His mailing address is: Department of Geology & Geophysics, c/o Dr. Richard L. Gibson, Texas A&M University, College Station, TX 77843-3115. His email address is Hoa.Bui@bp.com.

This document was typeset in LaTeX by Hoa Quang Bui.